NASA TECHNICAL MEMORANDUM

NASA TM X-1550

NASA TM X-1550

EFFECTS OF SIMULATED WING DAMAGE ON THE AERODYNAMIC CHARACTERISTICS OF A SWEPT-WING AIRPLANE MODEL

by Clyde Hayes

Langley Research Center

Langley Station, Hampton, Va.

NATIONAL AERONAUTICS AND SPACE ADMINISTRATION • WASHINGTON, D. C. • APRIL 1968

NASA TM X-1550

EFFECTS OF SIMULATED WING DAMAGE ON THE AERODYNAMIC CHARACTERISTICS OF A SWEPT-WING AIRPLANE MODEL

By Clyde Hayes

Langley Research Center
Langley Station, Hampton, Va.

NATIONAL AERONAUTICS AND SPACE ADMINISTRATION

For sale by the Clearinghouse for Federal Scientific and Technical Information
Springfield, Virginia 22151 – CFSTI price $3.00

EFFECTS OF SIMULATED WING DAMAGE ON THE AERODYNAMIC CHARACTERISTICS OF A SWEPT-WING AIRPLANE MODEL

By Clyde Hayes
Langley Research Center

SUMMARY

An investigation has been conducted to determine the effects of simulated wing damage on the aerodynamic characteristics of a swept-wing airplane model. Wing damage was simulated by removal of either a leading-edge portion or a trailing-edge portion of one wing panel or by removal of an entire wing panel. The investigation was conducted at Mach numbers from 1.70 to 2.86 at a constant Reynolds number of 2.25×10^6 per foot (7.38×10^6 per meter).

The results of the investigation indicated that removing the leading- or trailing-edge portion of the wing or removing the entire wing panel led to a decrease in both lift-curve slope and maximum lift-drag ratio. At the lower Mach numbers, removal of the trailing edge caused a rolling moment slightly larger than that caused by removal of the leading edge. At the higher Mach numbers, however, the effect on rolling moment due to removal of the trailing edge was less than that caused by removal of the leading edge even though a larger area of the wing was removed. Except when the entire wing panel was removed, the roll induced by wing asymmetry could be offset by sideslip within reasonable limits of angle of attack and sideslip.

INTRODUCTION

As an aid in assessing the aerodynamic effects of battle damage that might be sustained by military aircraft, a wind-tunnel investigation has been conducted in which wing damage was simulated by removal of all, or portions of, one wing panel of a research model. The model used consisted of an ogive-cylinder fuselage, a swept midwing, and a vertical tail. Wing damage was simulated by removal of either a leading-edge or a trailing-edge portion of the right wing panel or by removal of the entire right wing panel. Removal of the leading-edge portion of the wing resulted in an 11-percent reduction of the exposed wing-panel area S_e, and removal of the trailing-edge portion resulted in a 17-percent reduction. No attempt was made to apply control deflections required to trim the model.

The investigation was performed in the Langley Unitary Plan wind tunnel at Mach numbers from 1.70 to 2.86 at a Reynolds number of 2.25×10^6 per foot (7.38×10^6 per meter). The angle of attack was varied from about -4° to 22° and sideslip angle was varied from about -5° to 10°.

SYMBOLS

All aerodynamic data except those for lift and drag are presented in coefficient form referred to the body-axis system. The lift and drag data are referred to the stability axis system. The moments are referred to a point on the body center line 59.6 percent of the body length aft of the nose. Measurements for this investigation were taken in the U.S. customary units and in the International System of Units.

b	wing span, 20.00 in. (50.80 centimeters)
$\bar{c}$	mean aerodynamic chord, 8.611 in. (21.872 centimeters)
C_D	drag coefficient, $\frac{\text{Drag}}{qS}$
C_L	lift coefficient, $\frac{\text{Lift}}{qS}$
C_l	rolling-moment coefficient, $\frac{\text{Rolling moment}}{qSb}$
C_m	pitching-moment coefficient, $\frac{\text{Pitching moment}}{qS\bar{c}}$
C_n	yawing-moment coefficient, $\frac{\text{Yawing moment}}{qSb}$
C_Y	side-force coefficient, $\frac{\text{Side force}}{qS}$
C_{L_α}	lift-curve slope at $\alpha = 0^\circ$, per deg
$\Delta C_m / \Delta C_L$	longitudinal stability parameter at $C_L = 0$
L/D	lift-drag ratio
M	Mach number
q	dynamic pressure, lb/ft^2 (newtons/meter^2)

S total wing area, 1.042 ft^2 (0.0968 $meter^2$)

S_e exposed area of one wing panel, 0.383 ft^2 (0.0356 $meter^2$)

α angle of attack, deg

β sideslip angle (modified wing on windward side for positive β), deg

Subscripts:

max maximum

min minimum

MODEL

Details of the model are presented in figure 1. The model consisted of an ogive-cylinder body having a fineness ratio of 13.8, a swept wing located in a midwing position, and a slab vertical tail with a wedge leading edge. The symmetrical configuration, herein referred to as "basic," had wing airfoil sections as shown in figure 1. The fixed center section had a constant chordwise thickness and tapered from a thickness of 0.40 inch (1.016 cm) at the root to 0.15 inch (0.381 cm) at the tip. The removable leading edge consisted of the forward portion of an NACA 63-006 airfoil and the removable trailing-edge portion tapered to a sharp edge. Asymmetrical wing configurations were achieved by removal of either the right leading- or trailing-edge portion (fig. 1) or the entire right wing panel. Removal of the leading-edge portion resulted in an 11-percent reduction in wing area of the exposed wing panel and removal of the trailing-edge portion resulted in a 17-percent reduction.

TESTS AND CORRECTIONS

The investigation was conducted in the low Mach number test section of the Langley Unitary Plan wind tunnel at Mach numbers of 1.70, 1.90, 2.36, and 2.86 at a constant Reynolds number of 2.25×10^6 per foot (7.38×10^6 per meter). The dewpoint was maintained below -30° F (239° K) to avoid any significant condensation effects. The variation of stagnation pressure and temperature with Mach number was as follows:

Mach number	Stagnation temperature		Stagnation pressure	
	^{o}F	^{o}K	psia	kN/m^2
1.70	150	339	9.20	63.434
1.90	150	339	9.83	67.778
2.36	150	339	12.35	85.153
2.86	150	339	16.08	110.872

Forces and moments were measured by a sting-mounted six-component strain-gage balance. The tests were made through an angle-of-attack range from approximately -4^{o} to 22^{o} and an angle of sideslip from approximately -5^{o} to 10^{o}. The results have been corrected for tunnel flow angularity and deflection of the sting and balance due to aerodynamic loads. The axial-force data have been adjusted to free-stream static pressure acting over the model base and chamber. Transition was not fixed on any of the model components.

PRESENTATION OF RESULTS

The results of the investigation are presented in the following figures:

DISCUSSION

Longitudinal Aerodynamic Characteristics

The effects of wing asymmetry on the longitudinal aerodynamic characteristics of the model for Mach numbers from 1.70 to 2.86 at $\beta = 0^{o}$ are presented in figure 2 and summarized in figure 3. Removing either the leading- or trailing-edge portion of a wing panel or removing the entire wing panel leads to a decrease in lift-curve slope throughout the test Mach number range. The decrease in lift coefficient for removing the leading edge or removing the entire panel is essentially proportional to the decrease in wing area, whereas removing the trailing edge of the wing panel generally causes less decrease in C_L than would be expected on the basis of wing area change alone, particularly at the higher test Mach numbers. Removal of the leading edge causes a slight increase in stability level, whereas removal of the trailing edge or an entire wing panel leads to a noticeable decrease in stability level. The general shape of the pitching-moment curves, however, remains essentially the same whether or not wing area is removed.

Removing the leading or trailing edge of a wing panel generally leads to small increases in minimum drag and decreases in maximum lift-drag ratio. Removing the entire wing panel leads to a decrease in minimum drag and a large increase in drag due to lift; therefore, the maximum lift-drag ratio is further reduced.

The effects of wing asymmetry on the longitudinal aerodynamic characteristics with sideslip are shown in figures 4 to 7 for various angles of attack at each test Mach number. There is generally little effect of sideslip angle on the longitudinal aerodynamic characteristics at positive angles of attack, other than a slight decrease in pitching-moment coefficient as sideslip varies from negative to moderate positive angles for the trailing-edge-off and panel-off configurations.

Lateral-Directional Aerodynamic Characteristics

The variation of lateral-directional aerodynamic coefficients with lift coefficient for the various test configurations for $\beta = 0^{o}$ is shown in figure 8. As might be expected from the effect on C_L, a positive rolling moment essentially proportional to the decrease in wing area is incurred by removal of the leading edge or removal of the entire wing panel. At the lower Mach numbers, removal of the trailing edge causes a rolling moment slightly larger than that caused by removal of the leading edge. At the higher Mach numbers, however, the effect on rolling moment due to removal of the trailing edge is less than that caused by removal of the leading edge even though a larger area of the wing is removed. An initial increment of negative C_Y occurs as portions of the right wing panel are removed, resulting in an increase in positive C_n. However,

when the entire wing panel is removed and as lift is increased, a progressive increase in negative C_n occurs. The negative C_n is apparently related to an increase in positive side force induced at the tail as well as to the increased induced drag provided by the left wing panel.

Lateral data in sideslip are presented in figures 9 to 12 for the test configurations at various angles of attack. At an angle of attack of 0^o, there is little or no difference in the lateral or directional stability due to removing part or all of the wing panel. There is, however, a shift in β of as much as 3^o for trim rolling moment for the wing panel off as compared with that for the basic model.

With increasing angle of attack, the predominant problem that occurs is the shift in rolling moment due to the wing asymmetry. At $M = 1.70$ (fig. 9), the rolling moment induced by removal of either the leading edge or trailing edge at $\alpha = 5^o$ can be compensated with a sideslip angle of between 2^o and 3^o. The sideslip angle required to balance this roll asymmetry increases to about 4.5^o at $\alpha = 10^o$ and 7.5^o at $\alpha = 17^o$. With the entire wing panel removed, roll trim could not be achieved within the sideslip limit of 10^o for angles of attack of 5^o and above. An interpolation of the data indicates that the panel-off configuration at $M = 1.70$ could be trimmed in roll within a sideslip range of about 5^o for angles of attack up to about 2^o. Thus it appears that the roll induced by wing asymmetry could be offset by sideslip within reasonable limits of angle of attack and sideslip when only the leading- or trailing-edge portion of the wing is removed but not when the entire wing panel is removed. Trimming the model in yaw does not appear to be a serious problem at angles of attack to 10^o for any of the configurations since a C_n of only about 0.005 need be obtained.

CONCLUSIONS

An investigation at Mach numbers from 1.70 to 2.86 to determine the effects of simulated wing damage on the aerodynamic characteristics of a swept-wing—body—vertical-tail configuration indicated the following conclusions:

1. Removing the leading- or trailing-edge portion of one wing panel or removing the entire wing panel led to a decrease in both lift-curve slope and maximum lift-drag ratio.

2. At the lower Mach numbers, removal of the trailing edge caused a rolling moment slightly larger than that caused by removal of the leading edge. At the higher Mach numbers, however, the effect on rolling moment due to removal of the trailing edge was less than that caused by removal of the leading edge even though a larger area of the wing was removed.

3. Except when the entire wing panel was removed, the roll induced by wing asymmetry could be offset by sideslip within reasonable limits of angle of attack and sideslip.

Langley Research Center,
National Aeronautics and Space Administration,
Langley Station, Hampton, Va., December 26, 1967,
126-13-02-04-23.

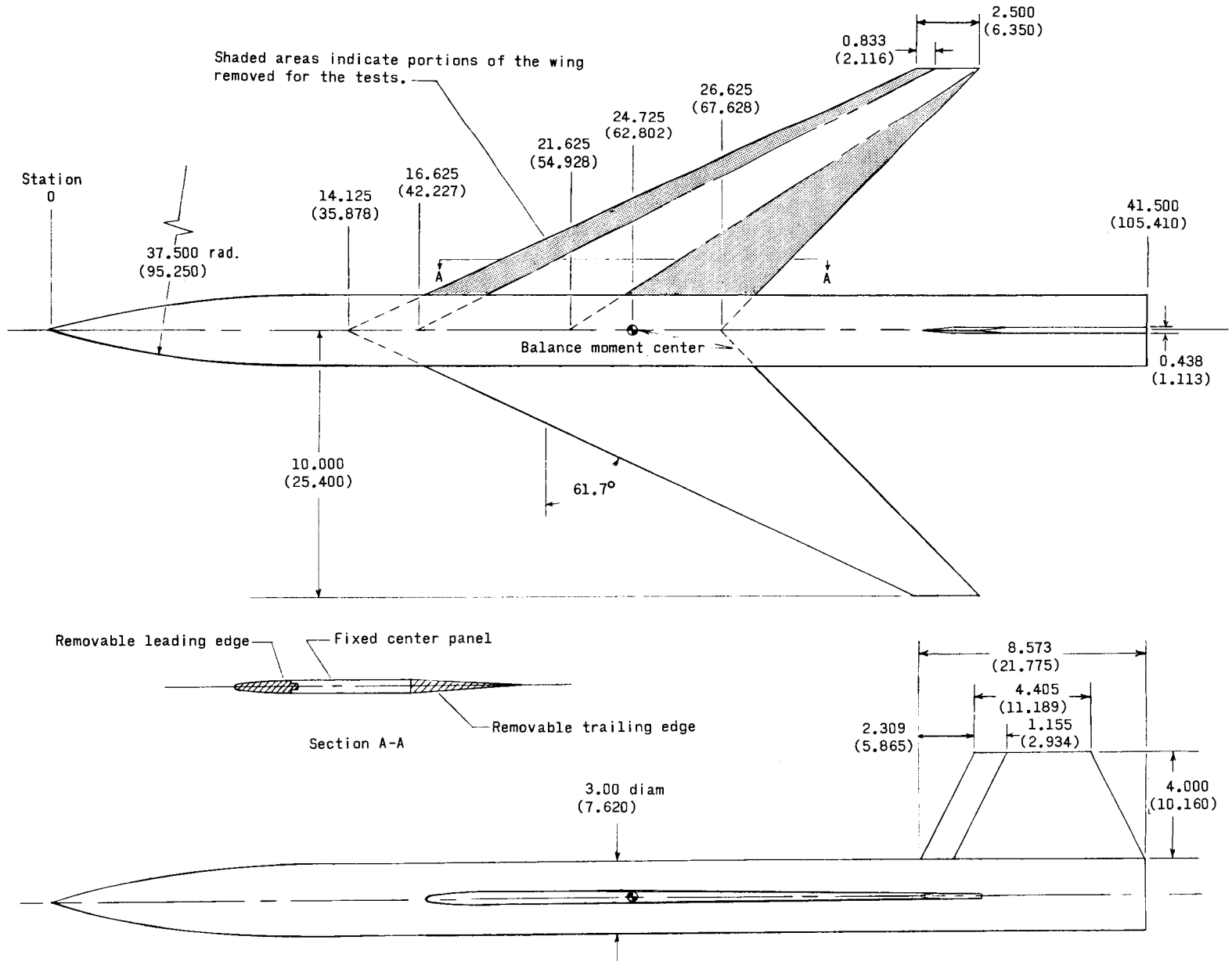

Figure 1.- Details of model. (All dimensions are given in inches and parenthetically in centimeters.)

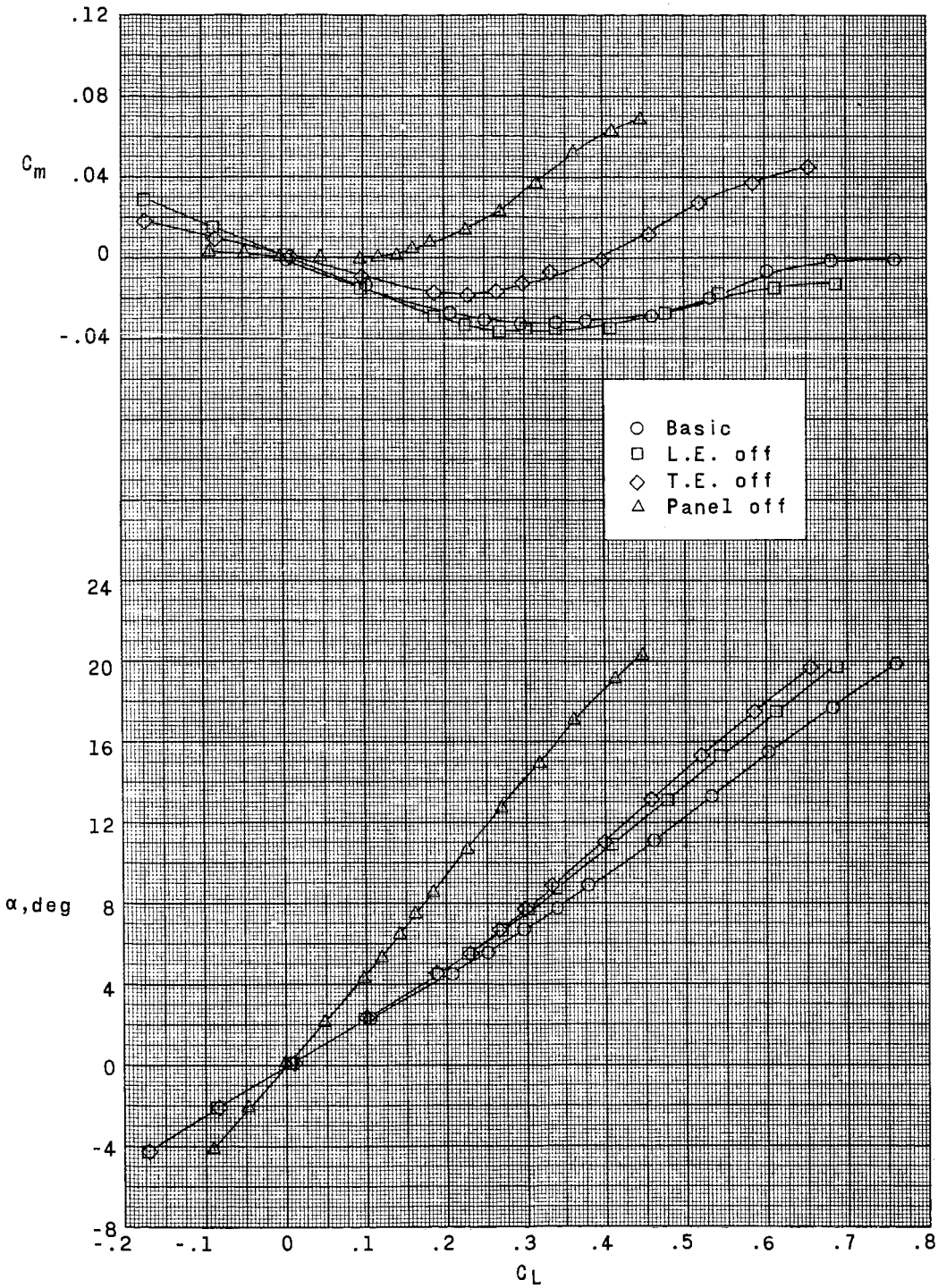

(a) M = 1.70.

Figure 2.- Effect of wing asymmetry on the longitudinal aerodynamic characteristics. $\beta = 0^{o}$.

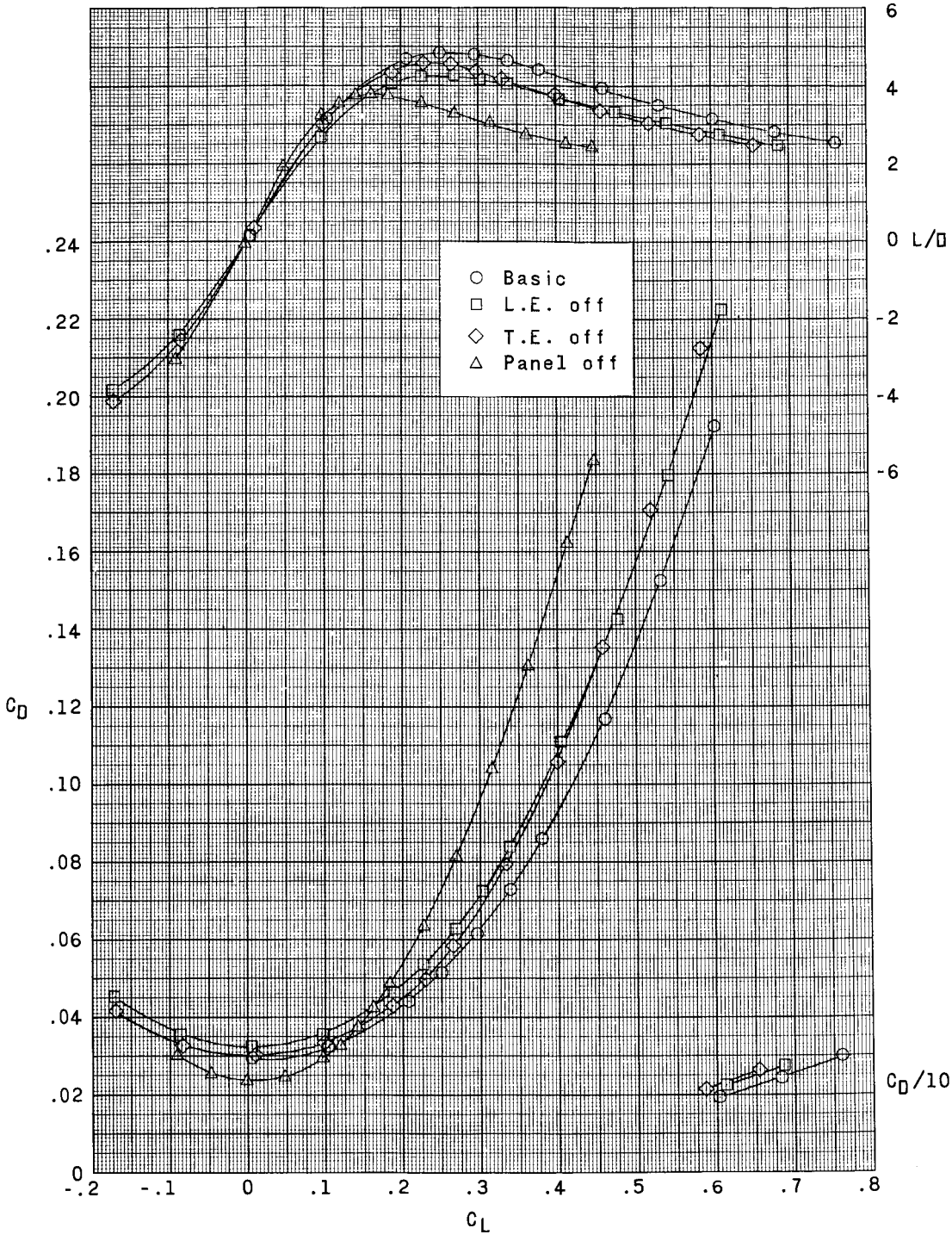

(a) Concluded.

Figure 2.- Continued.

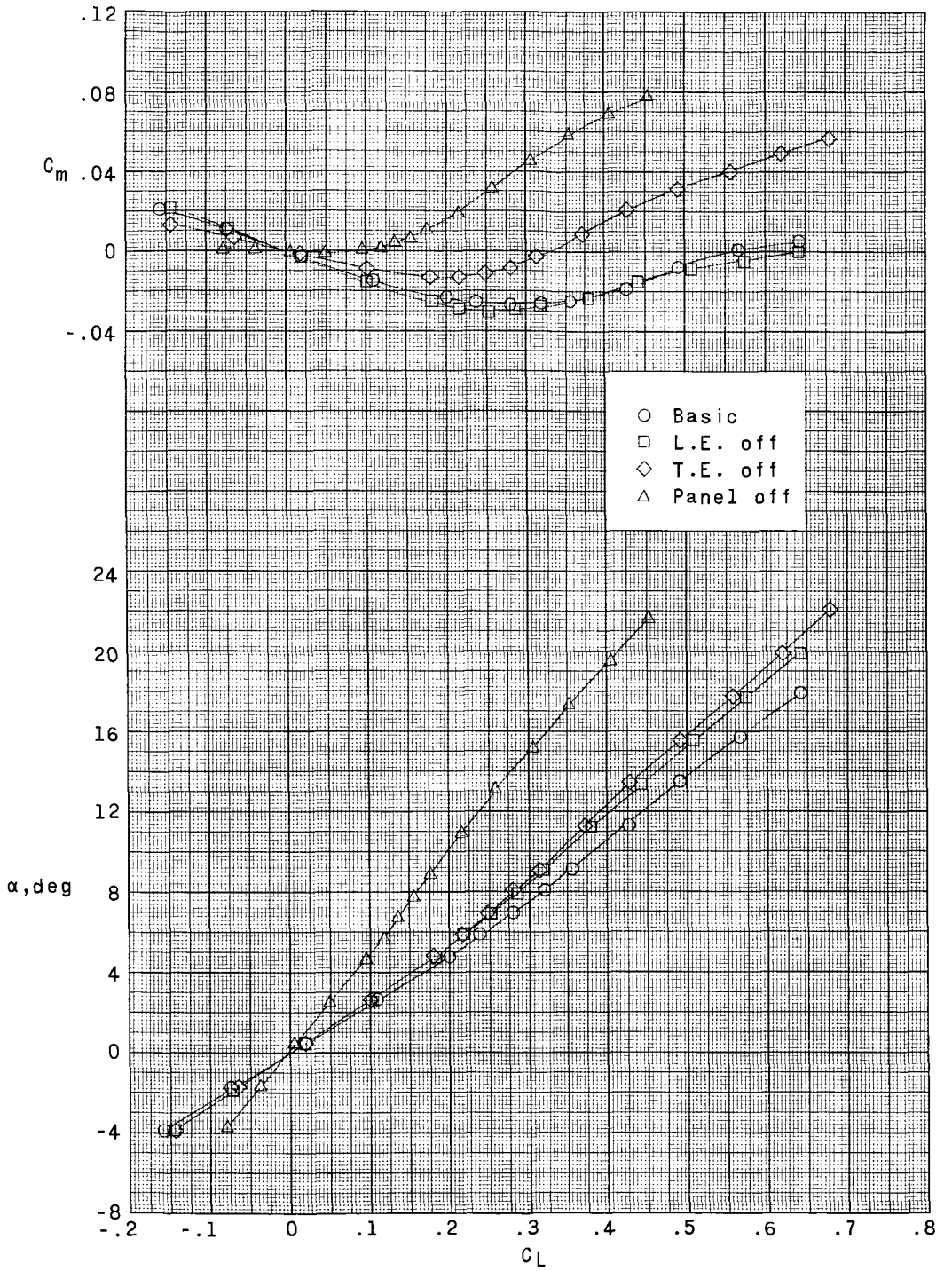

(b) M = 1.90.

Figure 2.- Continued.

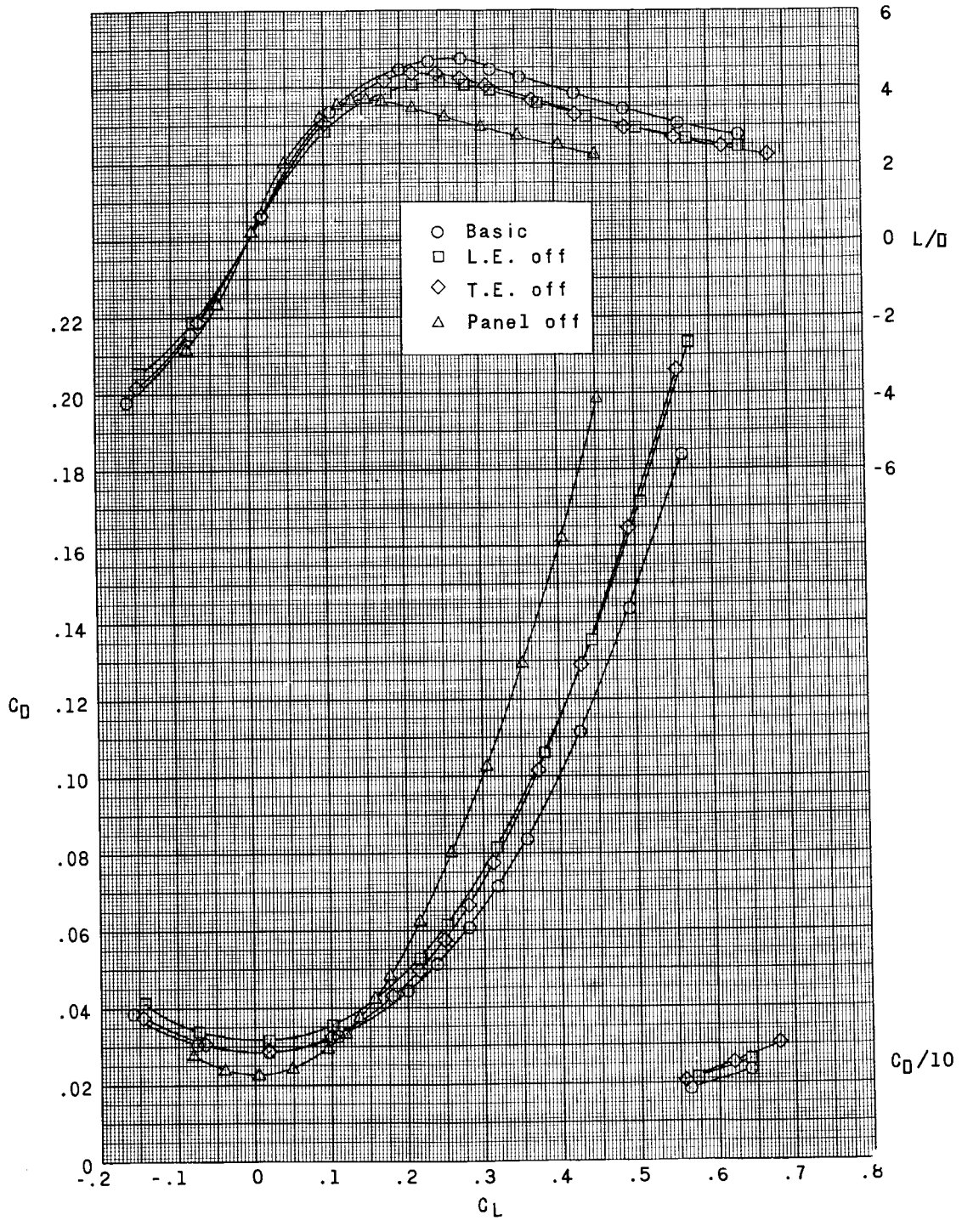

(b) Concluded.

Figure 2.- Continued.

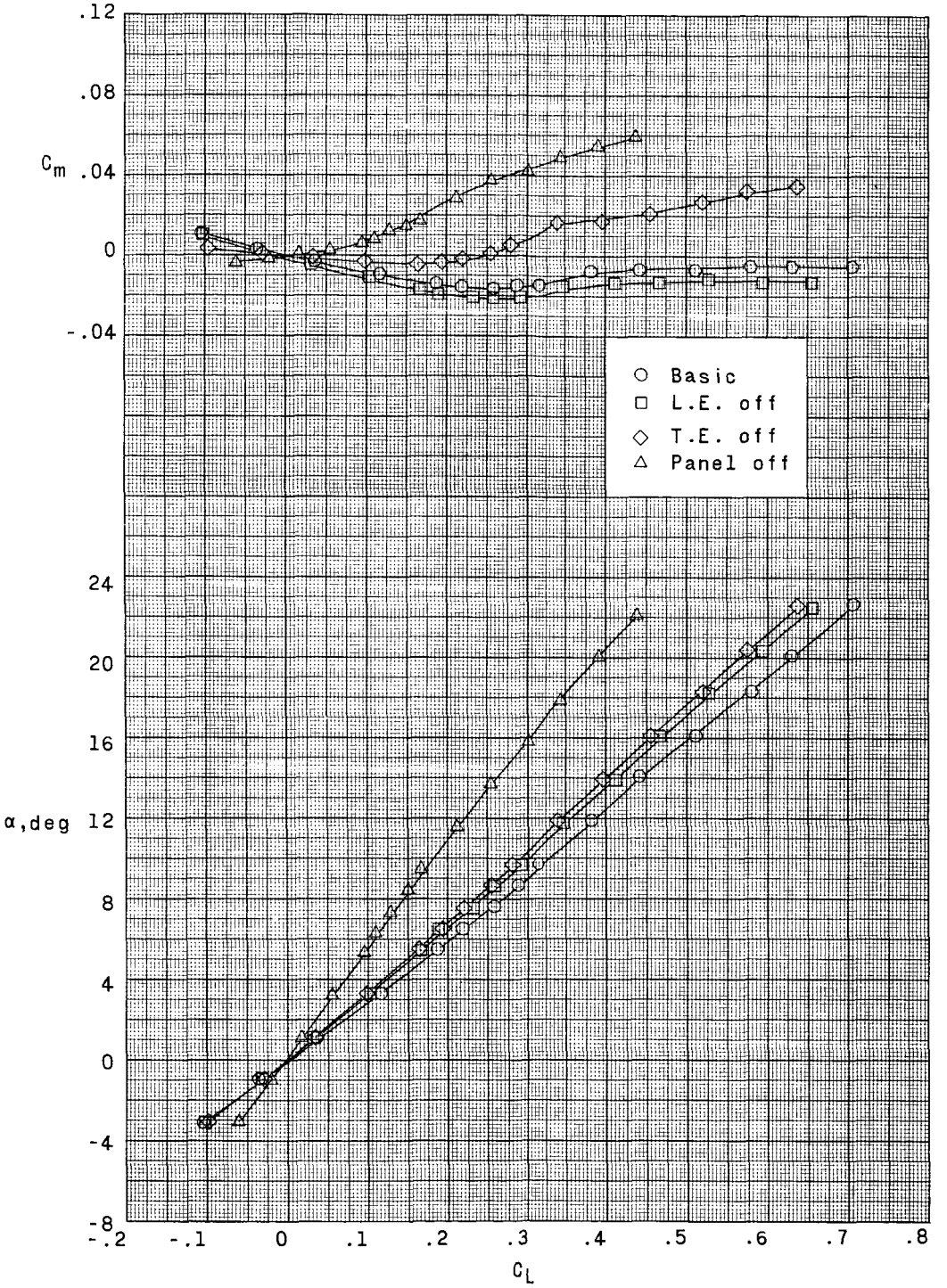

(c) M = 2.36.

Figure 2.- Continued.

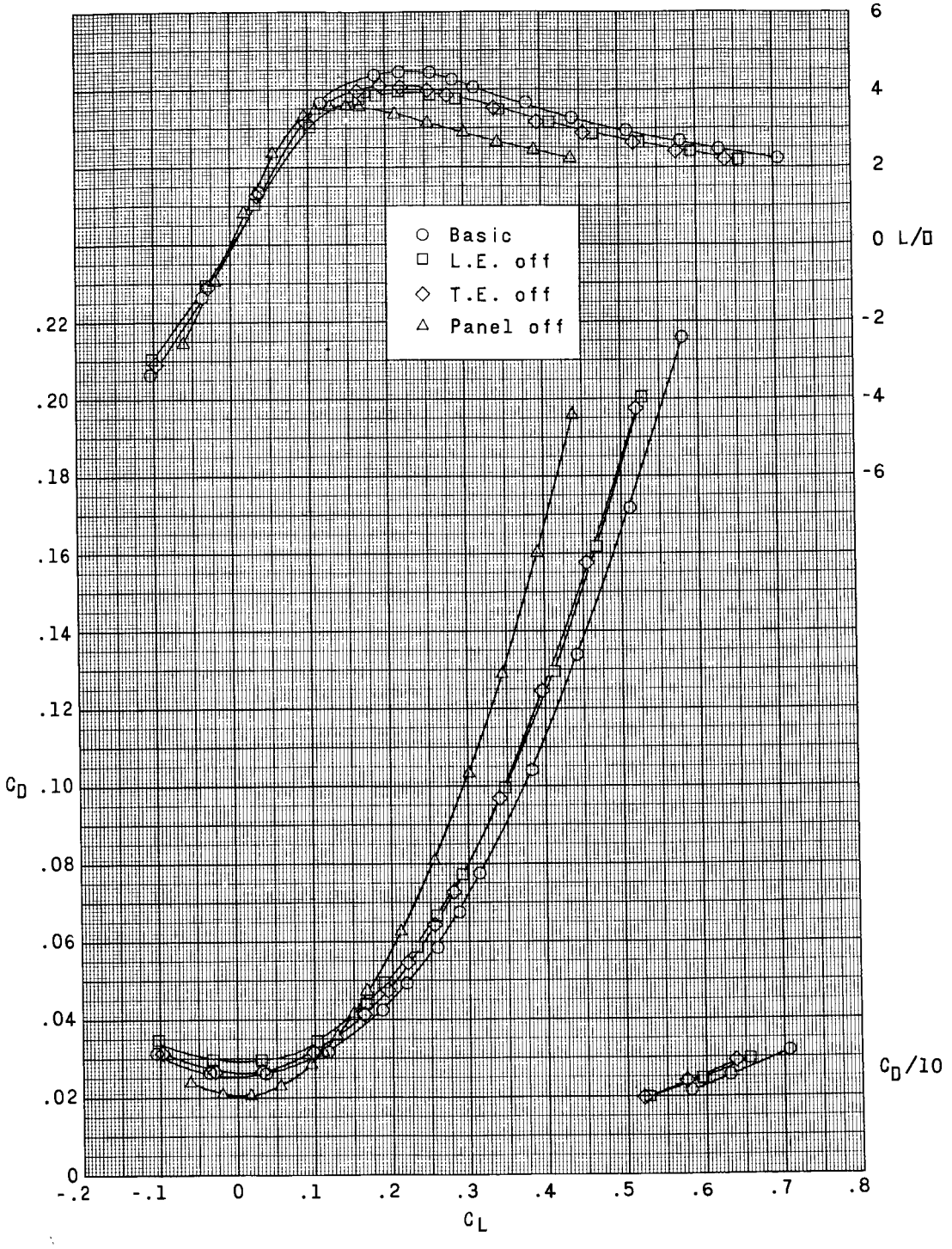

(c) Concluded.

Figure 2.- Continued.

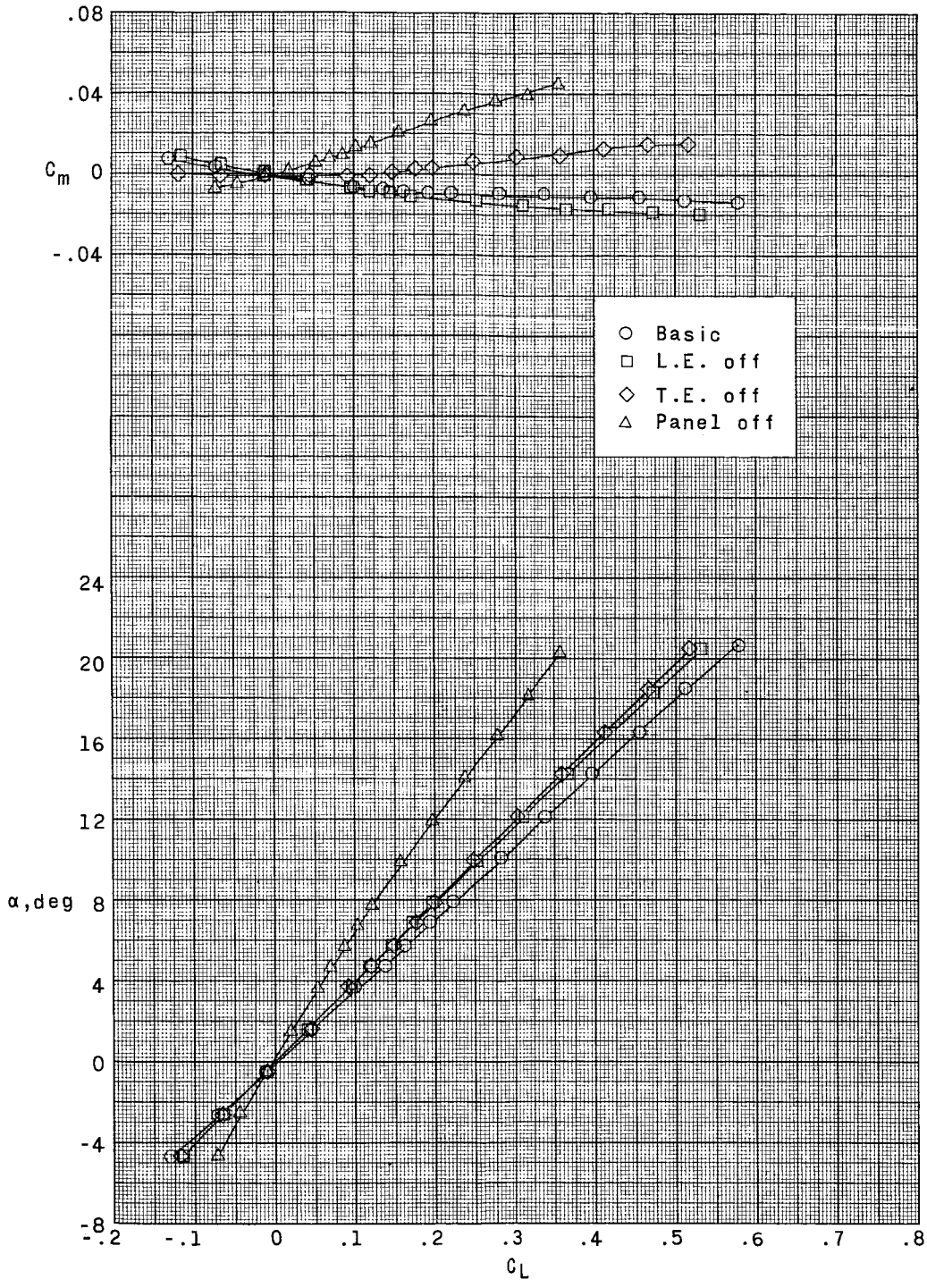

(d) M = 2.86.

Figure 2.- Continued.

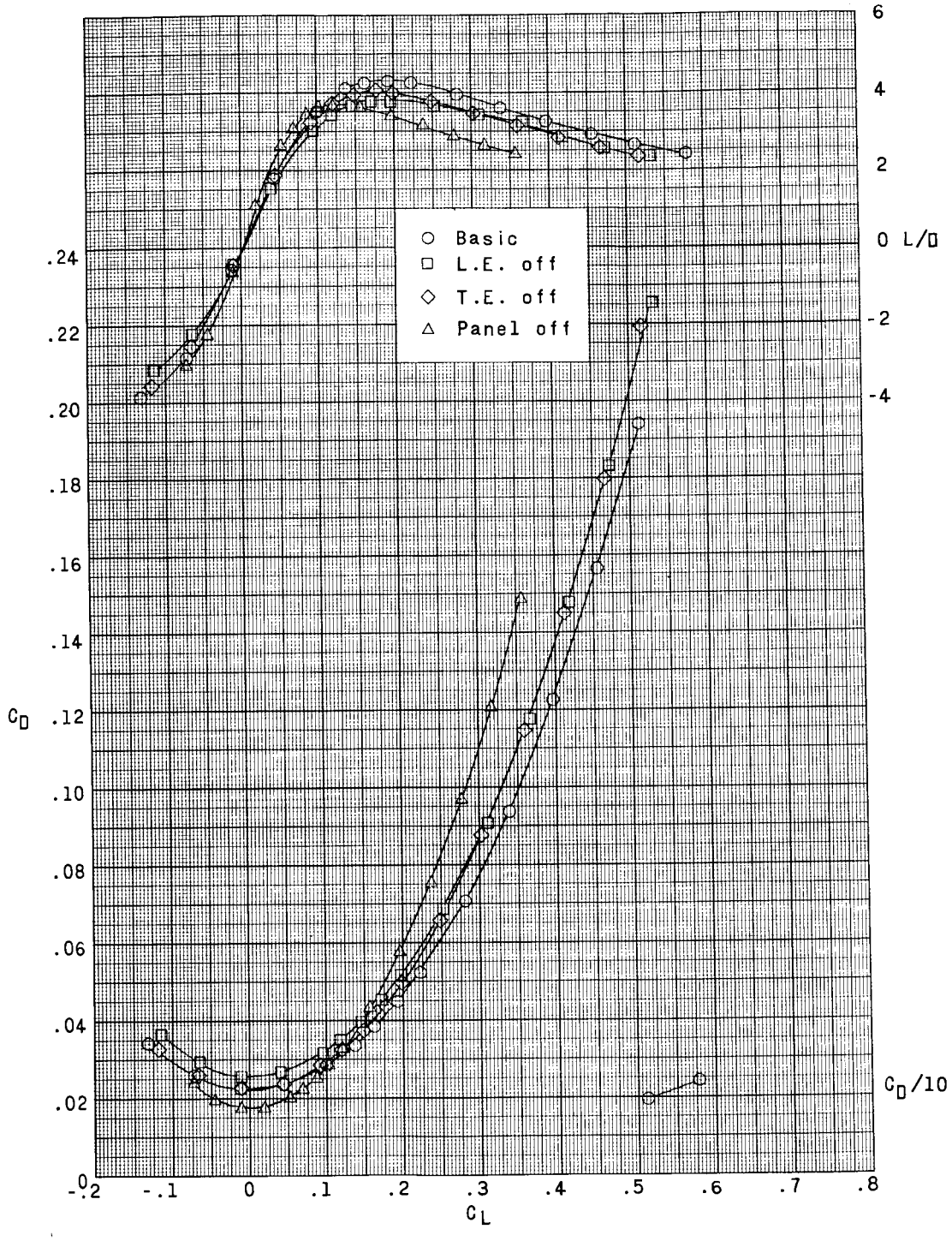

(d) Concluded.

Figure 2.- Concluded.

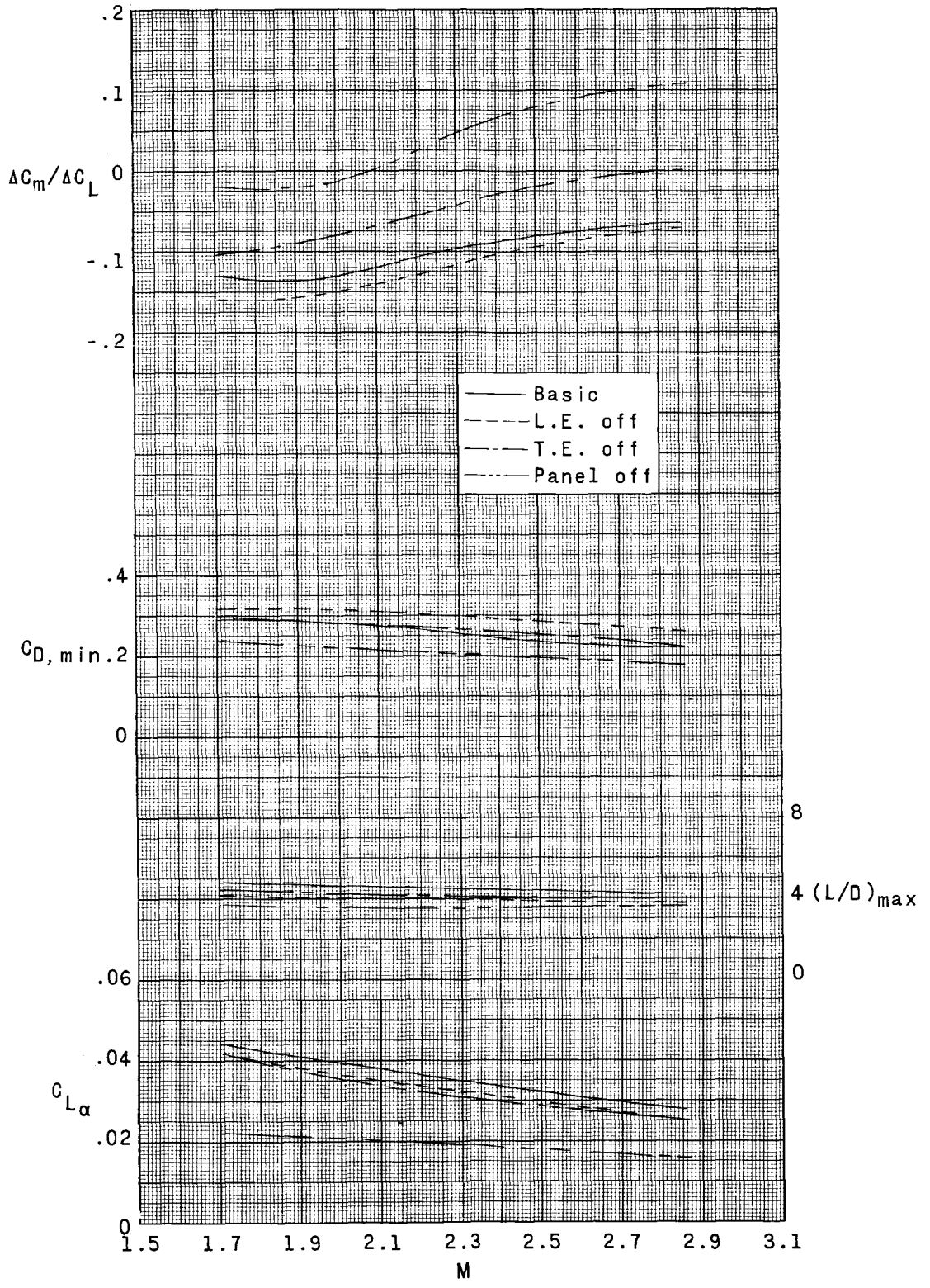

Figure 3.- Variation of the longitudinal aerodynamic characteristics with Mach number. $\beta = 0^0$.

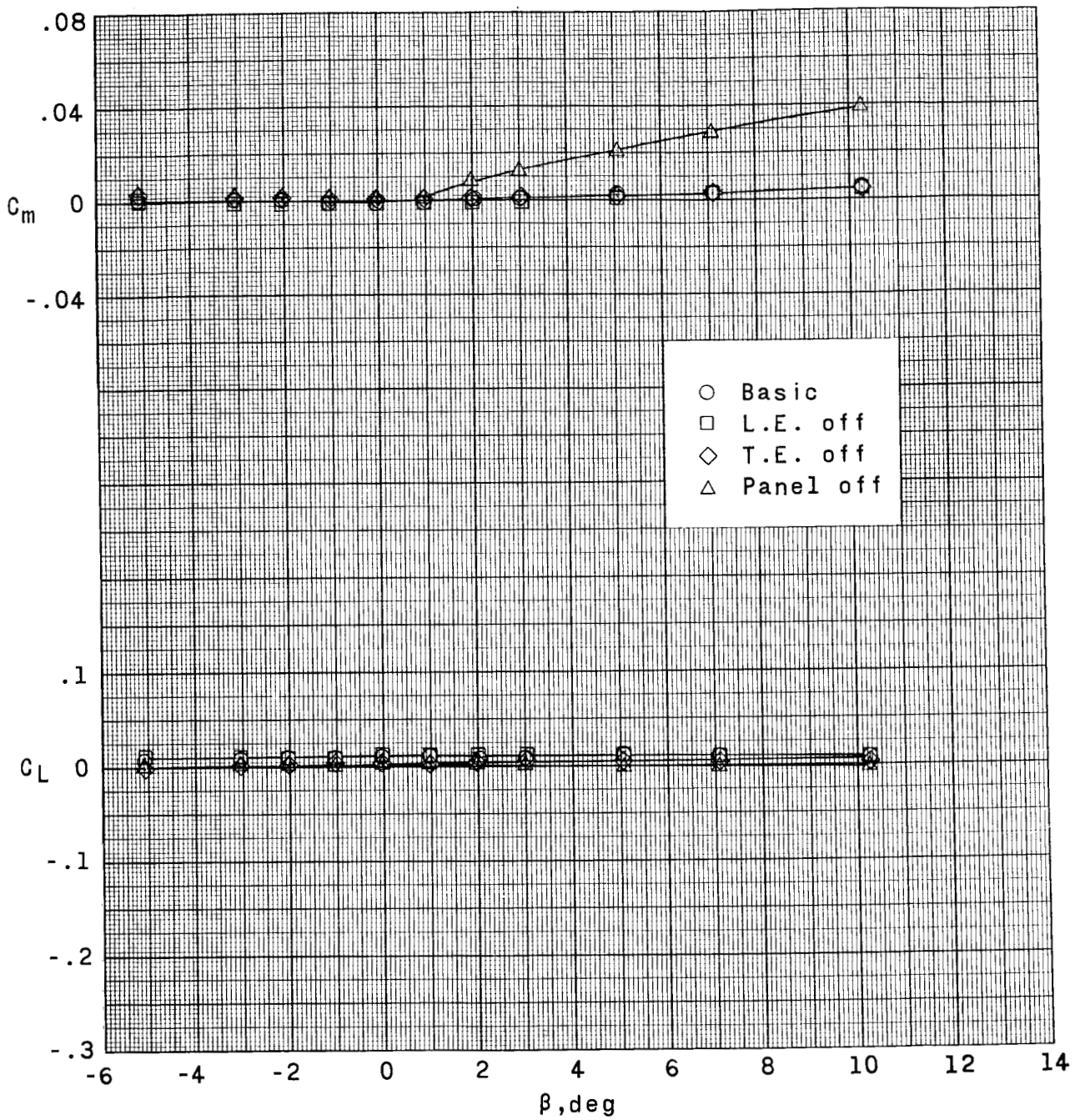

(a) $\alpha = 0^0$.

Figure 4.- Effect of wing asymmetry on the longitudinal aerodynamic characteristics with sideslip. M = 1.70.

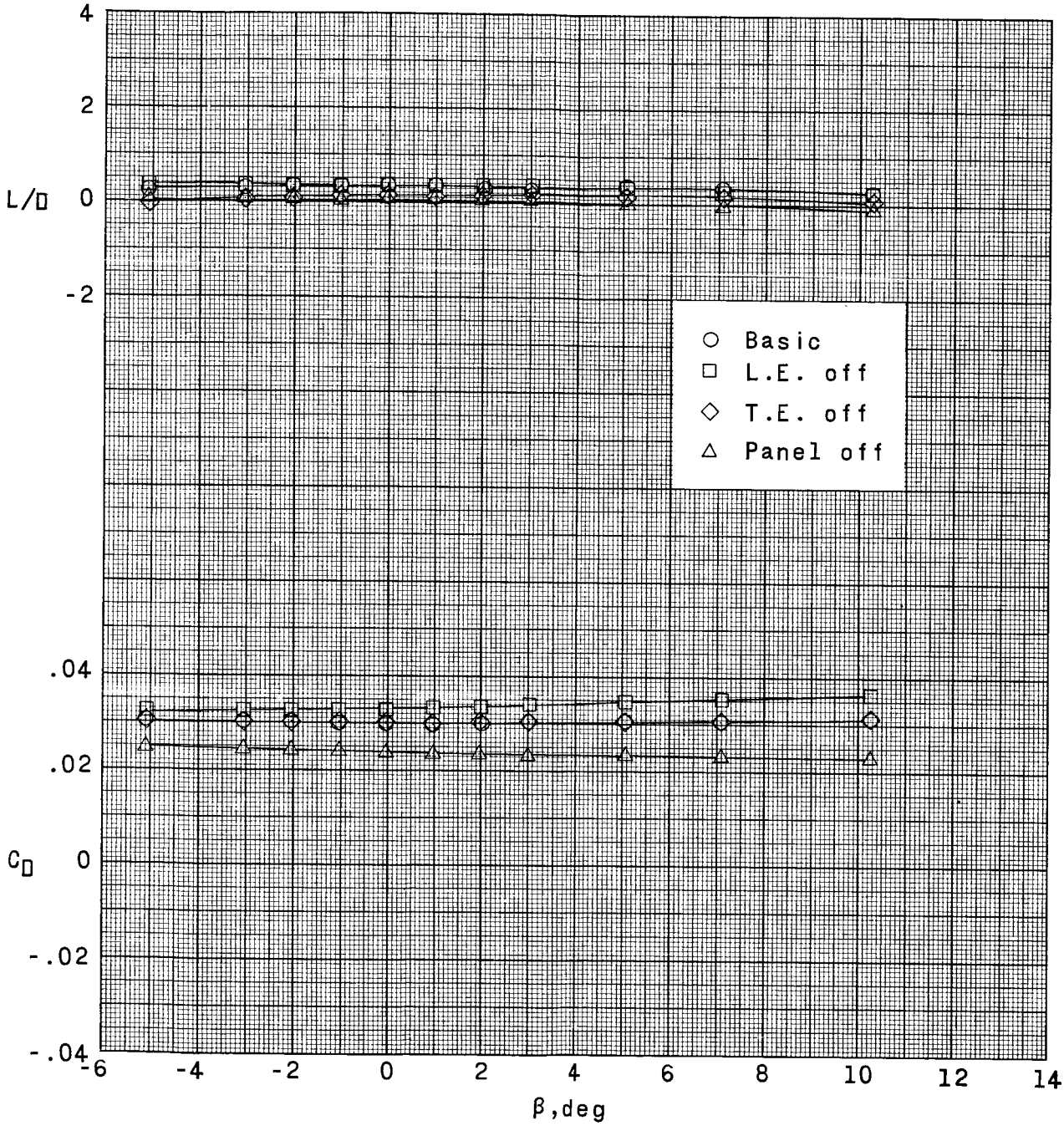

(a) Concluded.

Figure 4.- Continued.

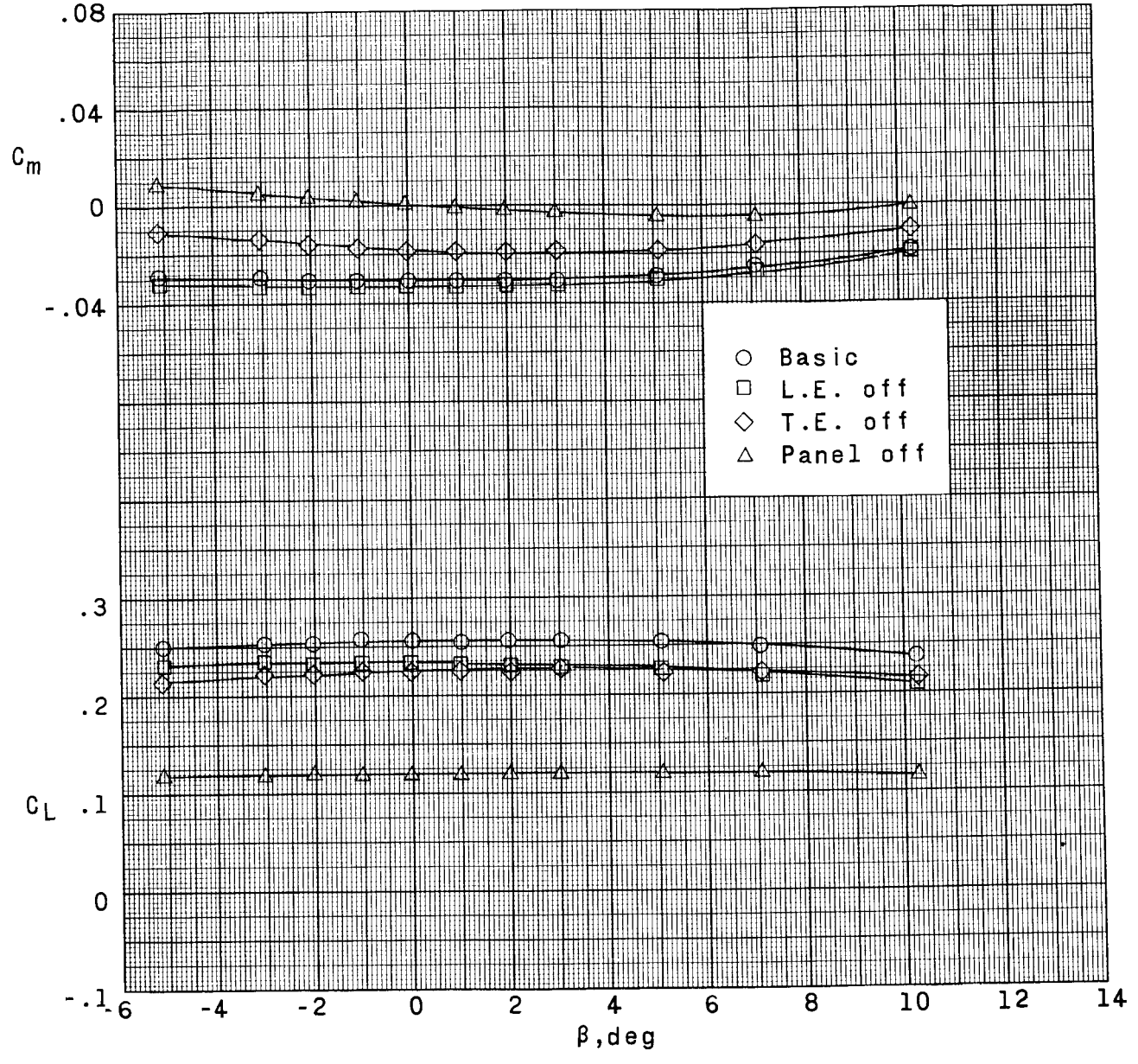

(b) $\alpha = 5.6^0$.

Figure 4.- Continued.

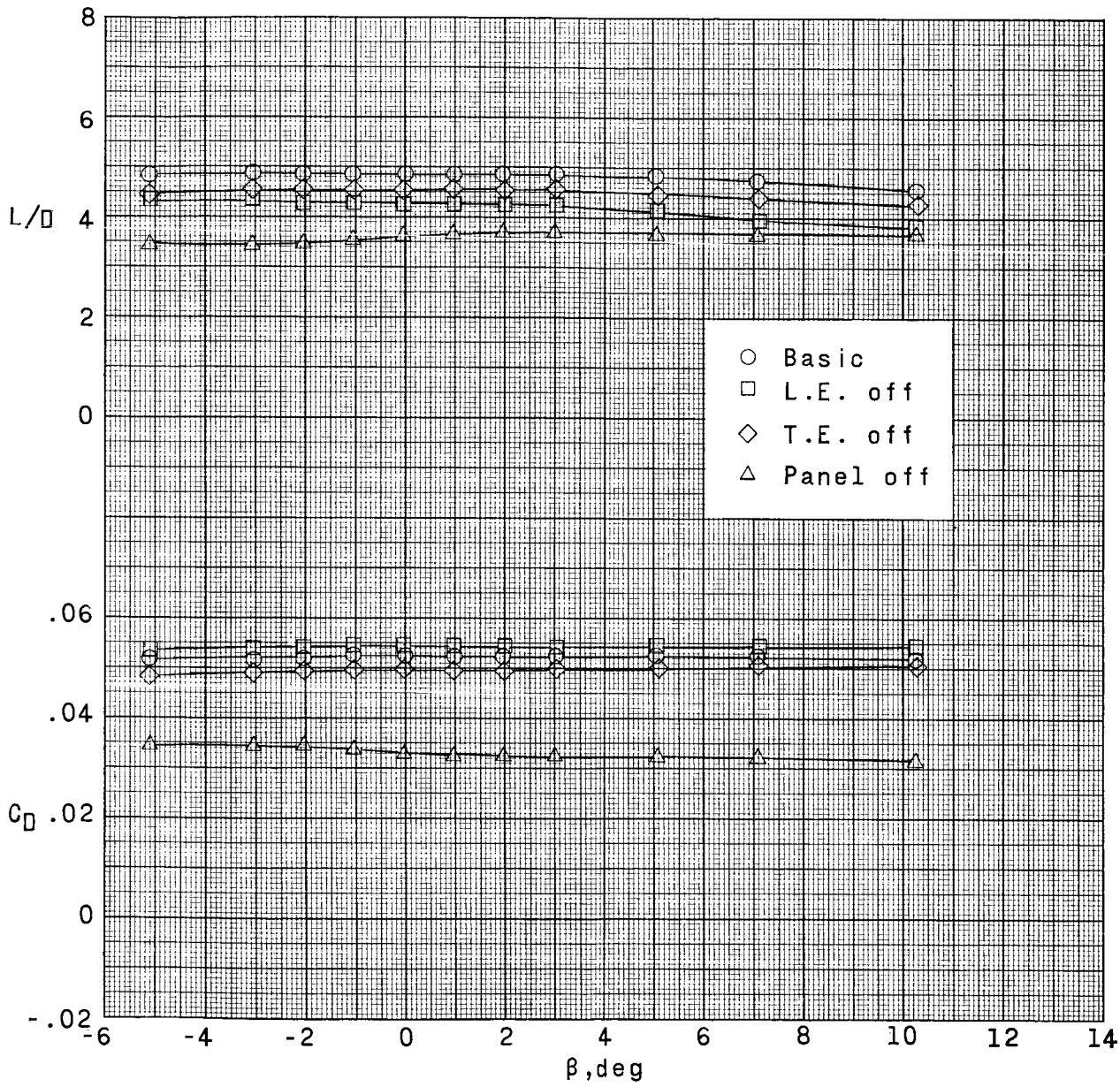

(b) Concluded.

Figure 4.- Continued.

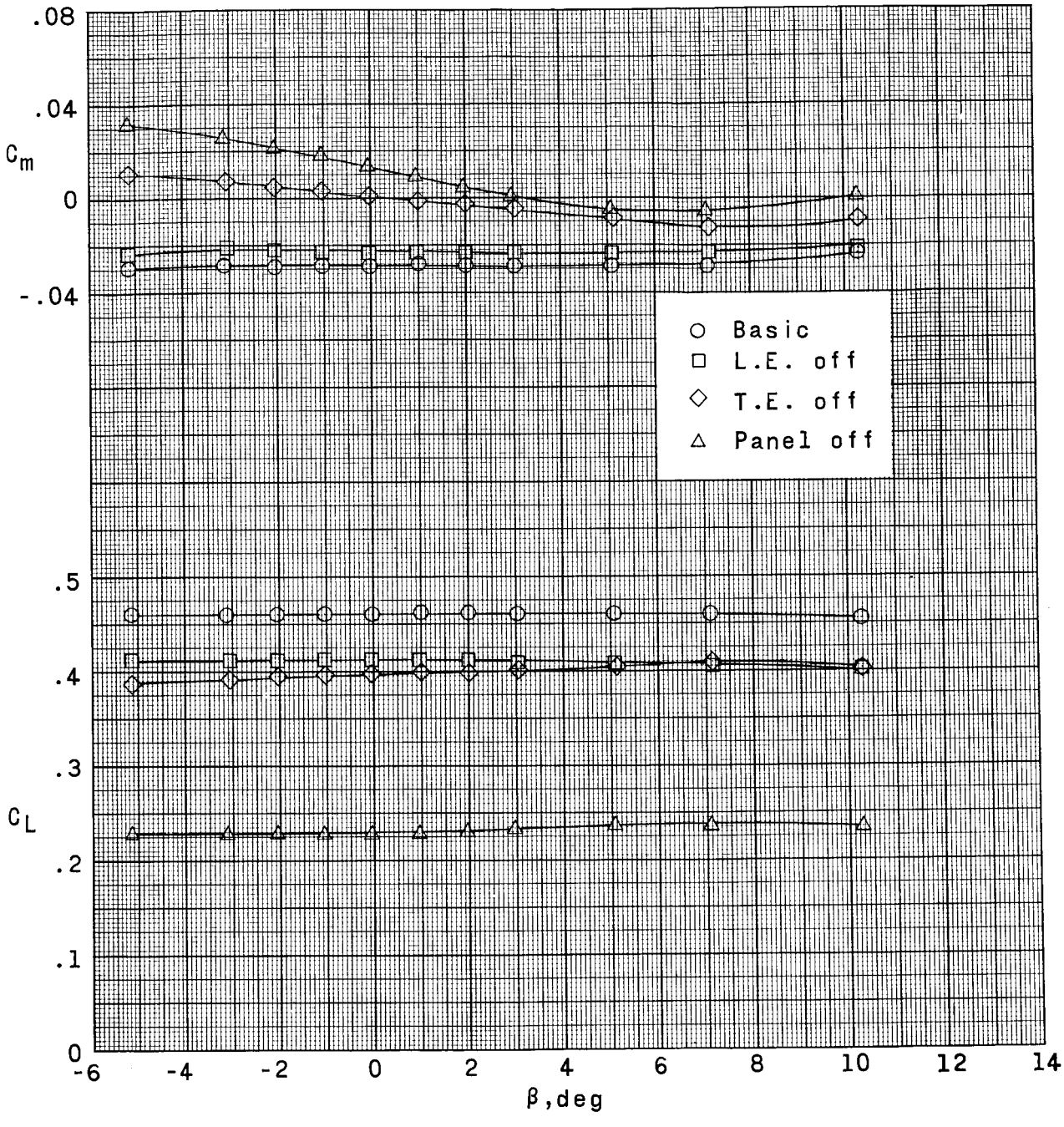

(c) $\alpha = 11.1^{0}$.

Figure 4.- Continued.

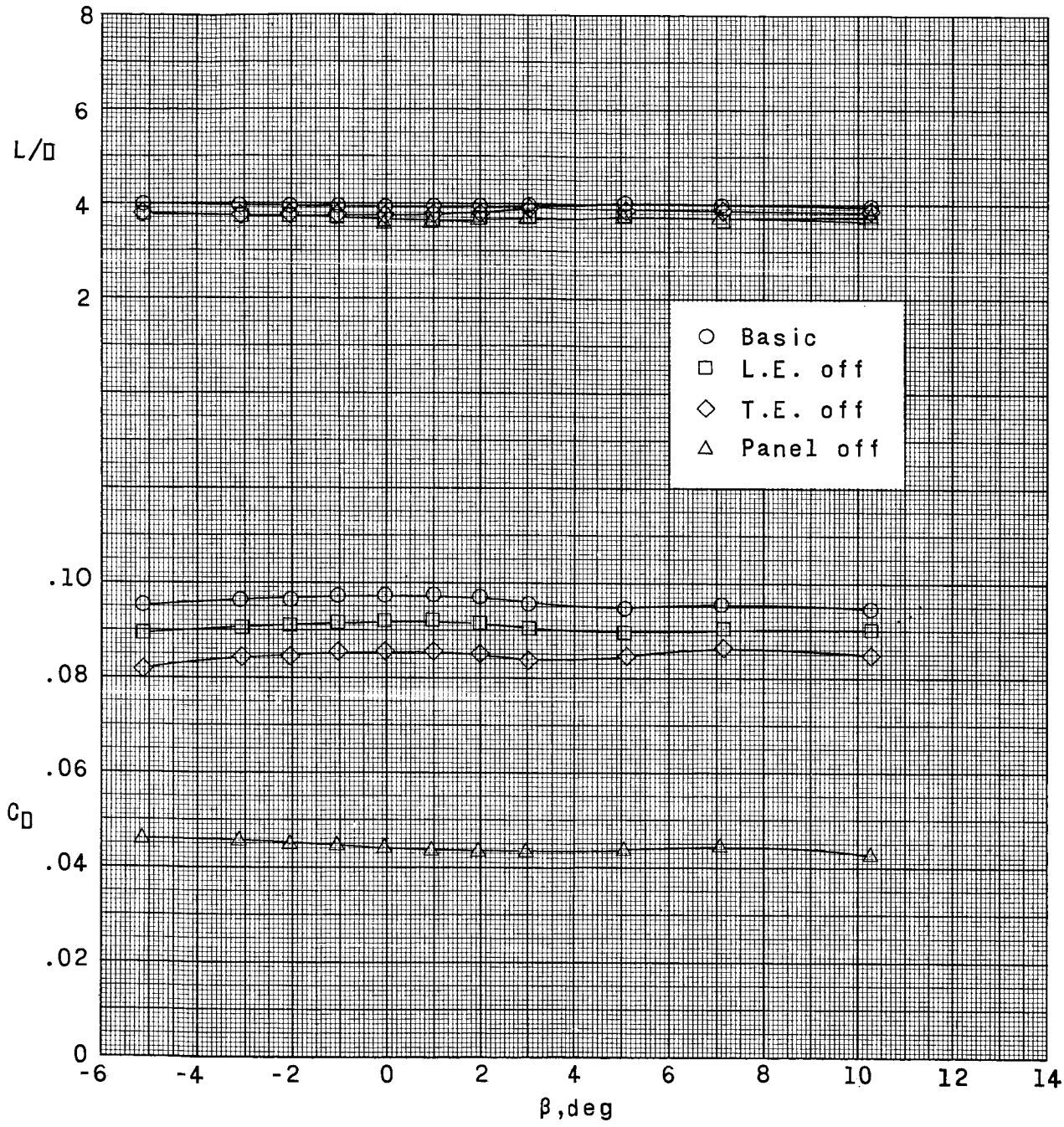

(c) Concluded.

Figure 4.- Continued.

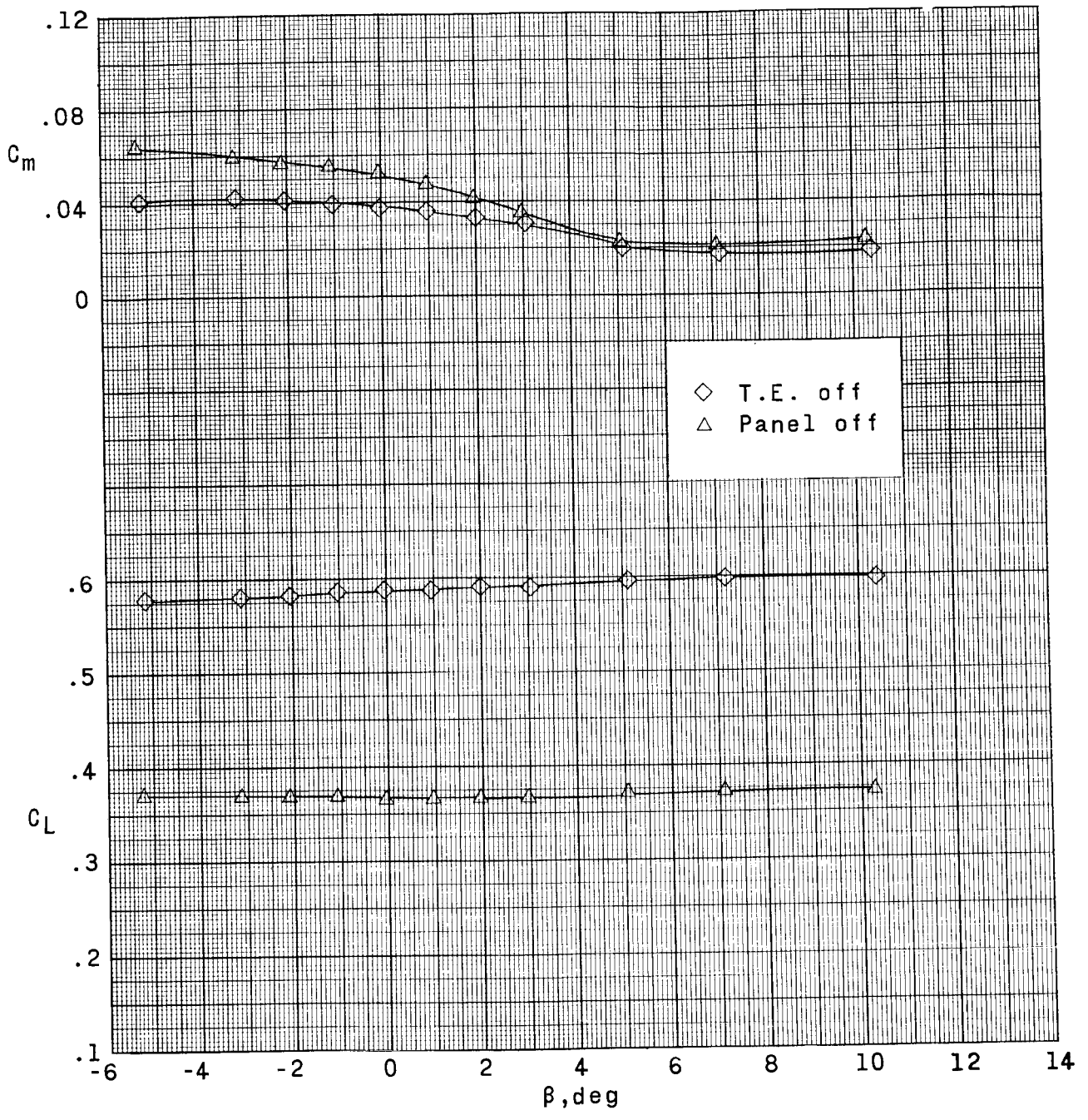

(d) $\alpha = 17.3^{0}$.

Figure 4.- Continued.

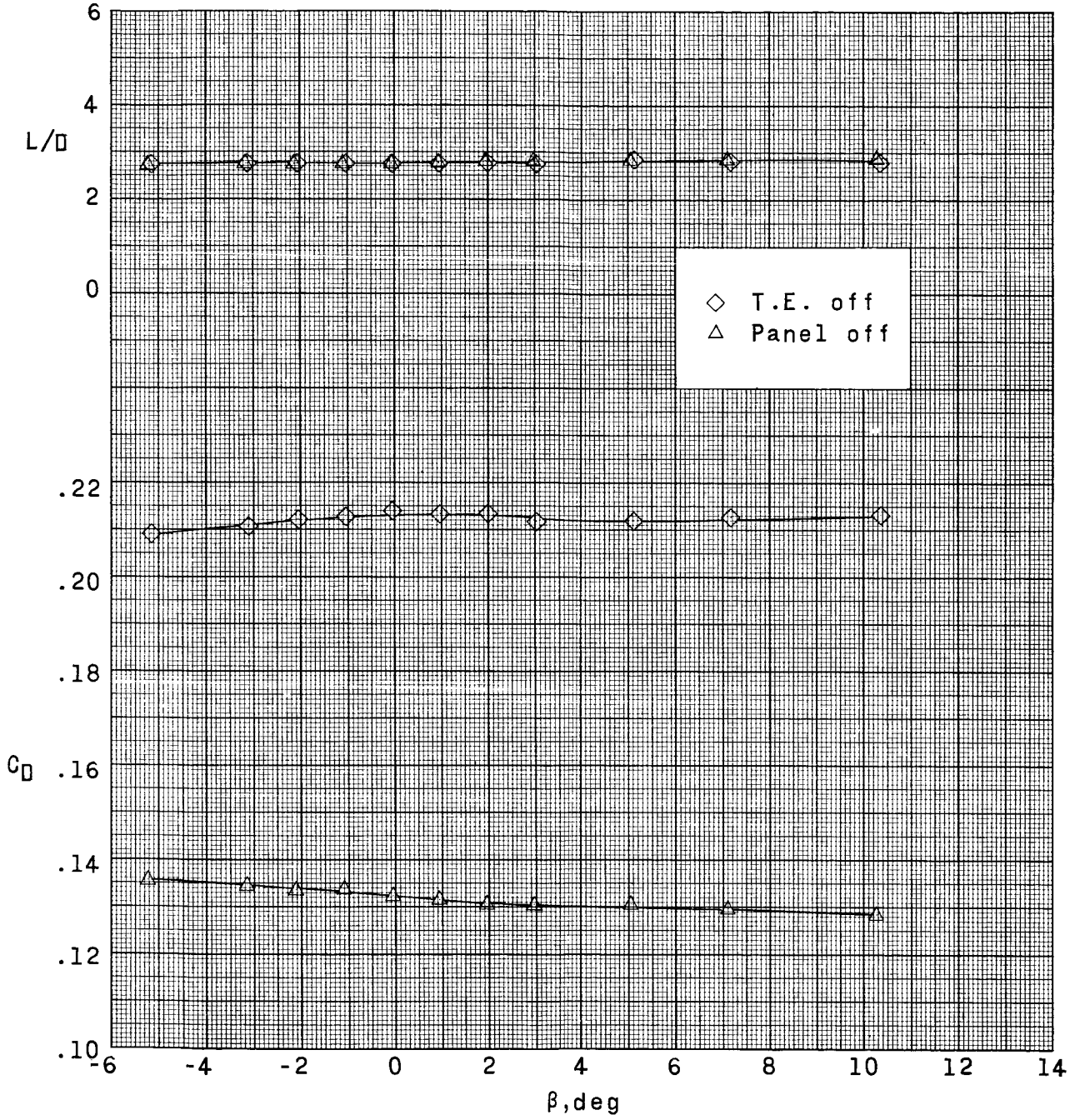

(d) Concluded.

Figure 4.- Concluded.

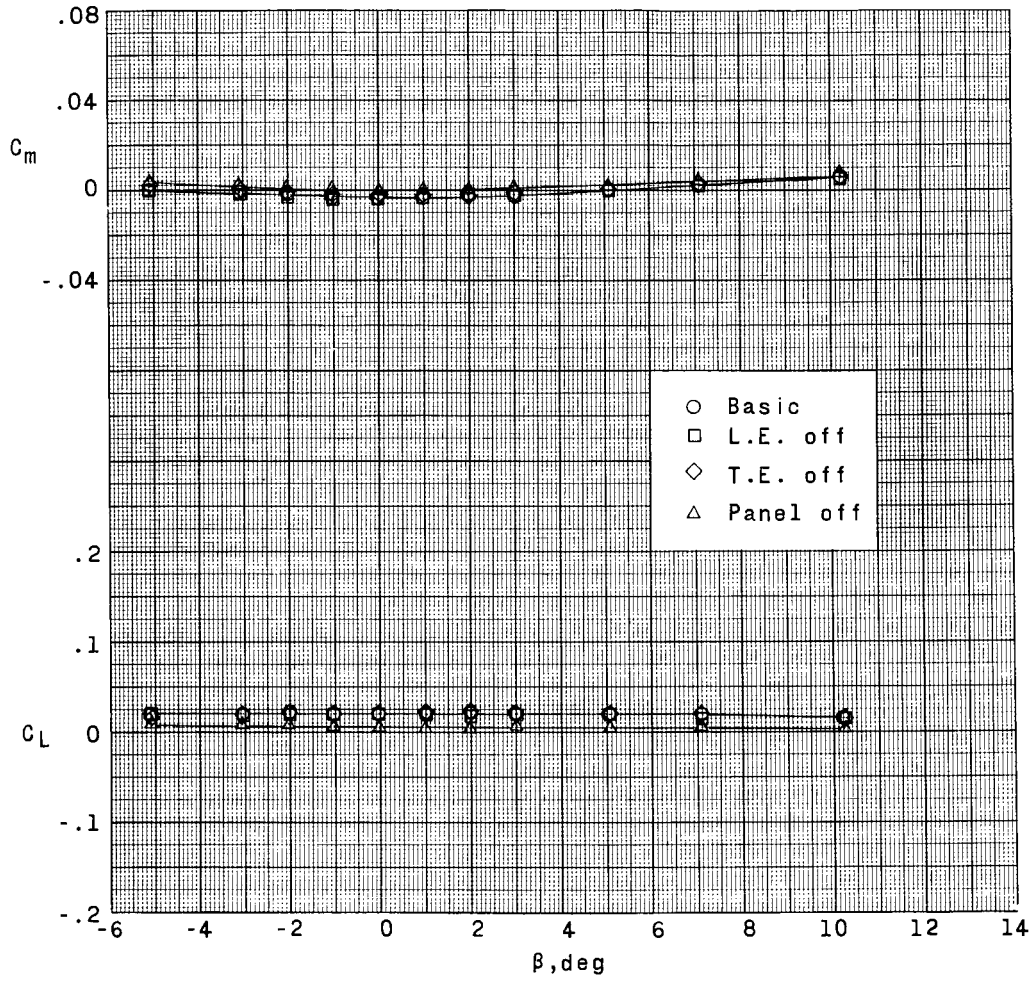

(a) $\alpha = 0.4^{o}$.

Figure 5.- Effect of wing asymmetry on the longitudinal aerodynamic characteristics with sideslip. M = 1.90.

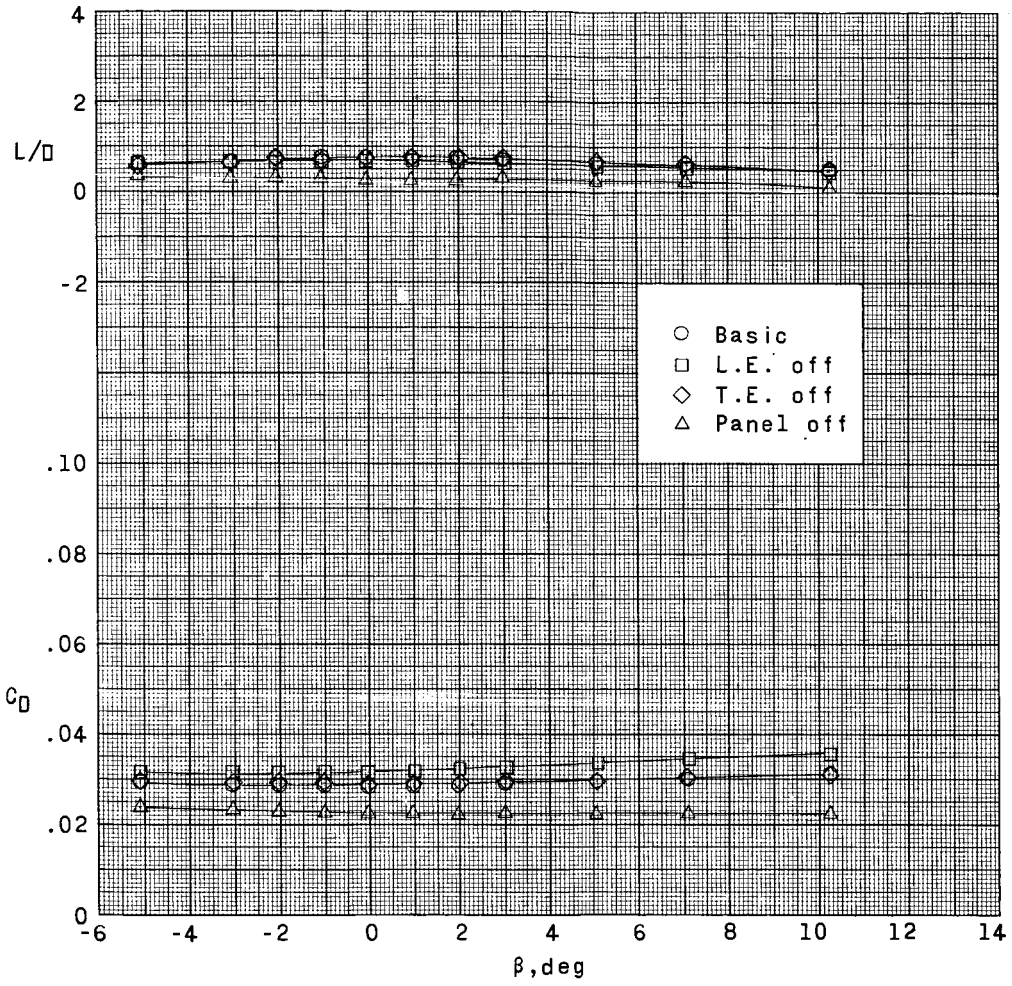

(a) Concluded.

Figure 5.- Continued.

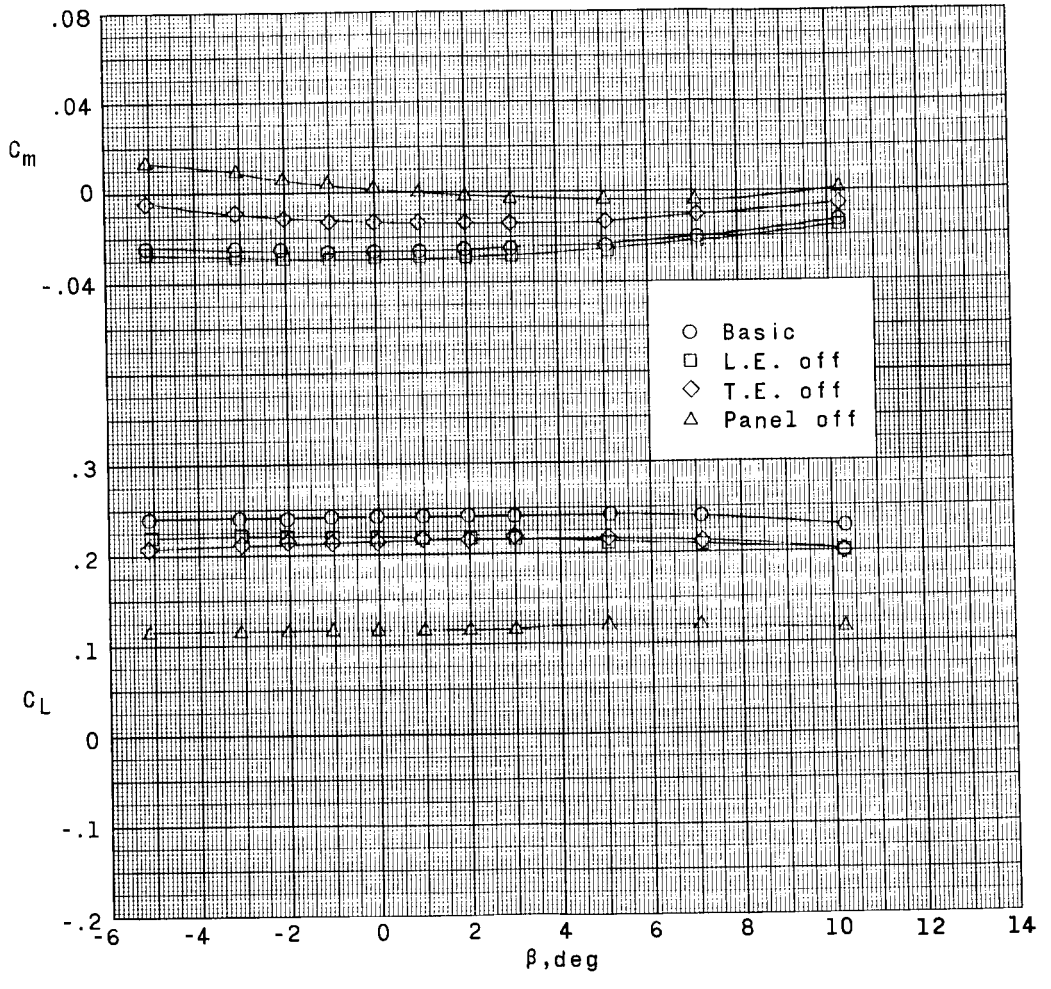

(b) $\alpha = 5.8^0$.

Figure 5.- Continued.

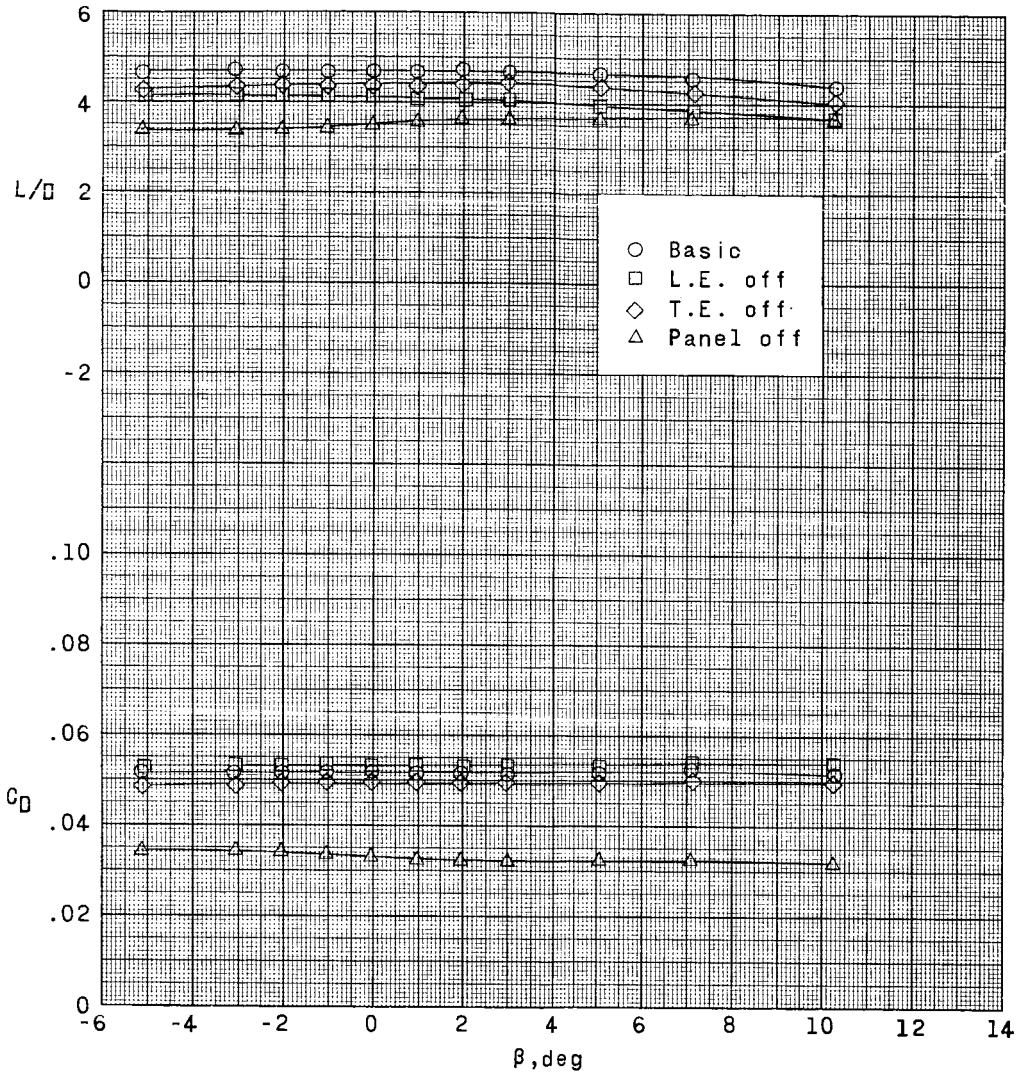

(b) Concluded.

Figure 5.- Continued.

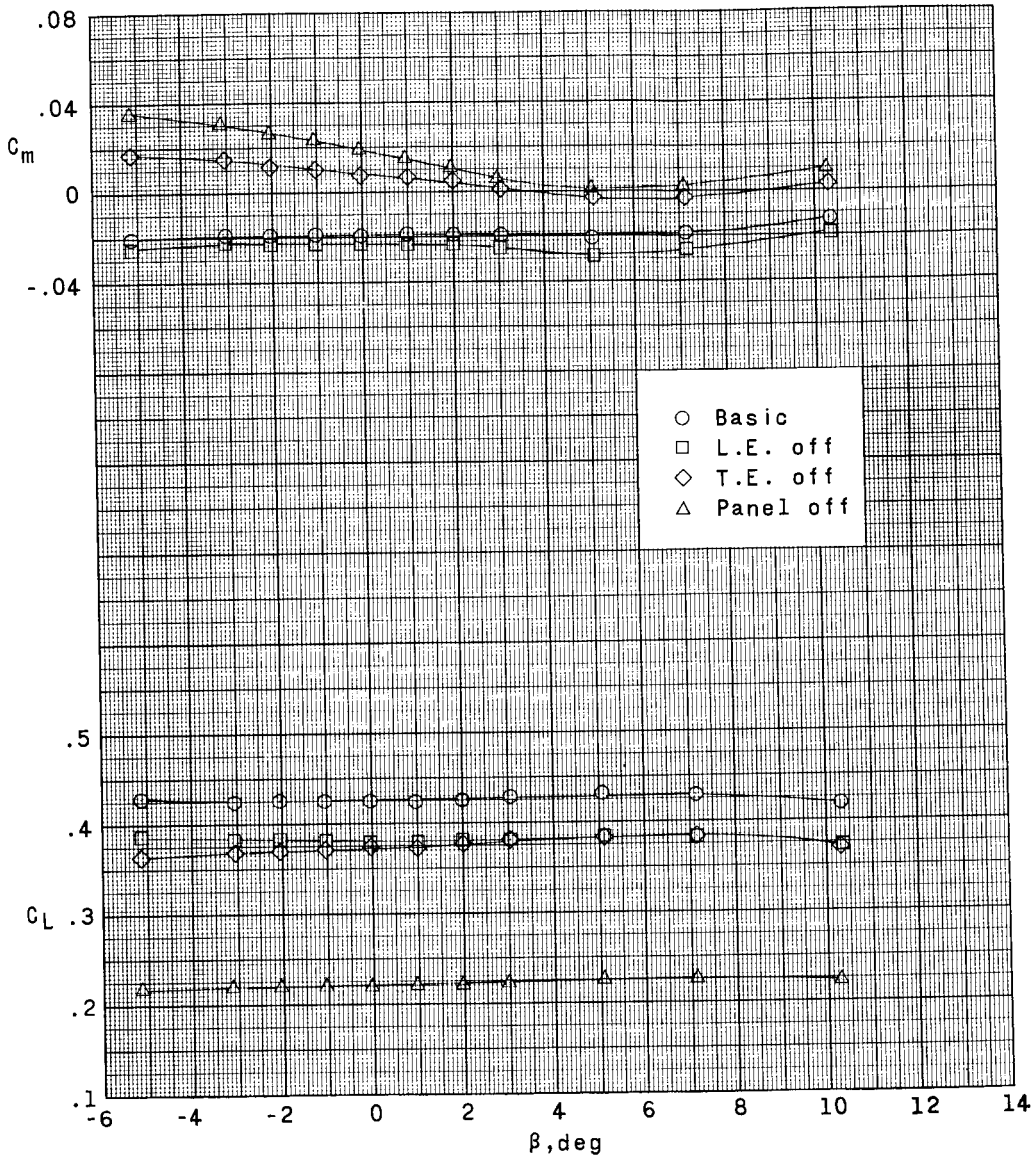

(c) $\alpha = 11.2^{o}$.

Figure 5.- Continued.

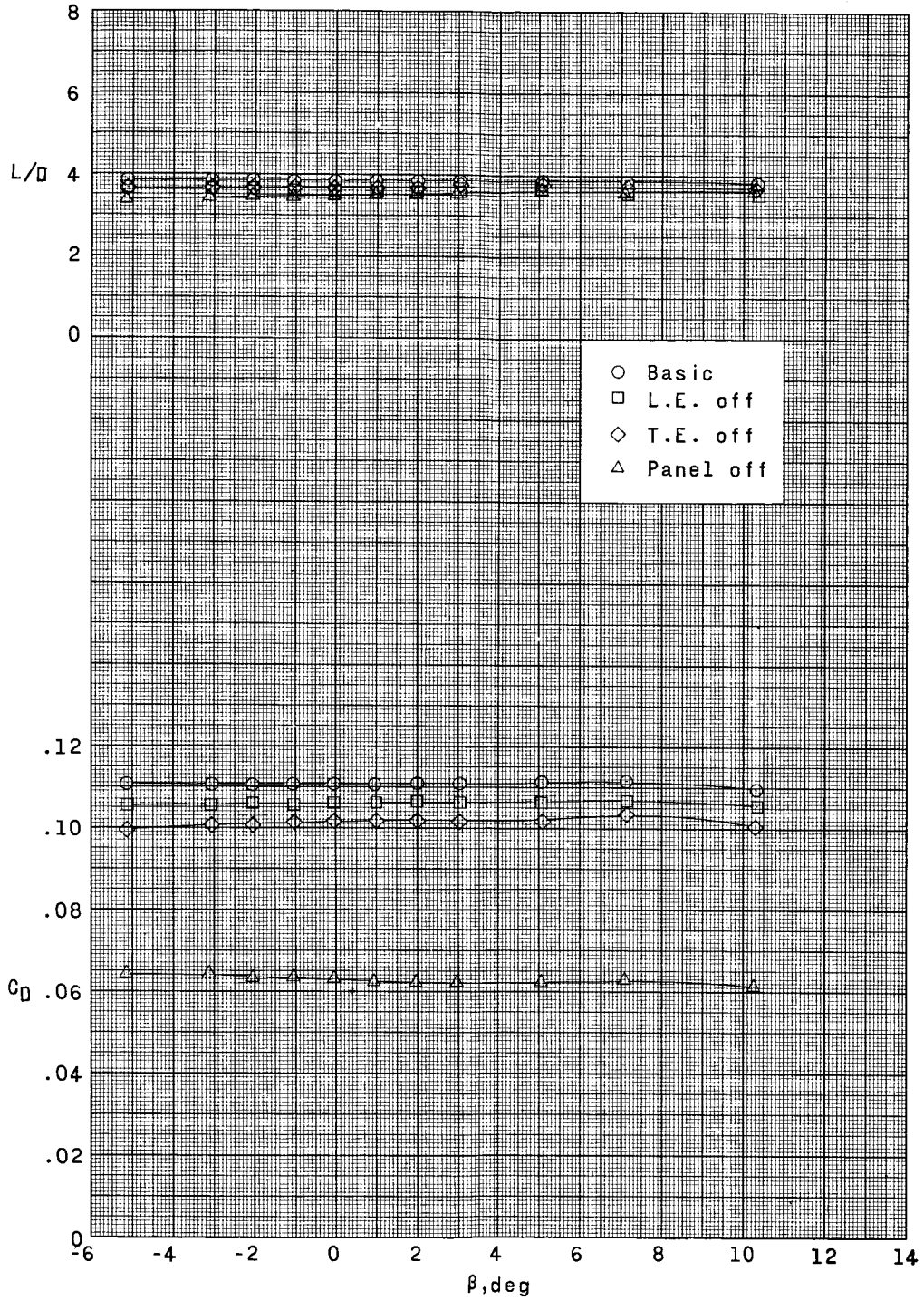

(c) Concluded.

Figure 5.- Continued.

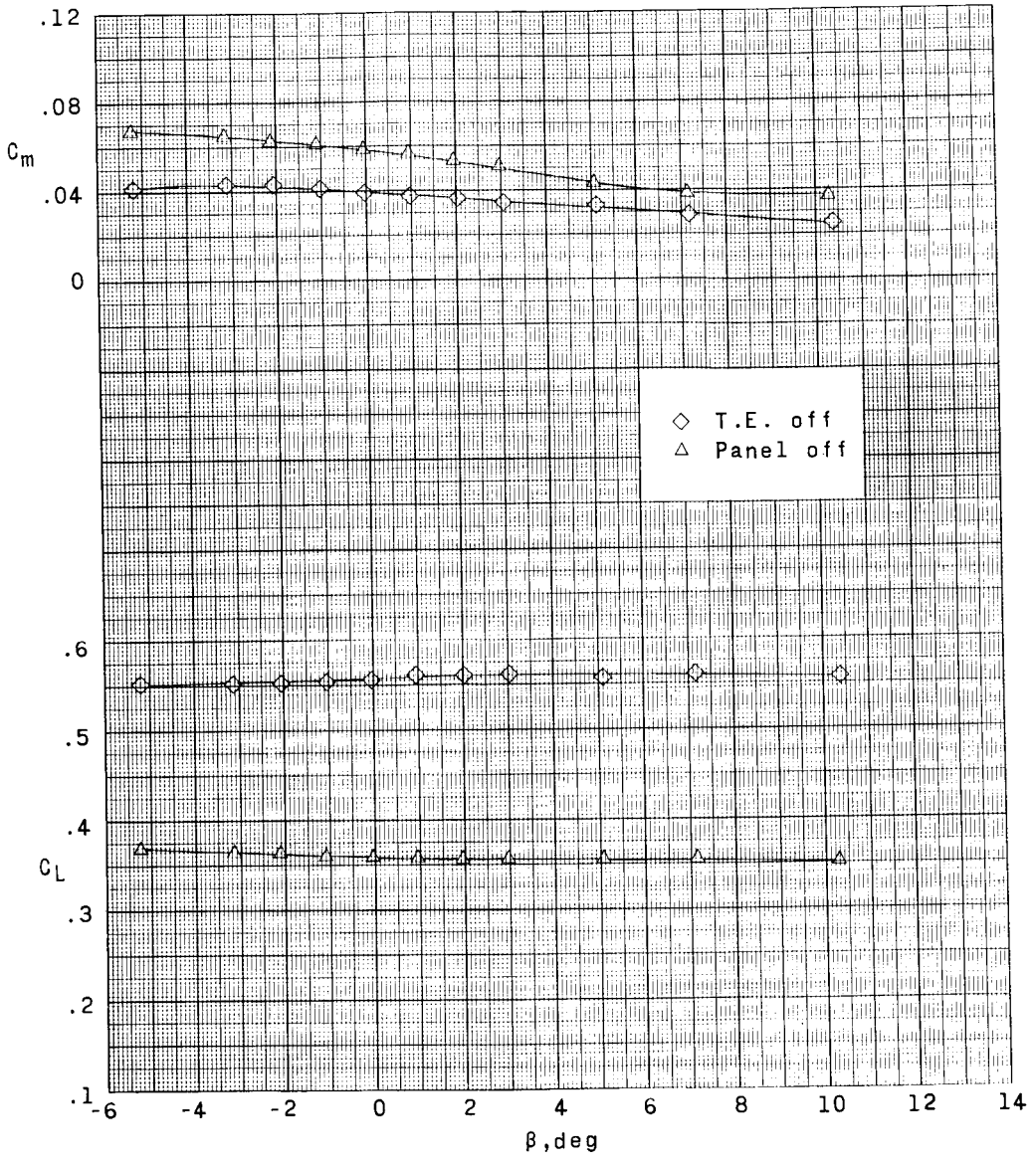

(d) $\alpha = 17.5^{0}$.

Figure 5.- Continued.

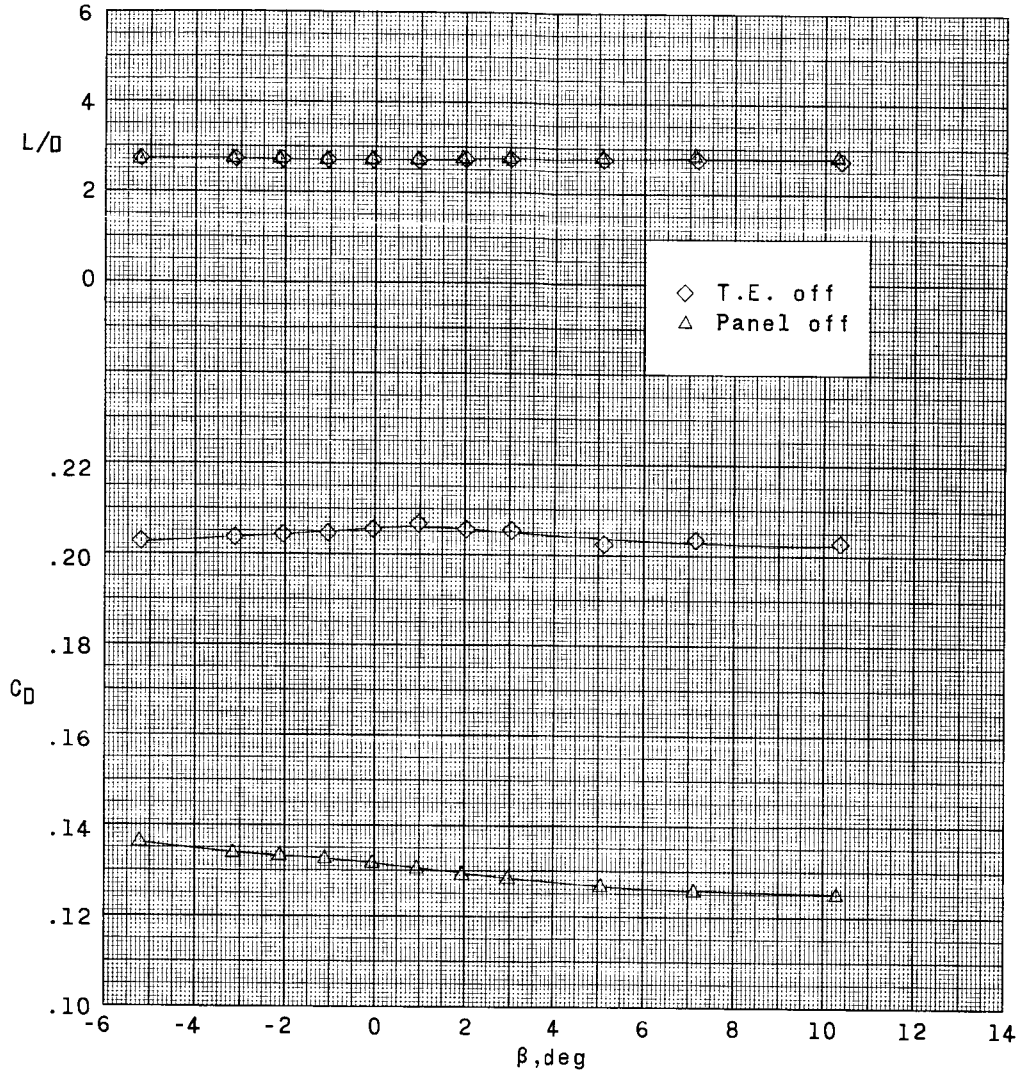

(d) Concluded.

Figure 5.- Concluded.

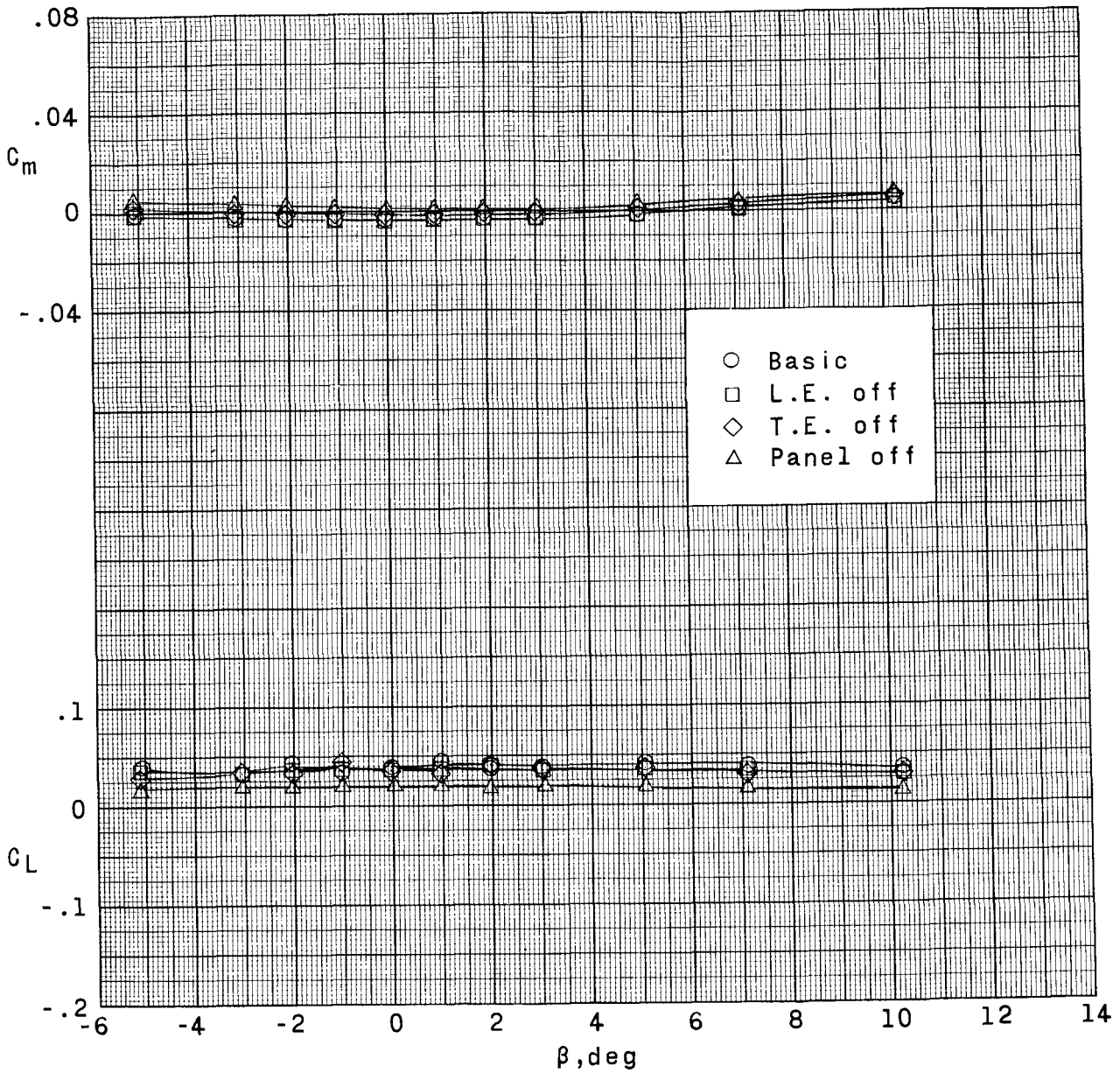

(a) $\alpha = 0^{o}$.

Figure 6.- Effect of wing asymmetry on the longitudinal aerodynamic characteristics with sideslip. M = 2.36.

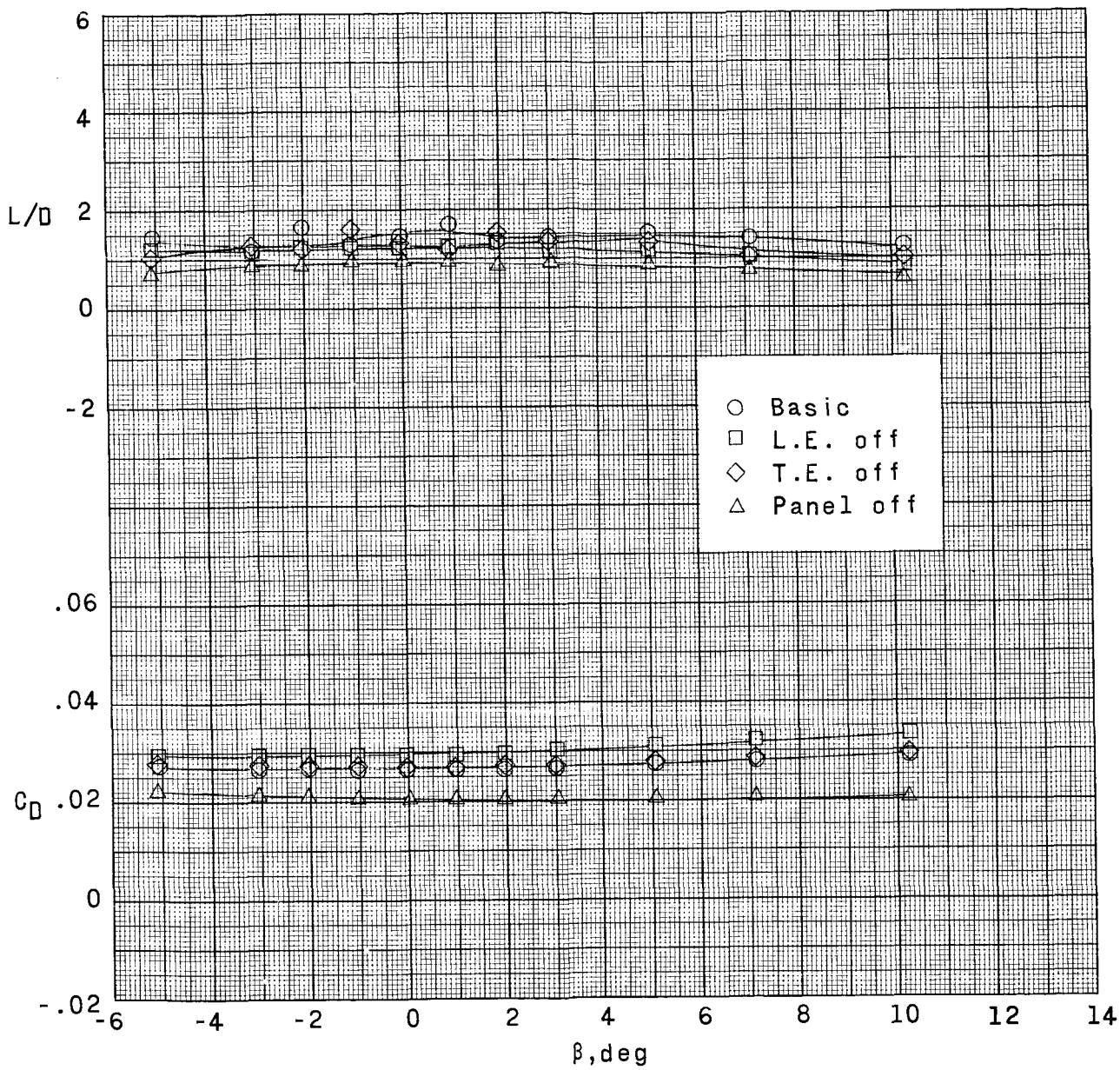

(a) Concluded.

Figure 6.- Continued.

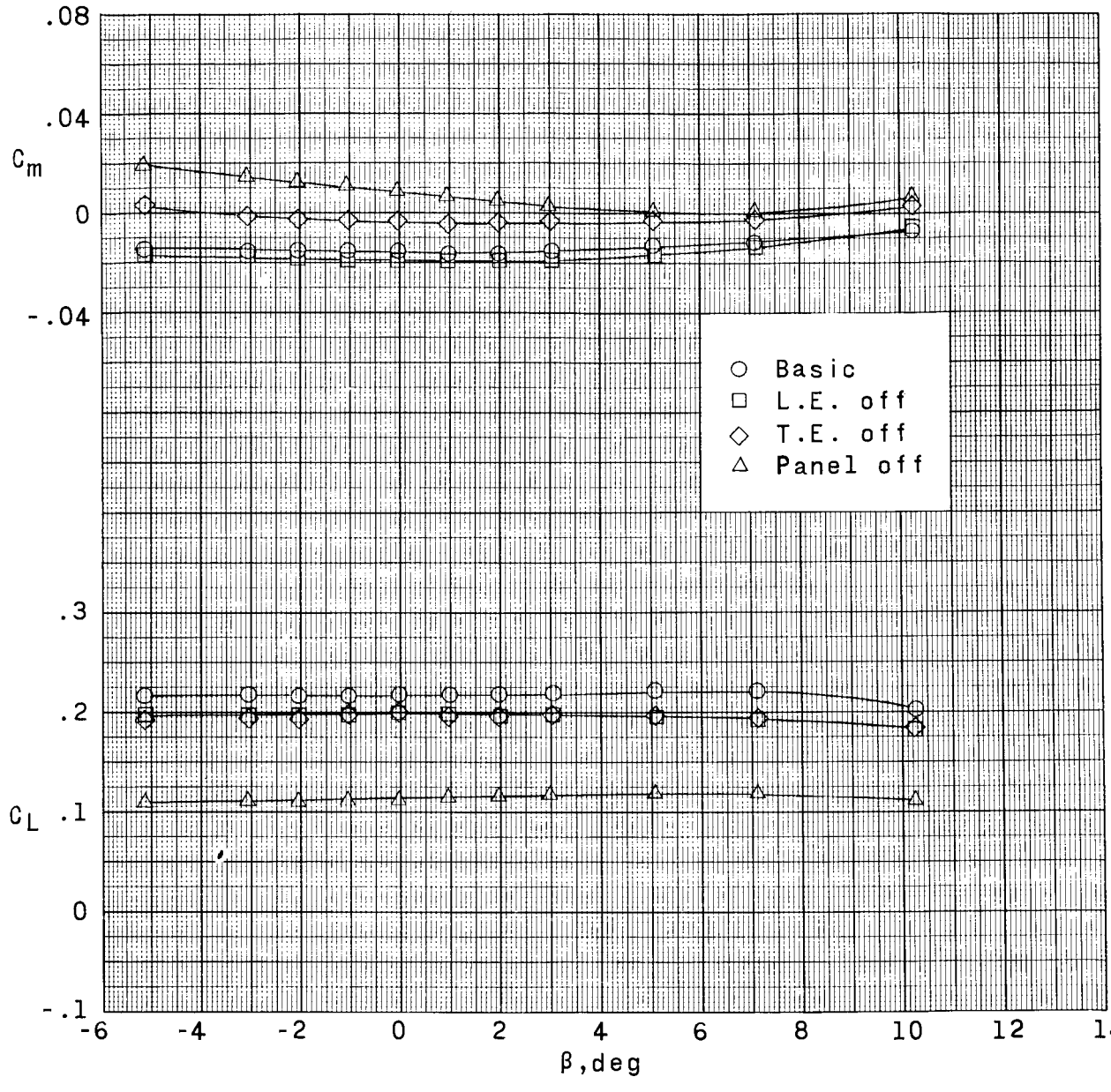

(b) $\alpha = 5^0$.

Figure 6.- Continued.

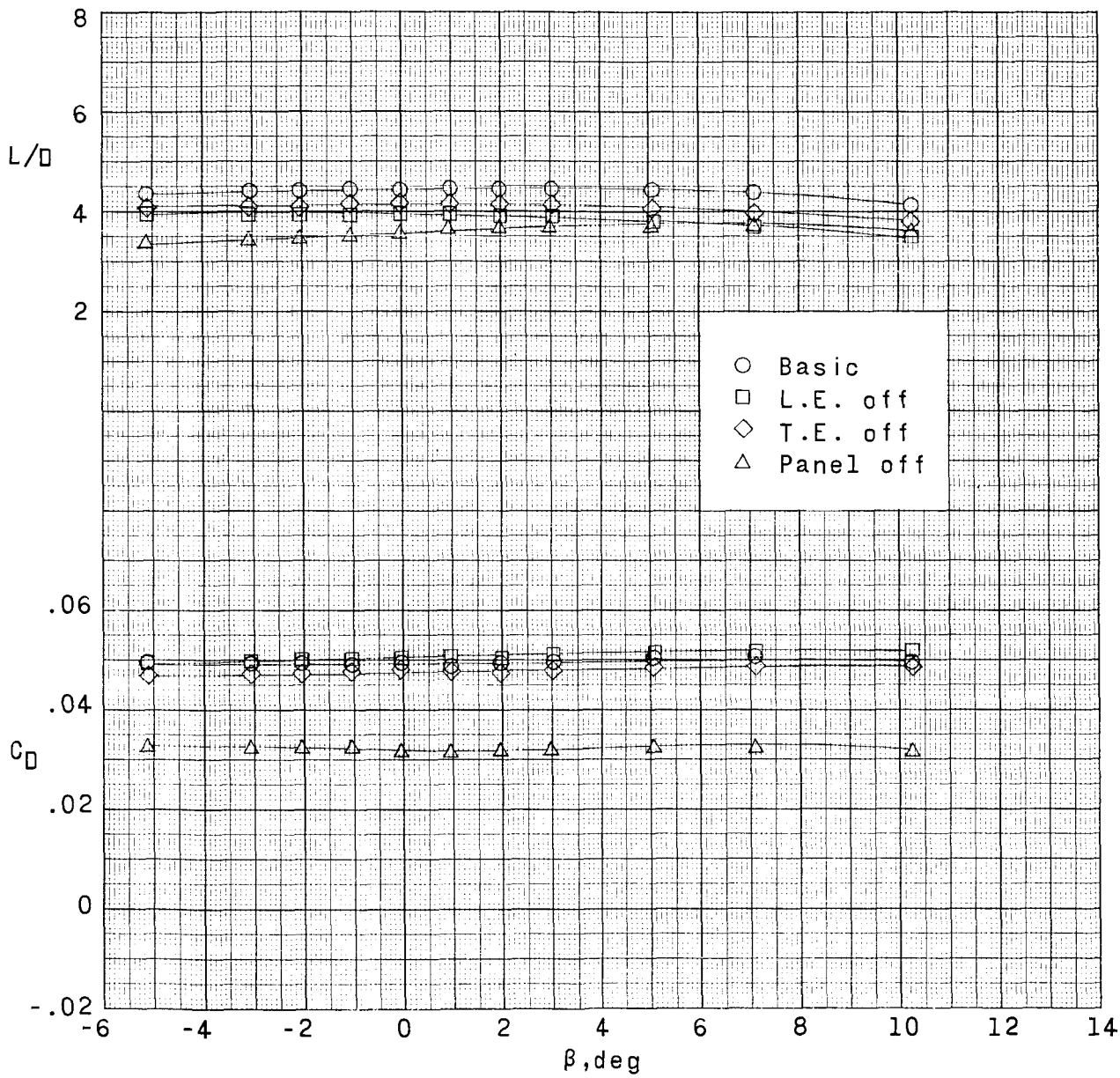

(b) Concluded.

Figure 6.- Continued.

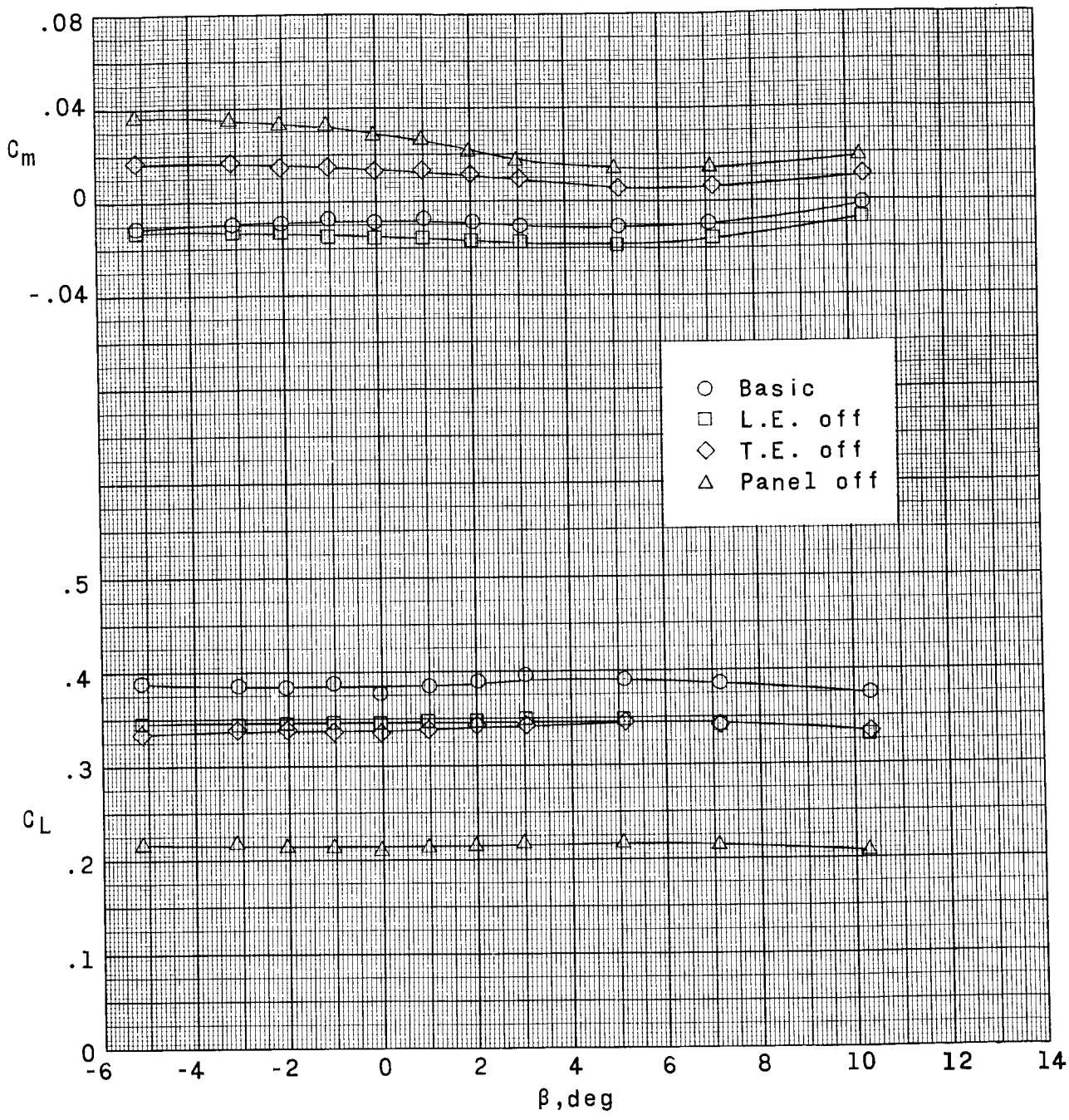

(c) $\alpha = 10^{o}$.

Figure 6.- Continued.

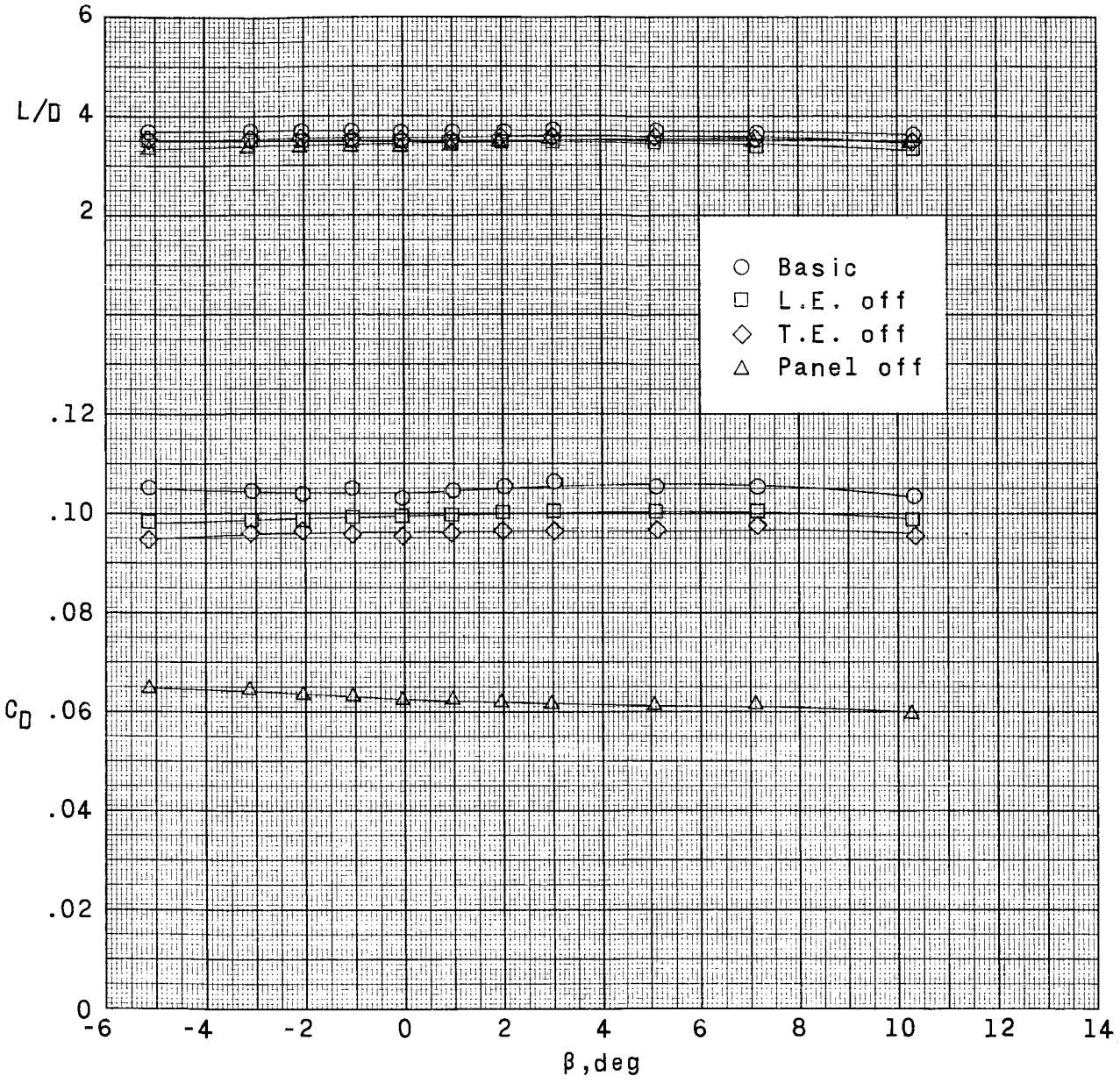

(c) Concluded.

Figure 6.- Continued.

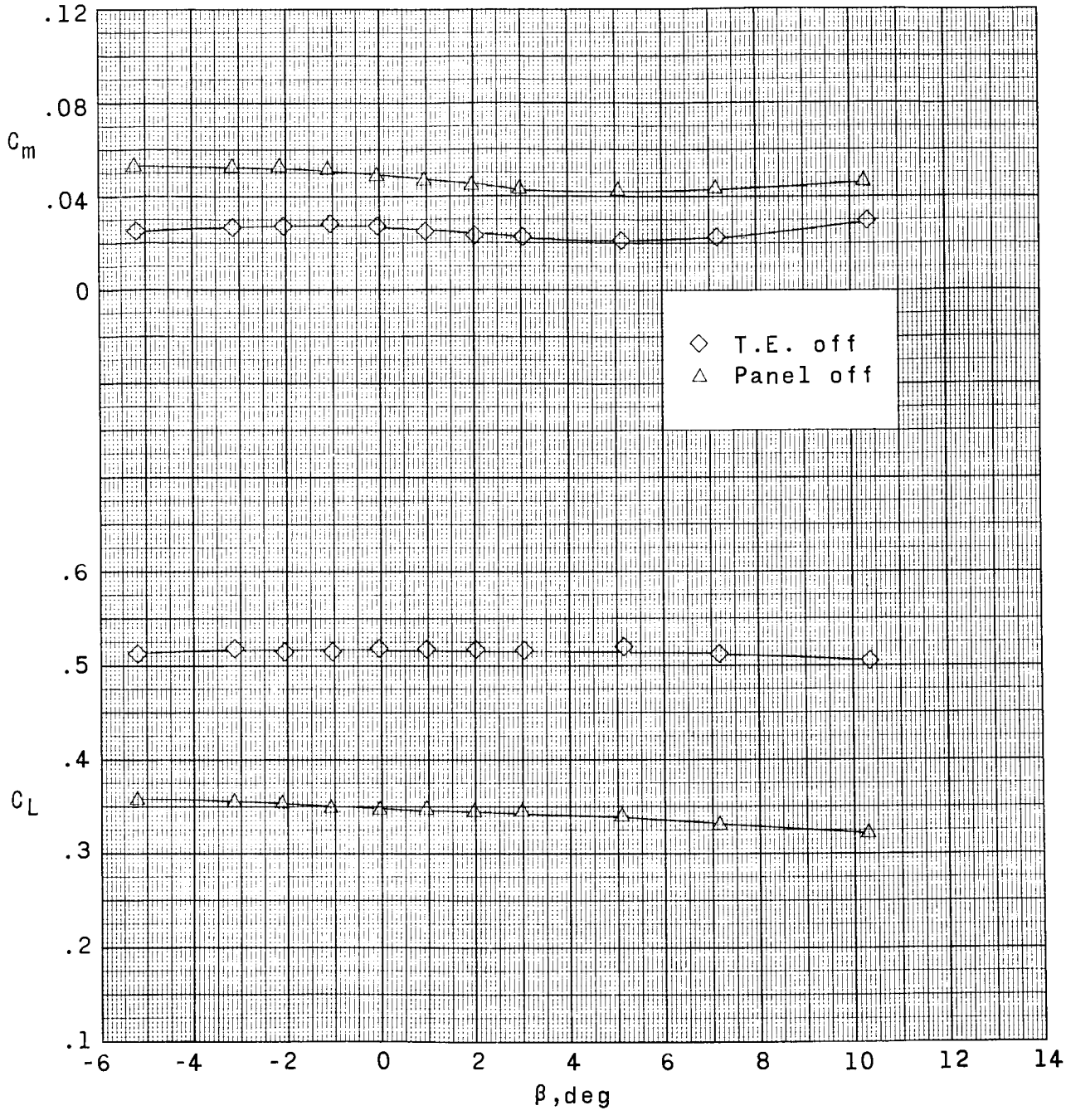

(d) $\alpha = 18^0$.

Figure 6.- Continued.

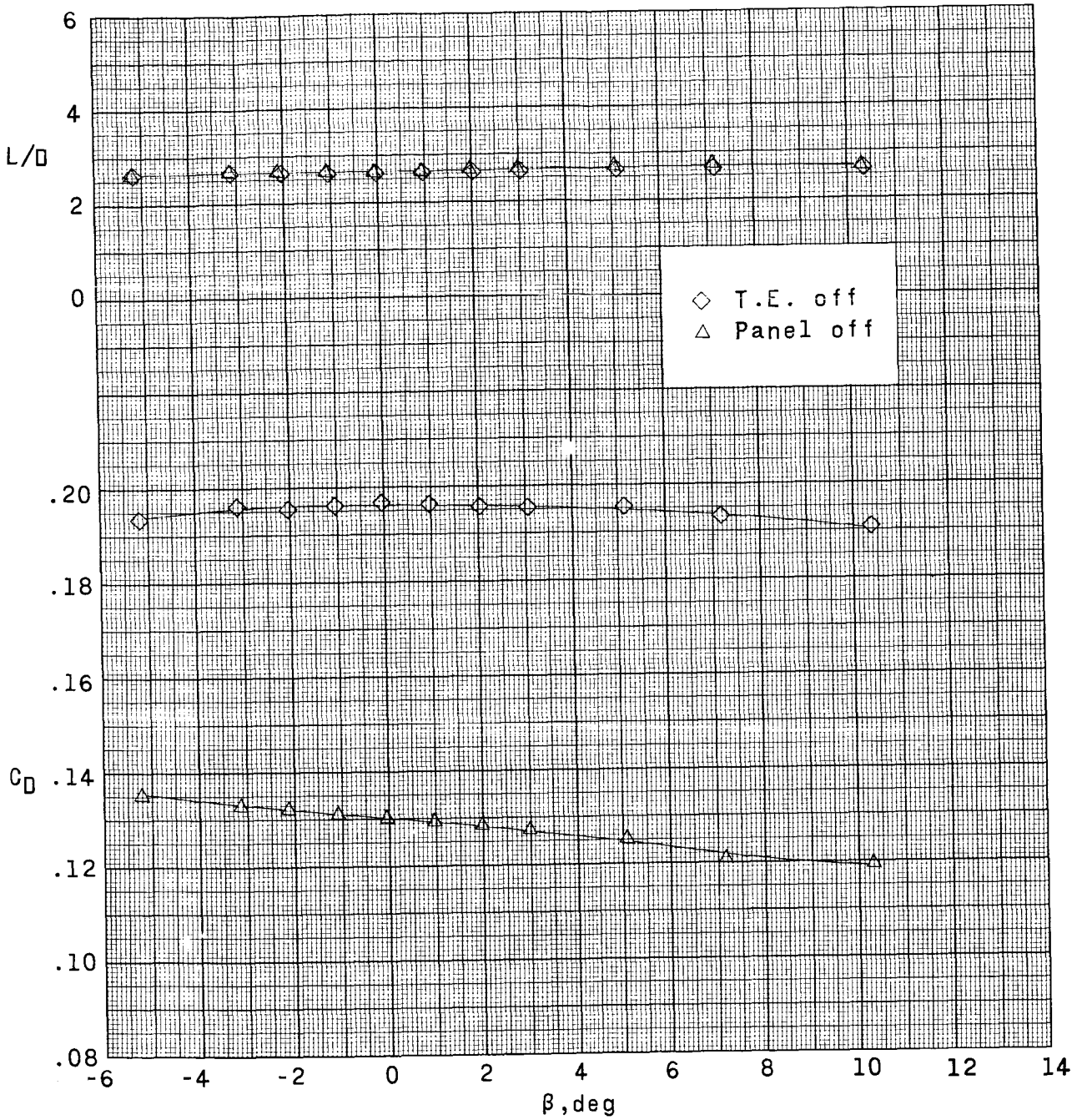

(d) Concluded.

Figure 6.- Concluded.

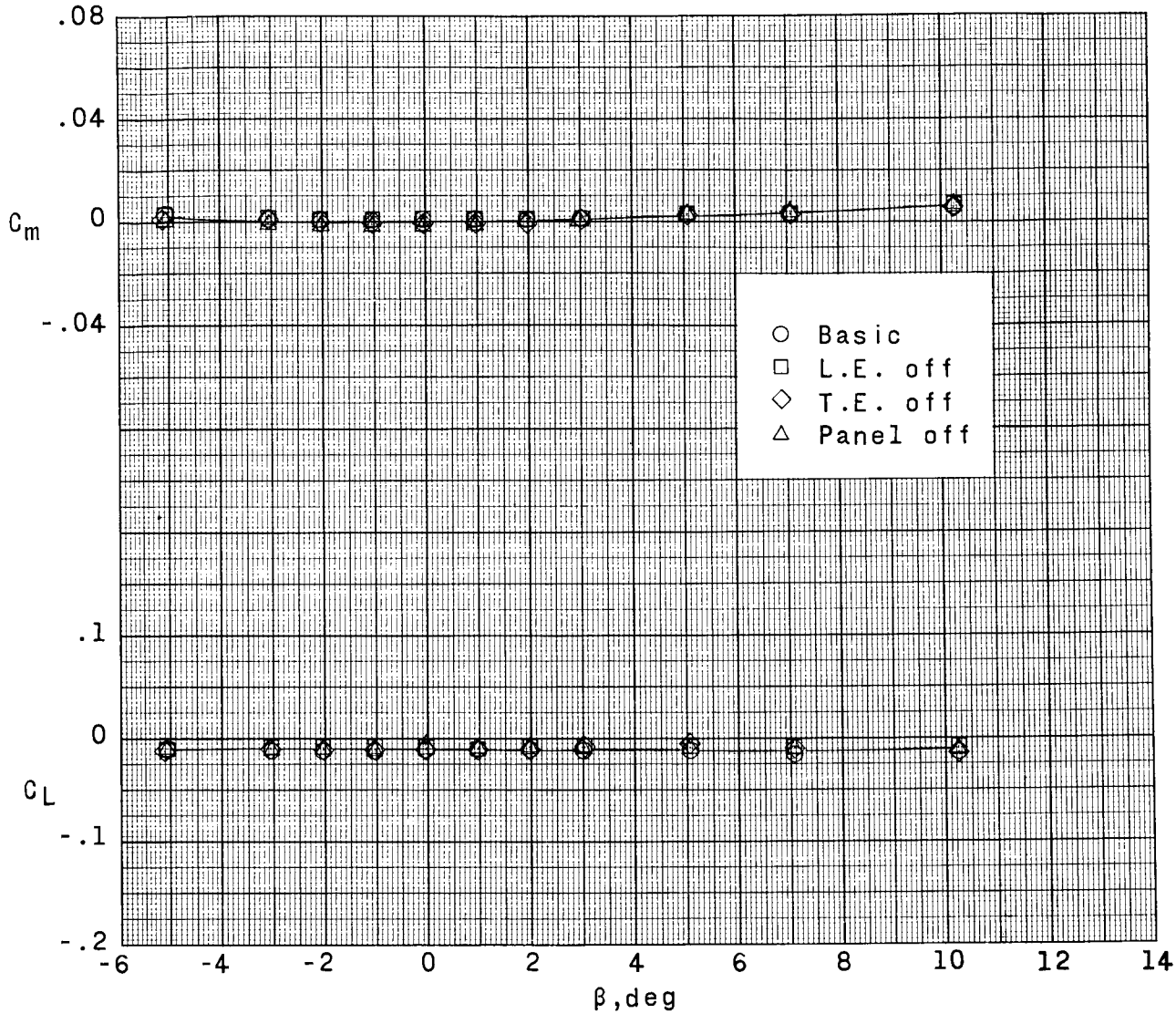

(a) $\alpha = 0^{o}$.

Figure 7.- Effect of wing asymmetry on the longitudinal aerodynamic characteristics with sideslip. M = 2.86.

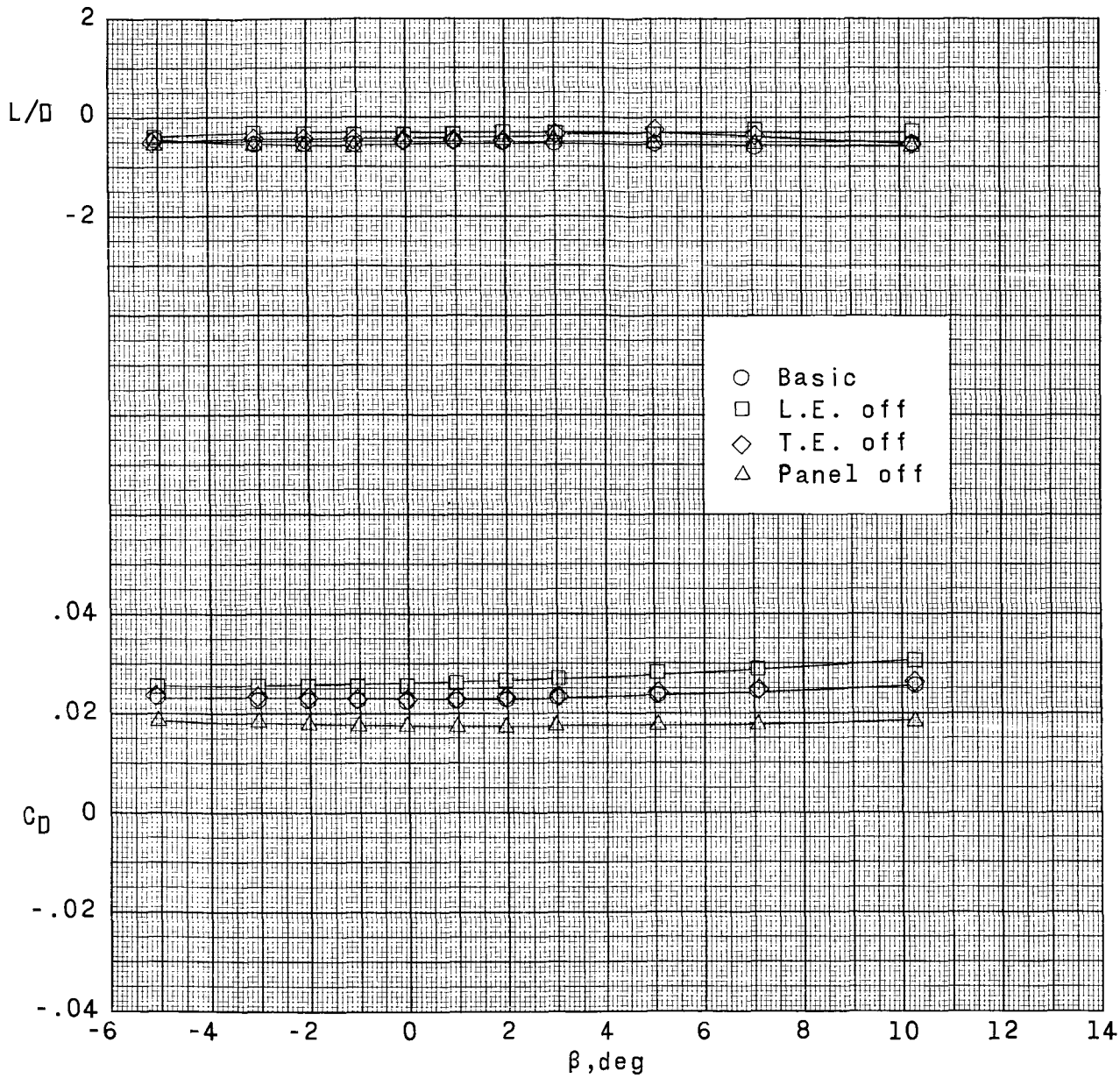

(a) Concluded.

Figure 7.- Continued.

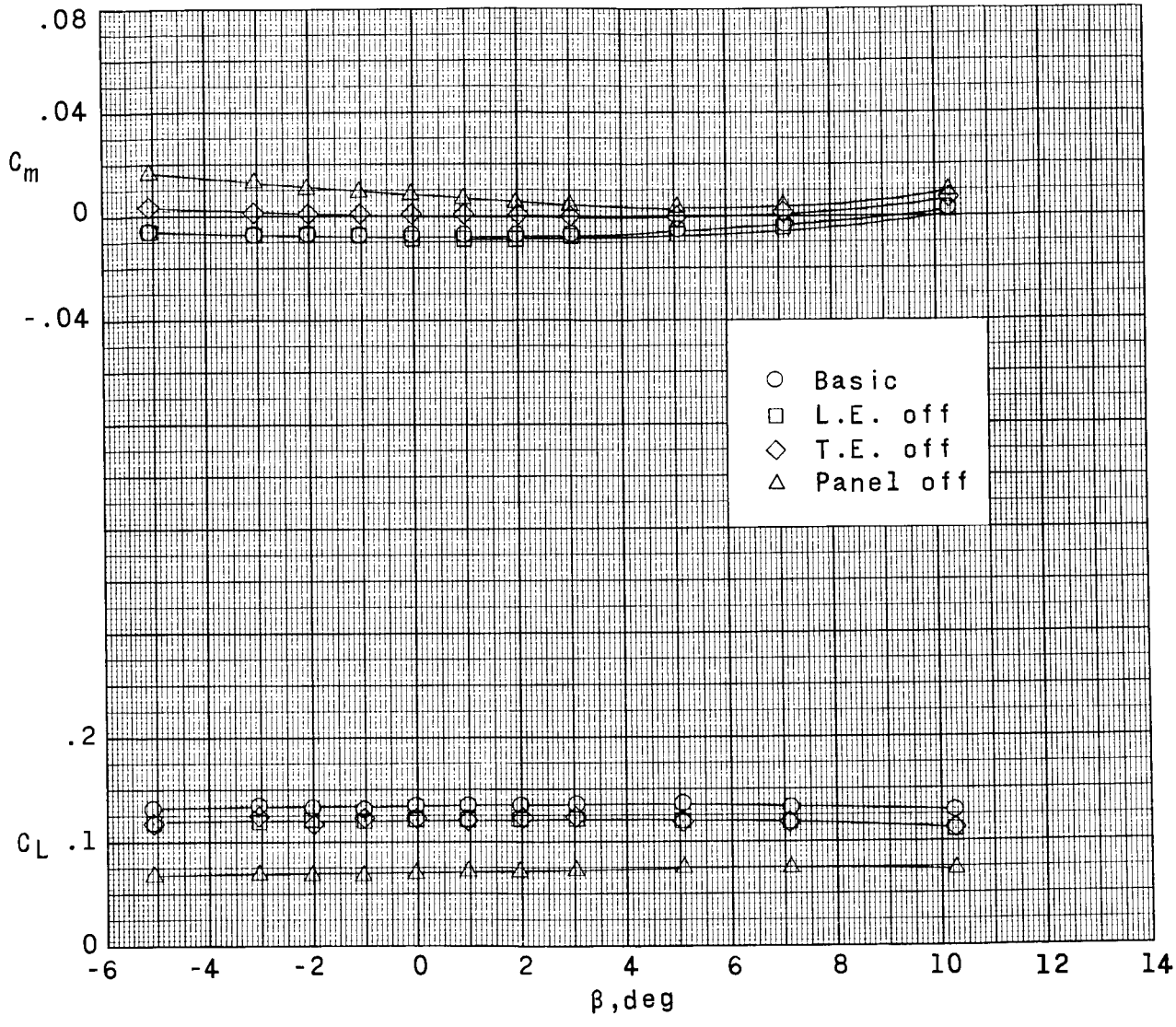

(b) $\alpha = 5^{\circ}$.

Figure 7.- Continued.

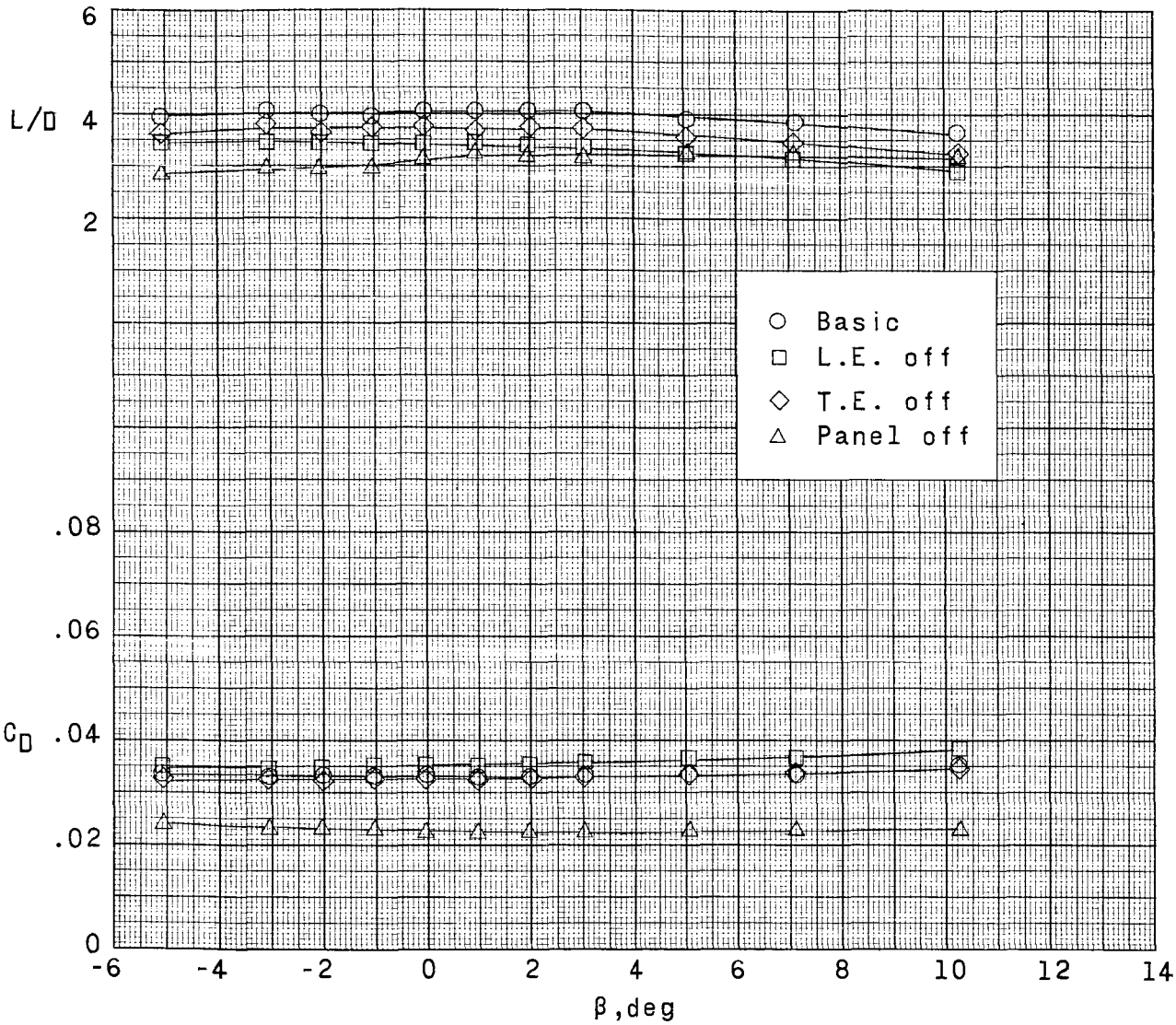

(b) Concluded.

Figure 7.- Continued.

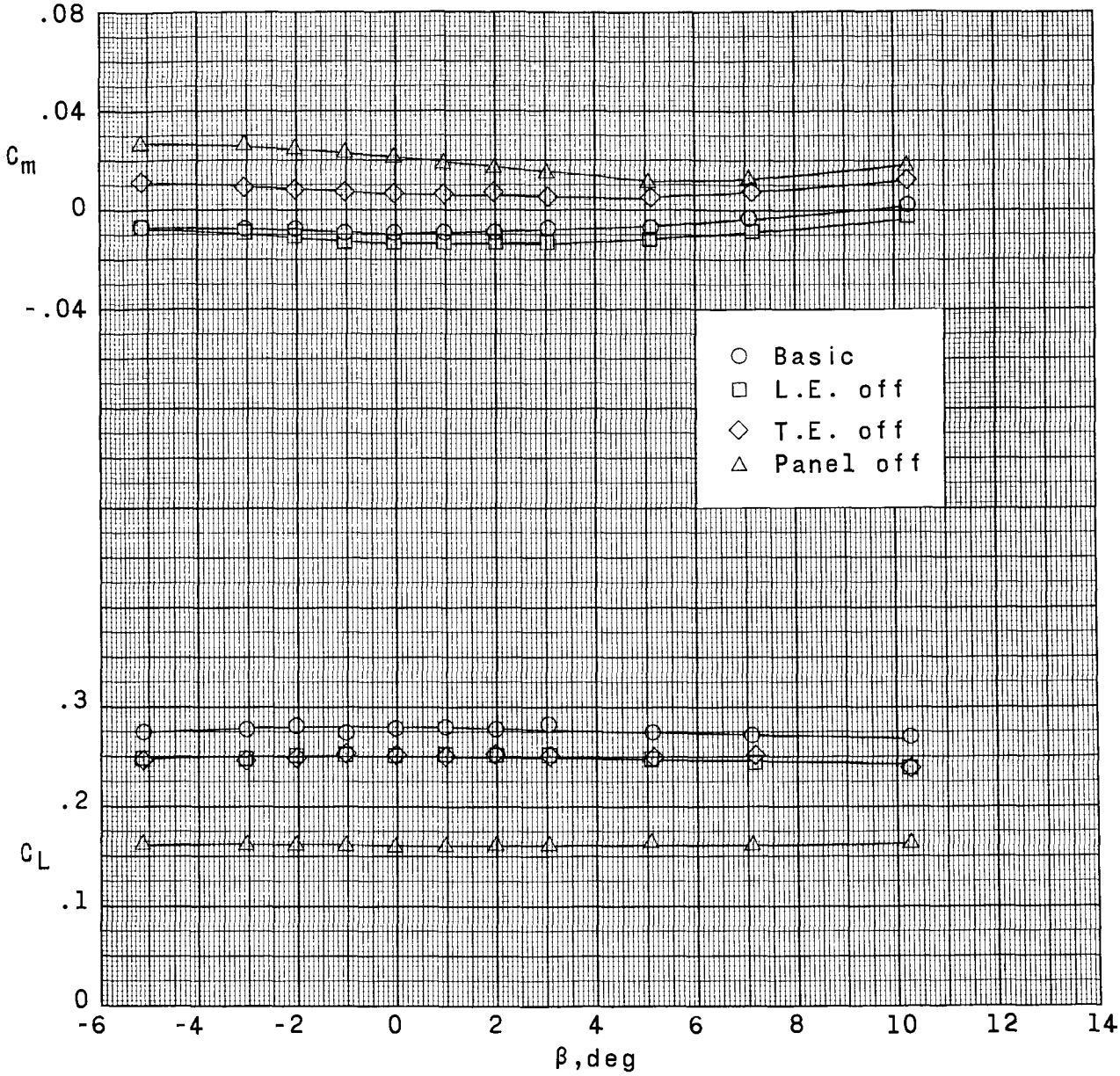

(c) $\alpha = 10^0$.

Figure 7.- Continued.

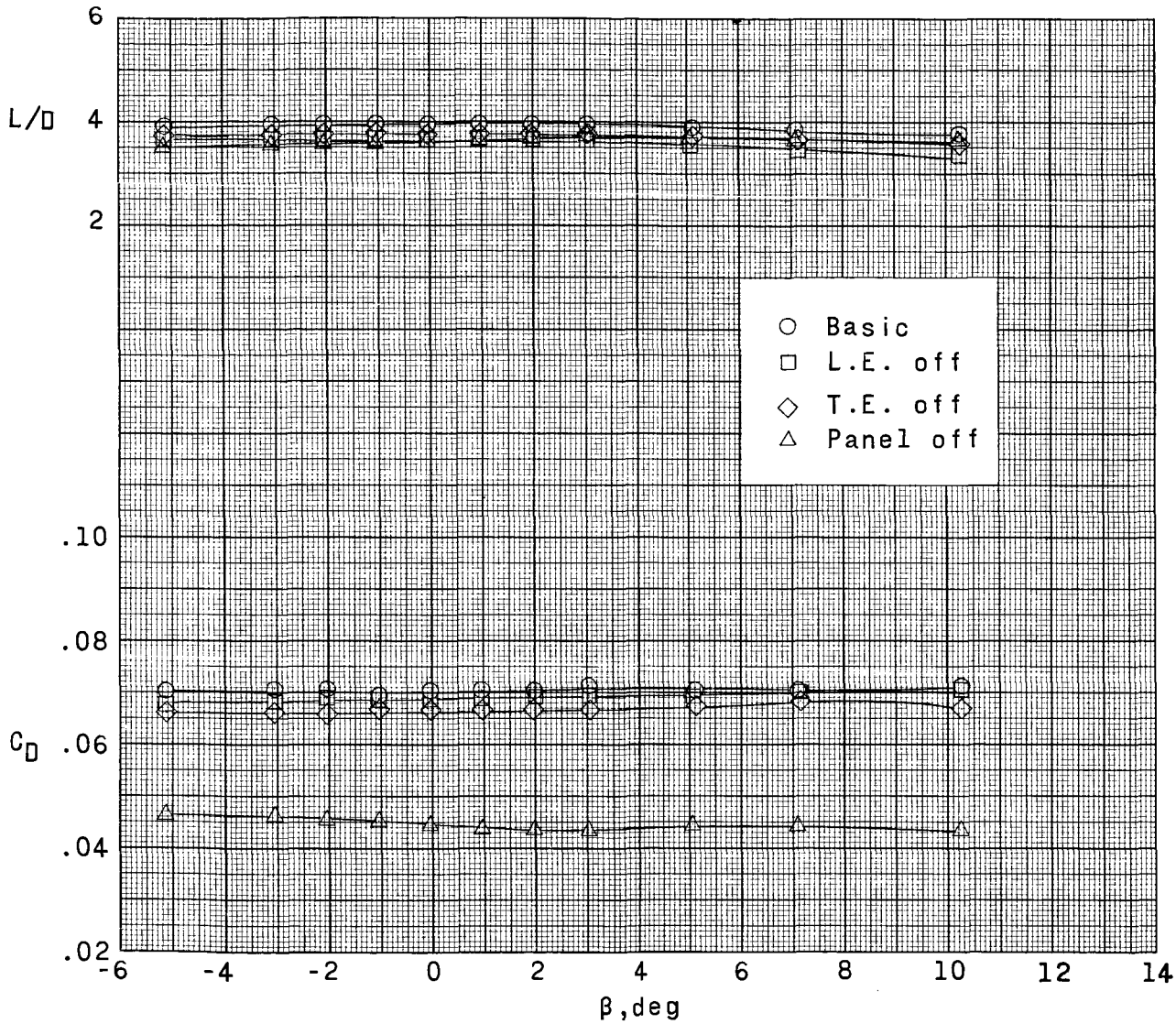

(c) Concluded.

Figure 7.- Continued.

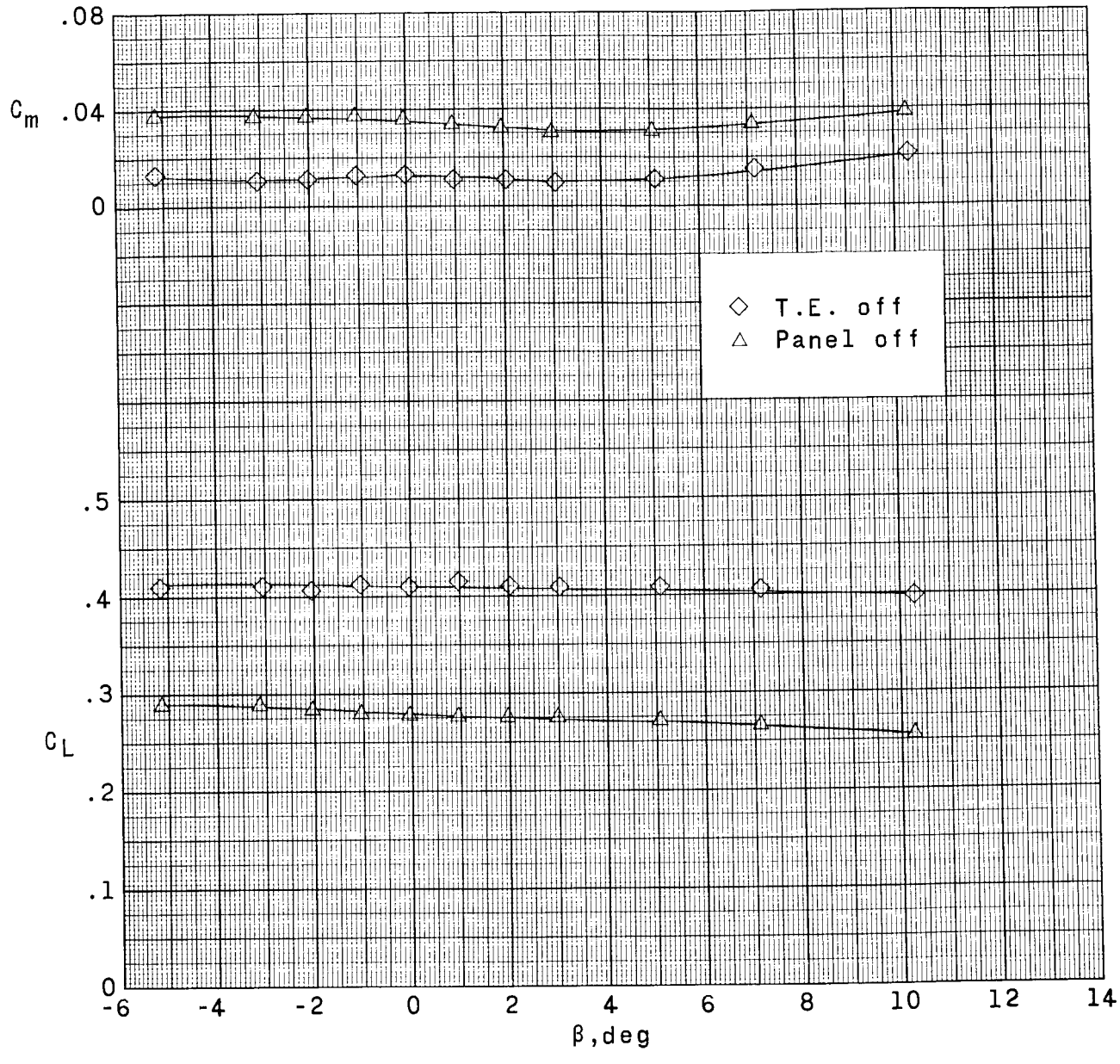

(d) $\alpha = 17^{0}$.

Figure 7.- Continued.

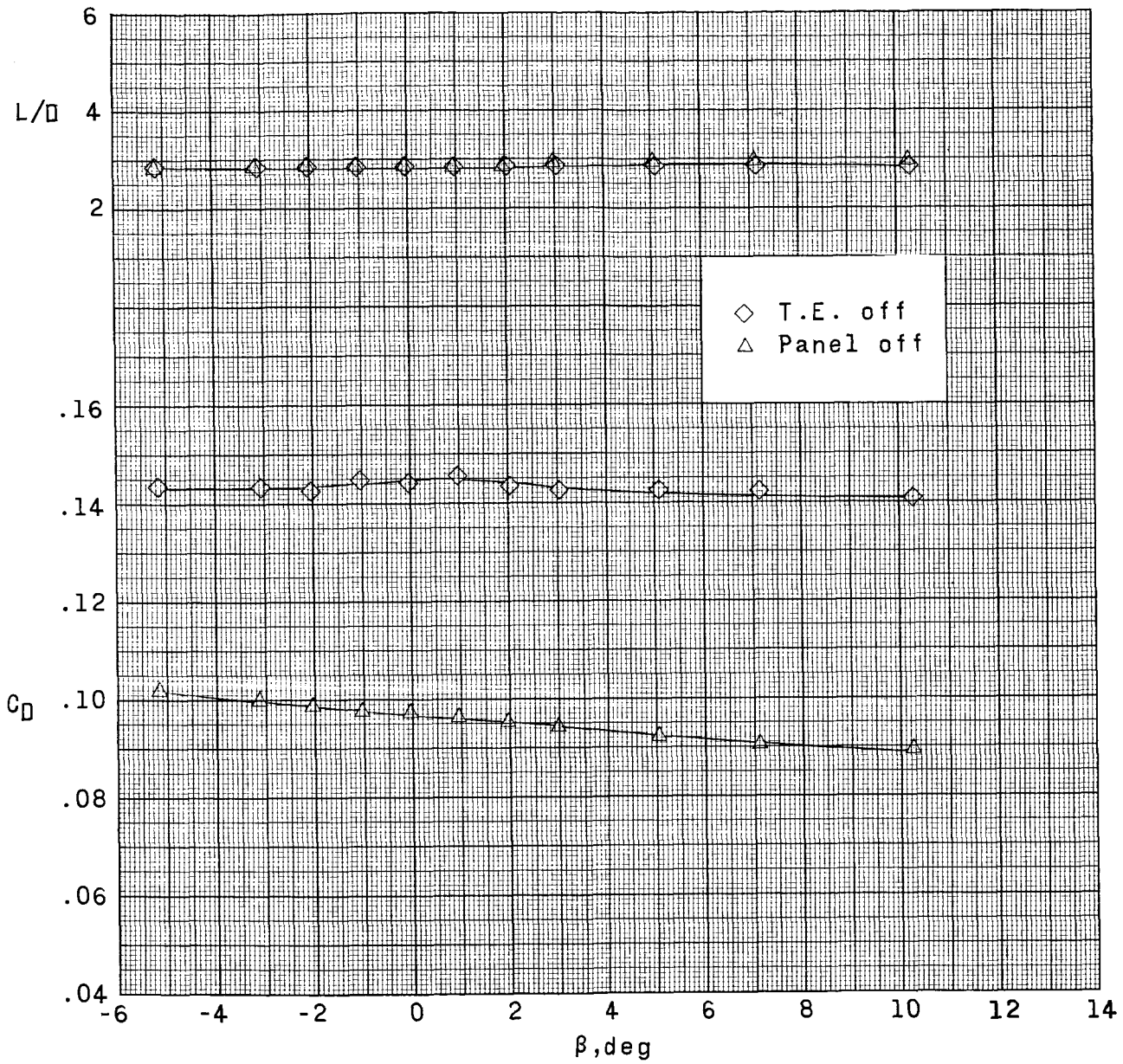

(d) Concluded.

Figure 7.- Concluded.

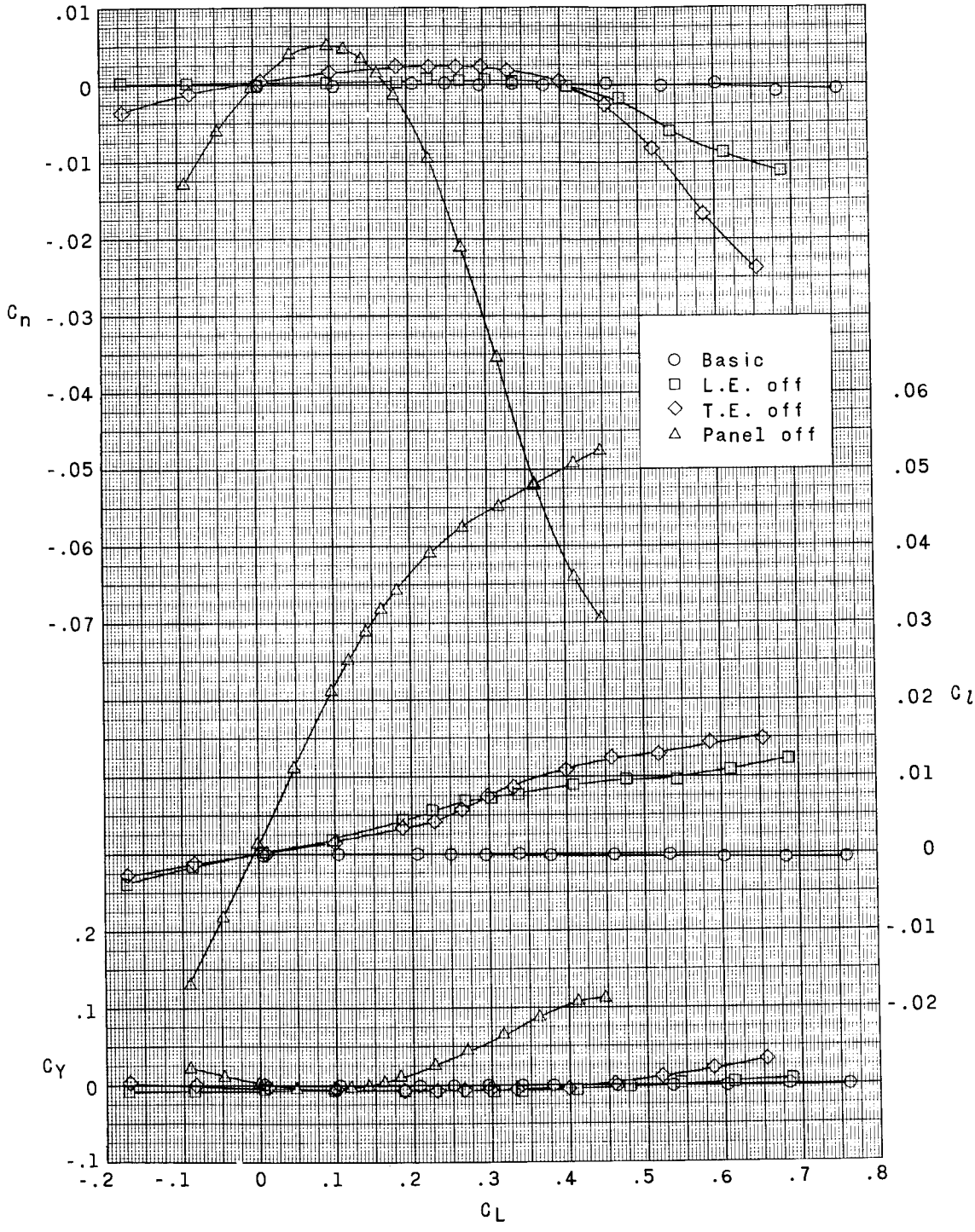

(a) M = 1.70.

Figure 8.- Effect of wing asymmetry on the lateral-directional aerodynamic characteristics. $\beta = 0^{o}$.

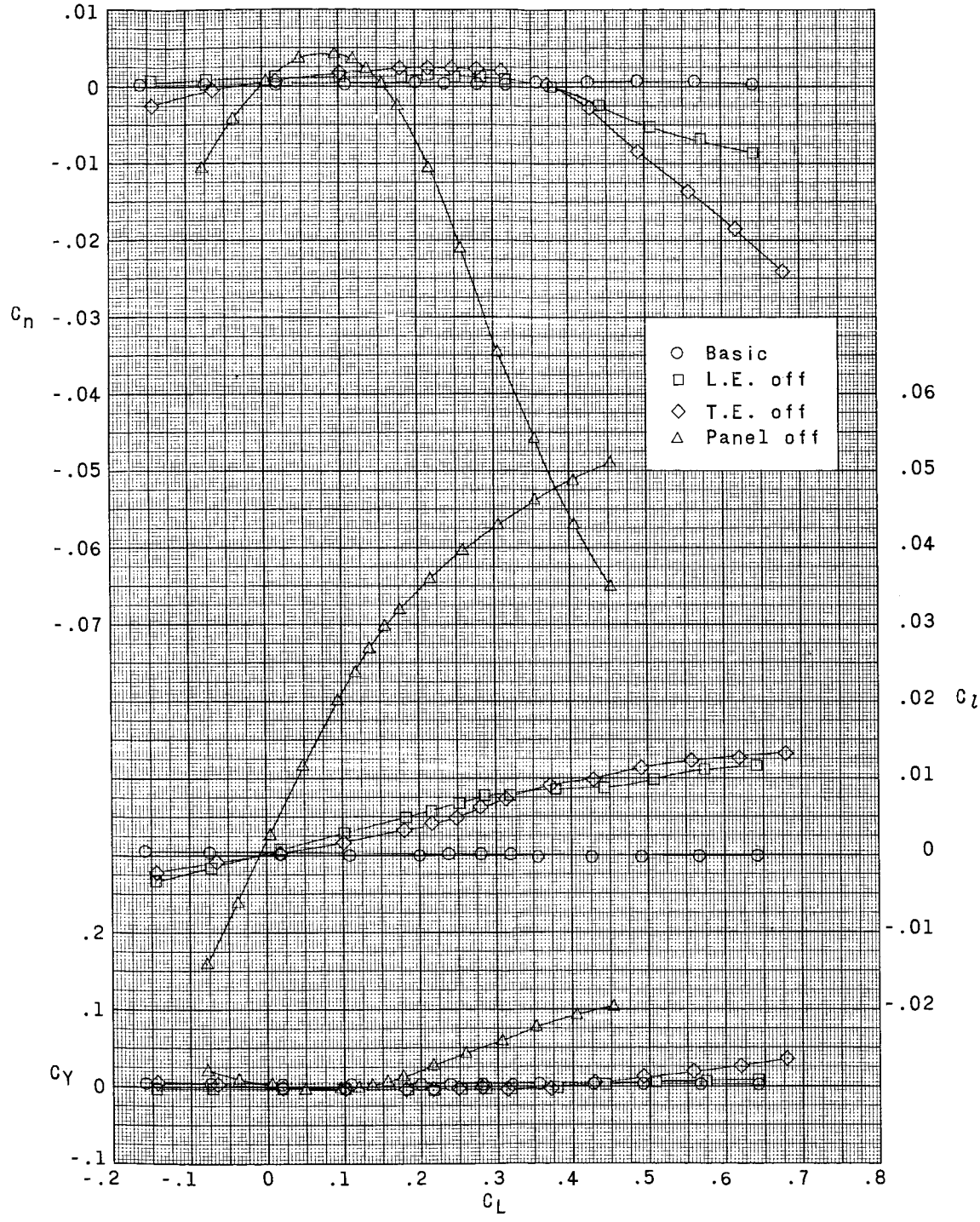

(b) M = 1.90.

Figure 8.- Continued.

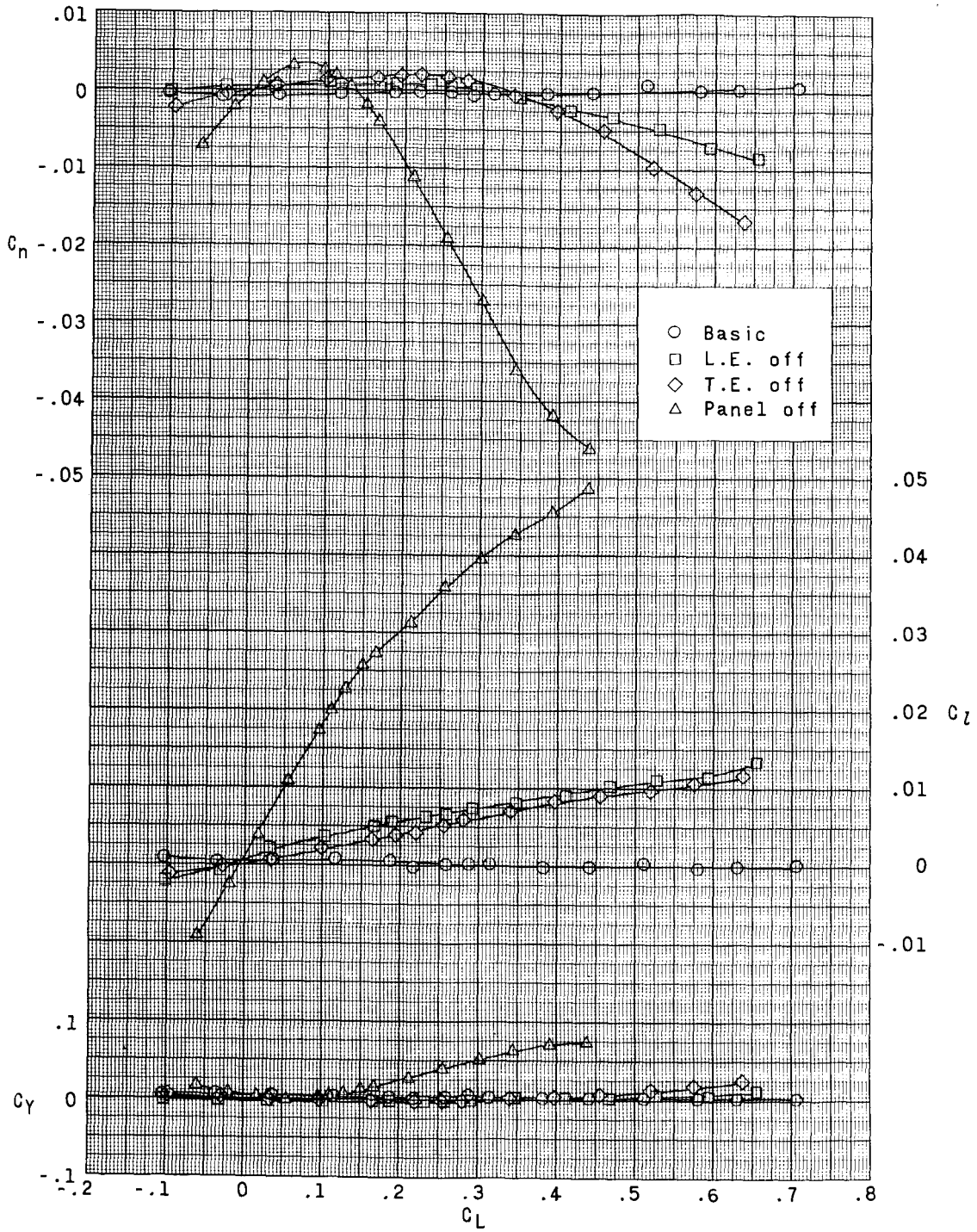

(c) M = 2.36.

Figure 8.- Continued.

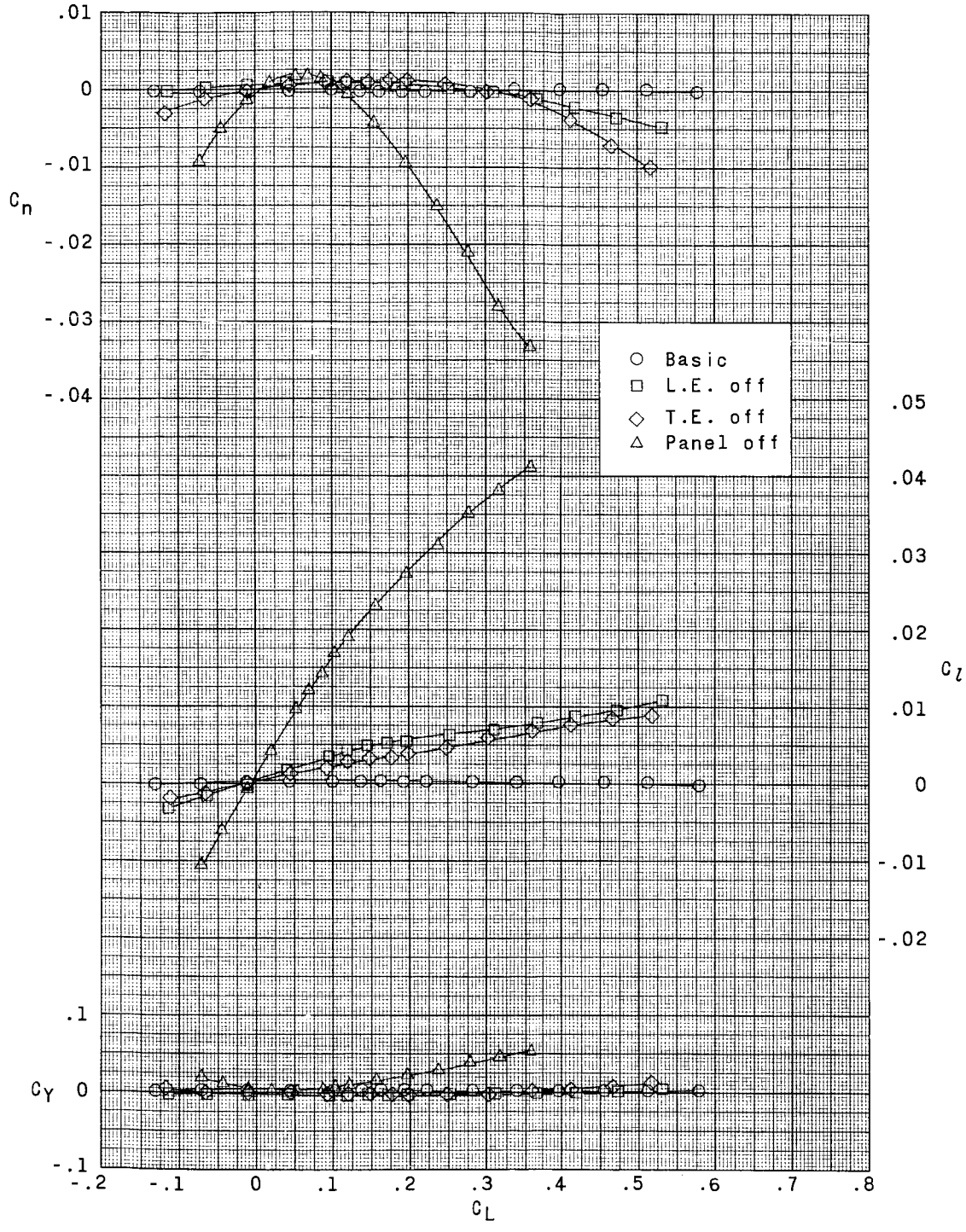

(d) M = 2.86.

Figure 8.- Concluded.

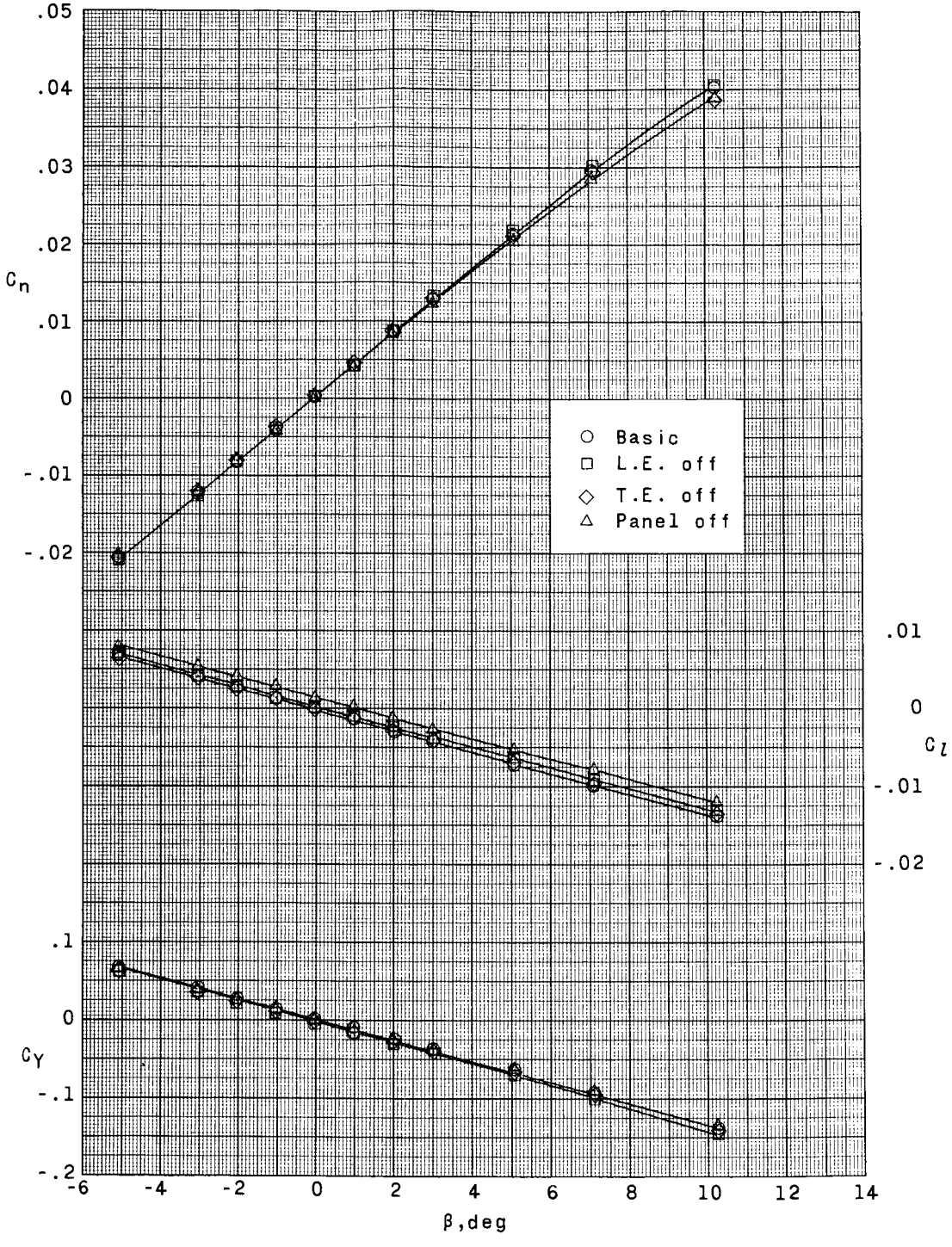

(a) $\alpha = 0^0$.

Figure 9.- Effect of wing asymmetry on the lateral-directional aerodynamic characteristics with sideslip. M = 1.70.

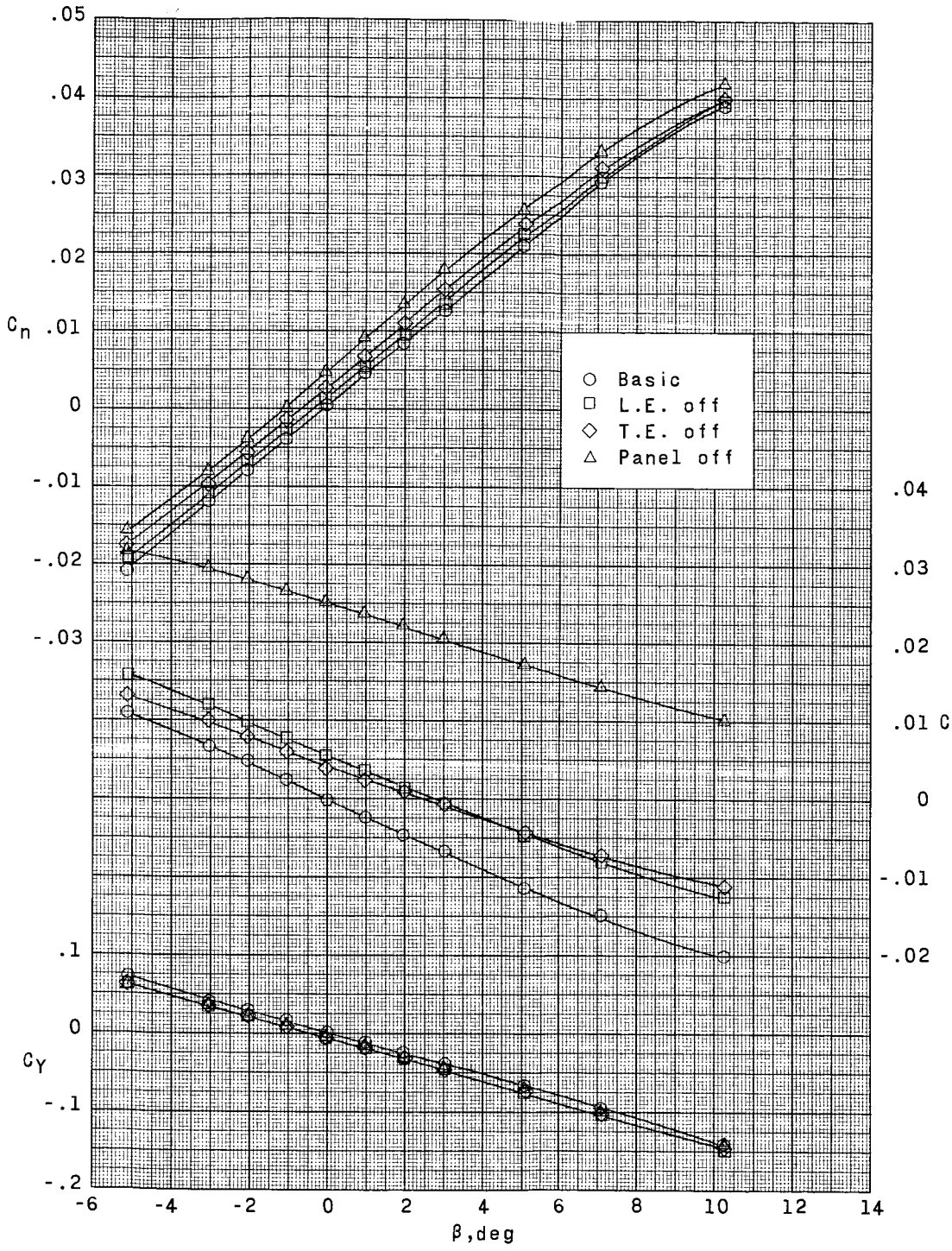

(b) $\alpha = 5^0$.

Figure 9.- Continued.

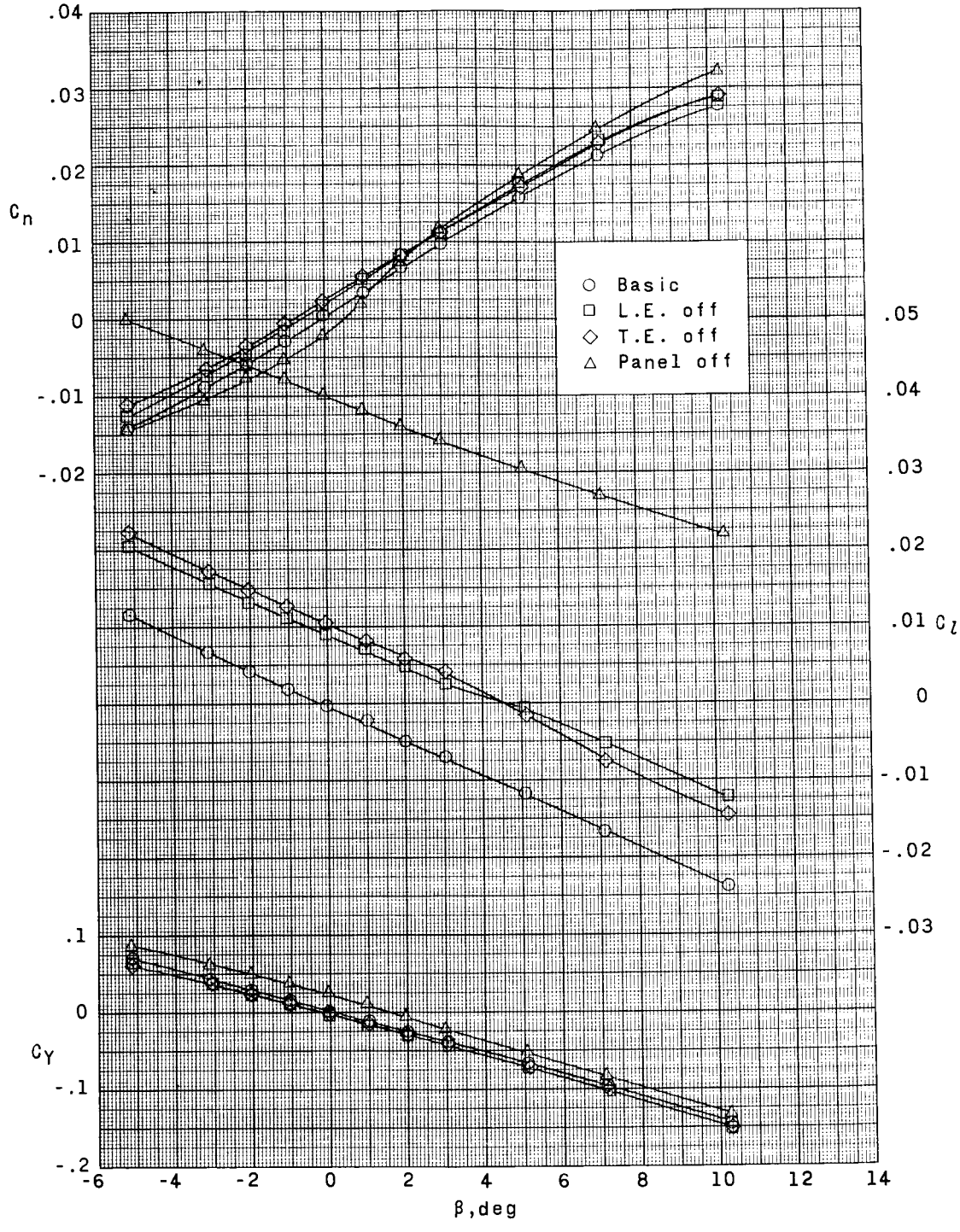

(c) $\alpha = 10^0$.

Figure 9.- Continued.

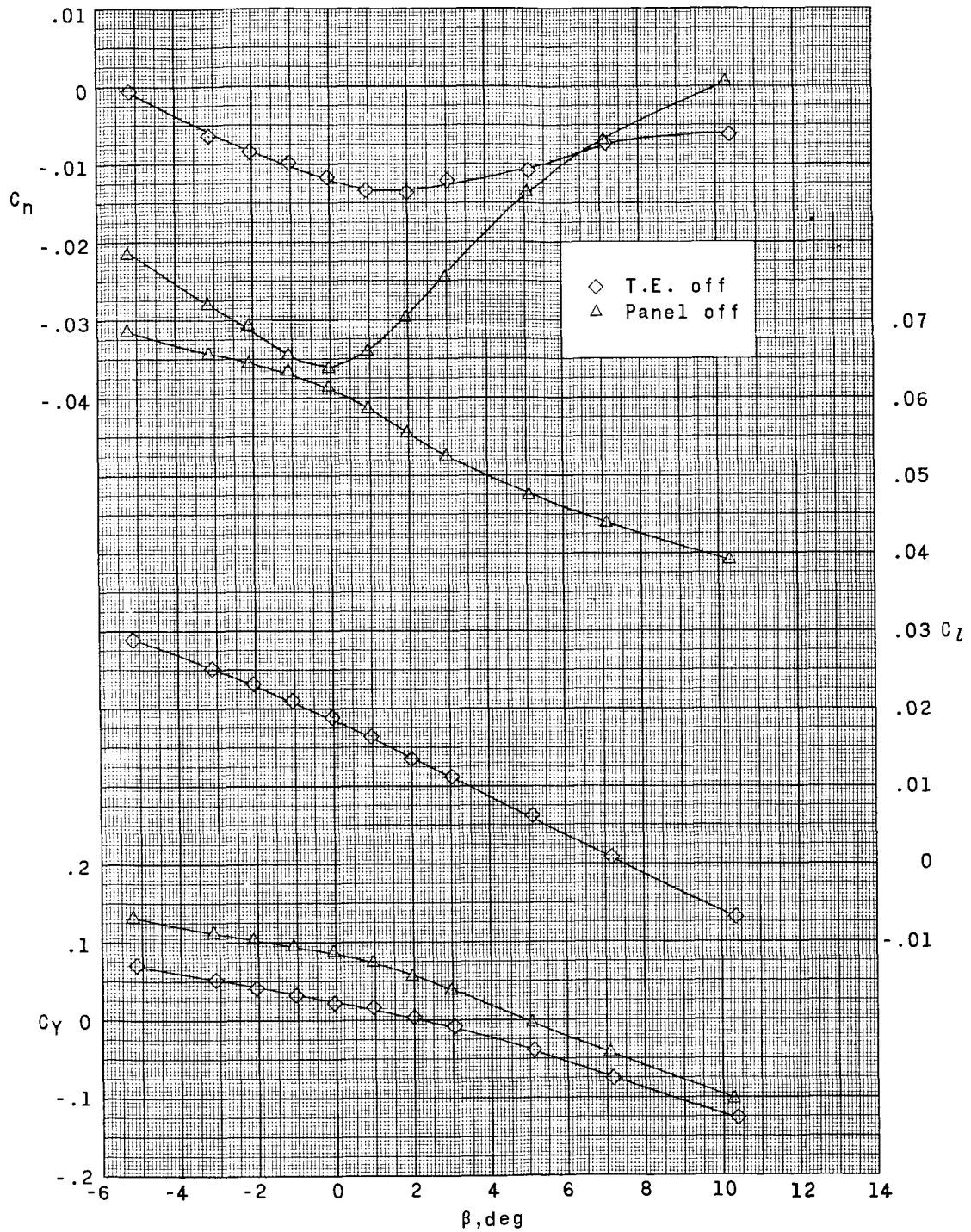

(d) $\alpha = 17^{0}$.

Figure 9.- Concluded.

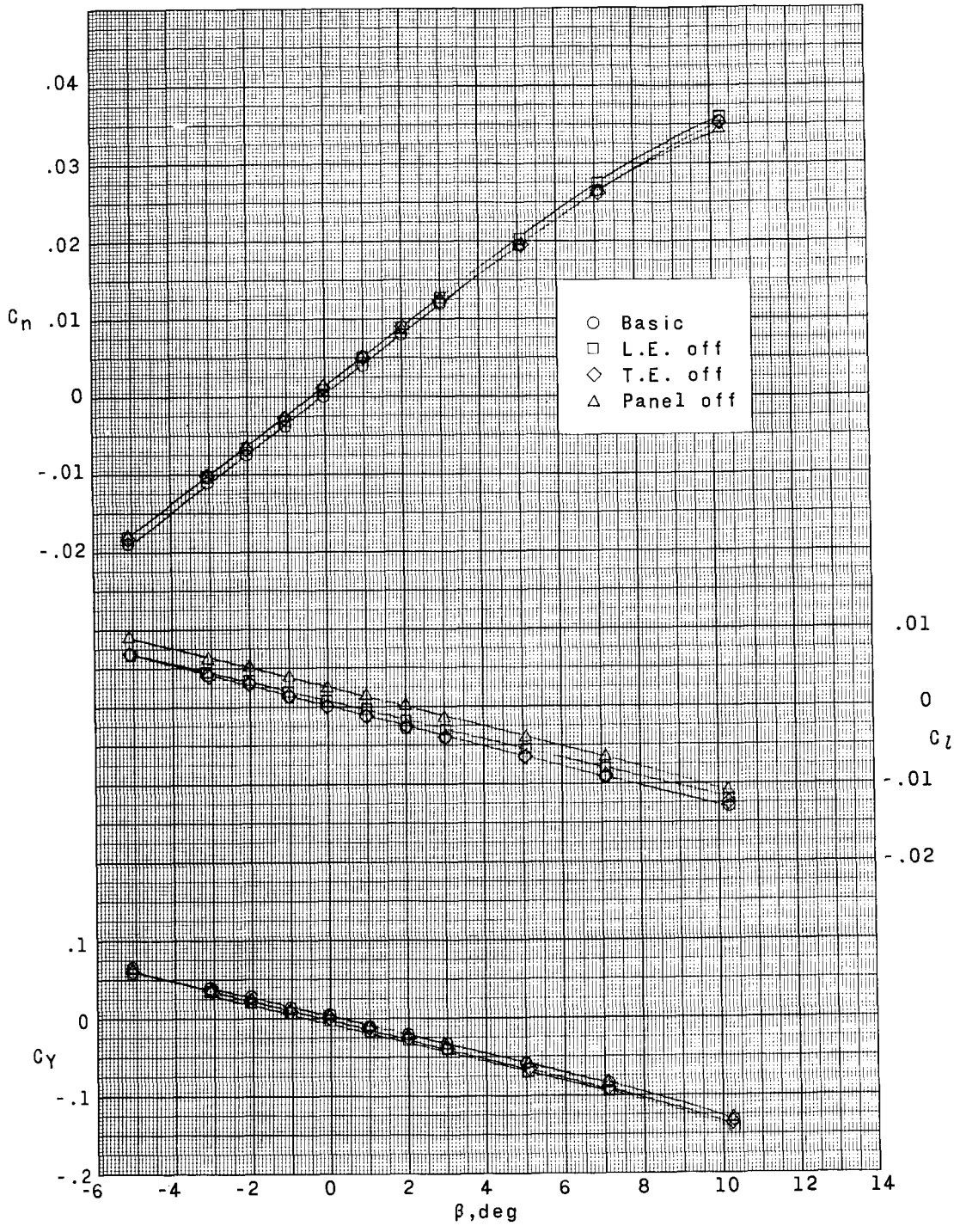

(a) $\alpha = 0^0$.

Figure 10.- Effect of wing asymmetry on the lateral-directional aerodynamic characteristics with sideslip. M = 1.90.

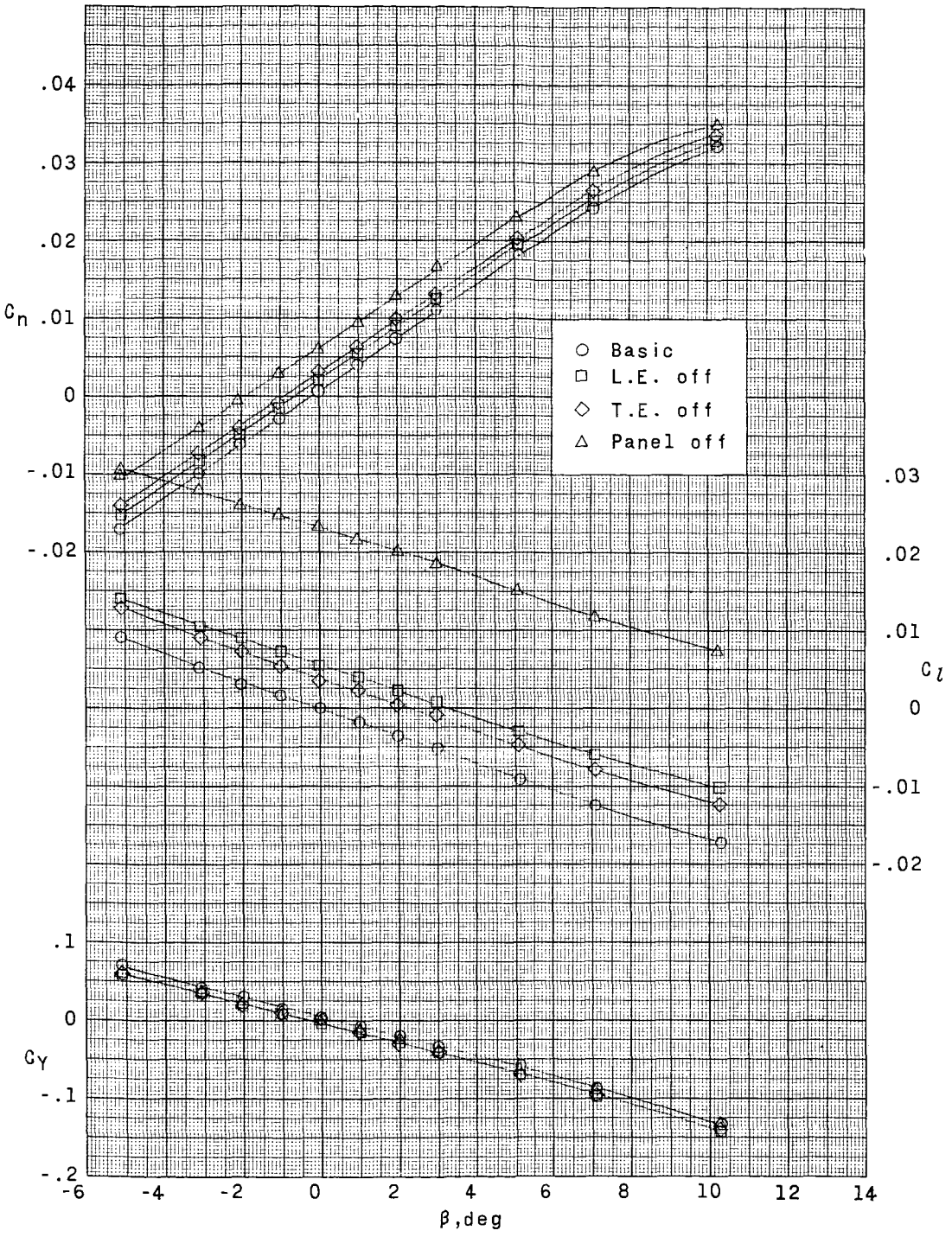

(b) $\alpha = 5^0$.

Figure 10.- Continued.

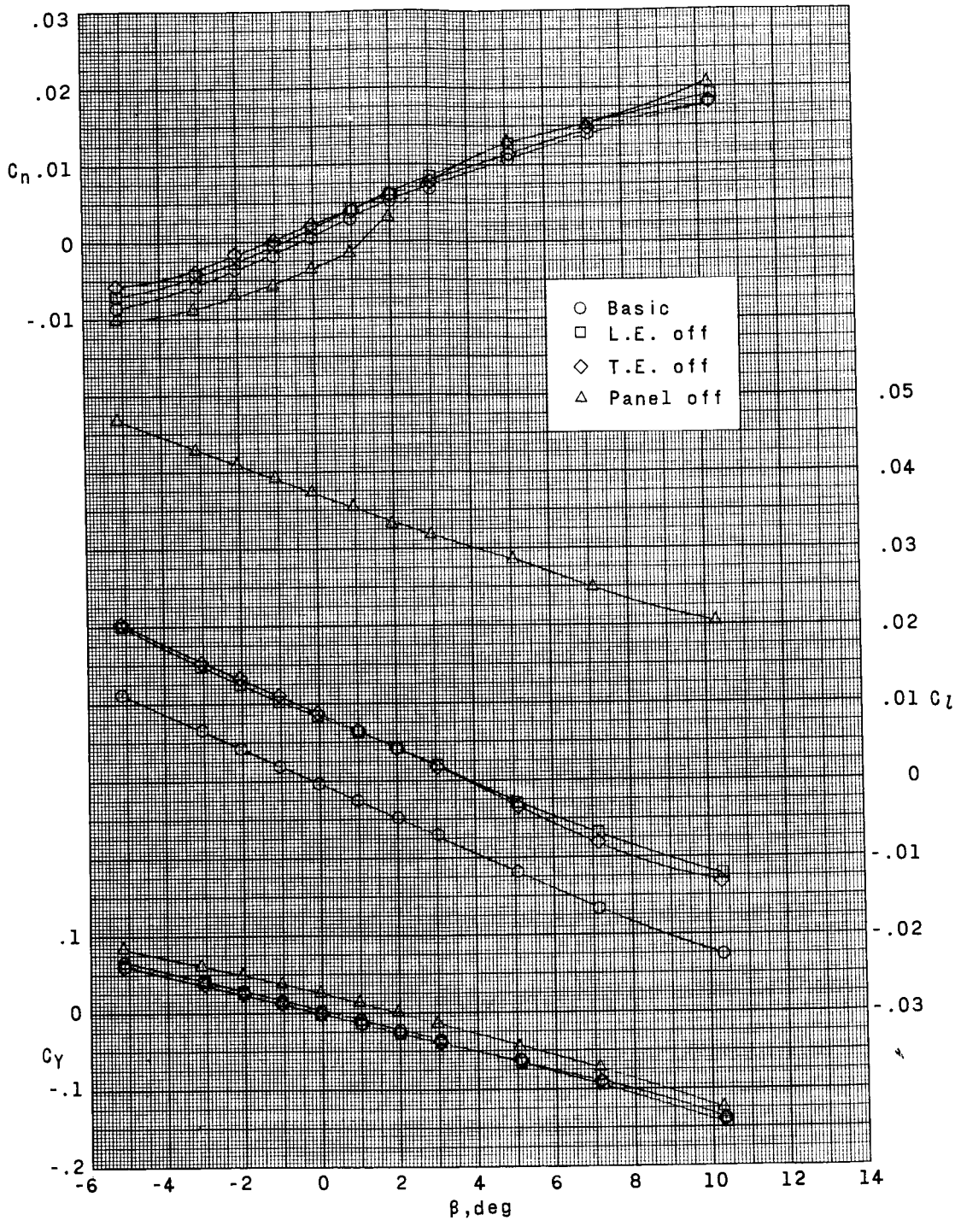

(c) $\alpha = 11^0$.

Figure 10.- Continued.

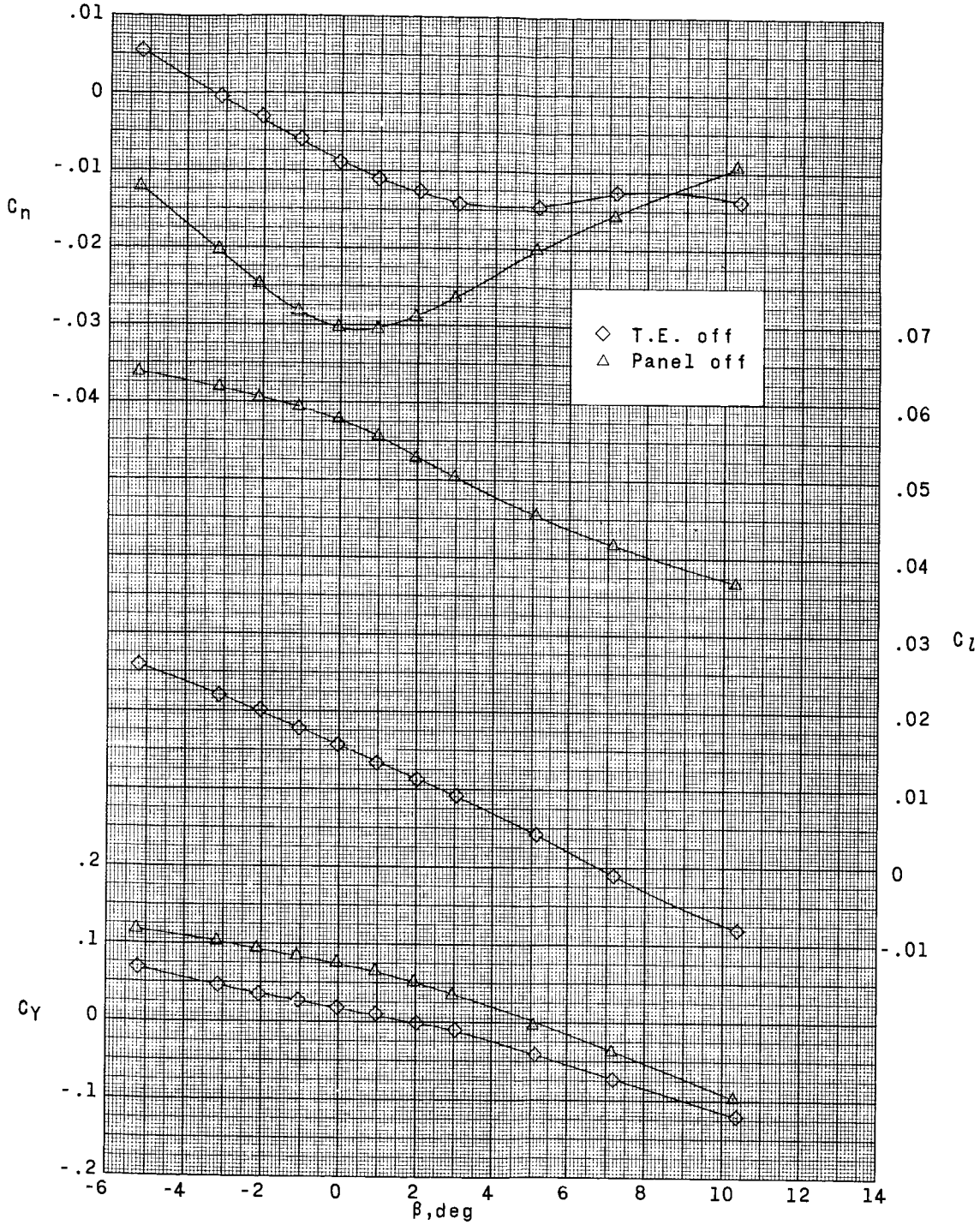

(d) $\alpha = 17^0$.

Figure 10.- Concluded.

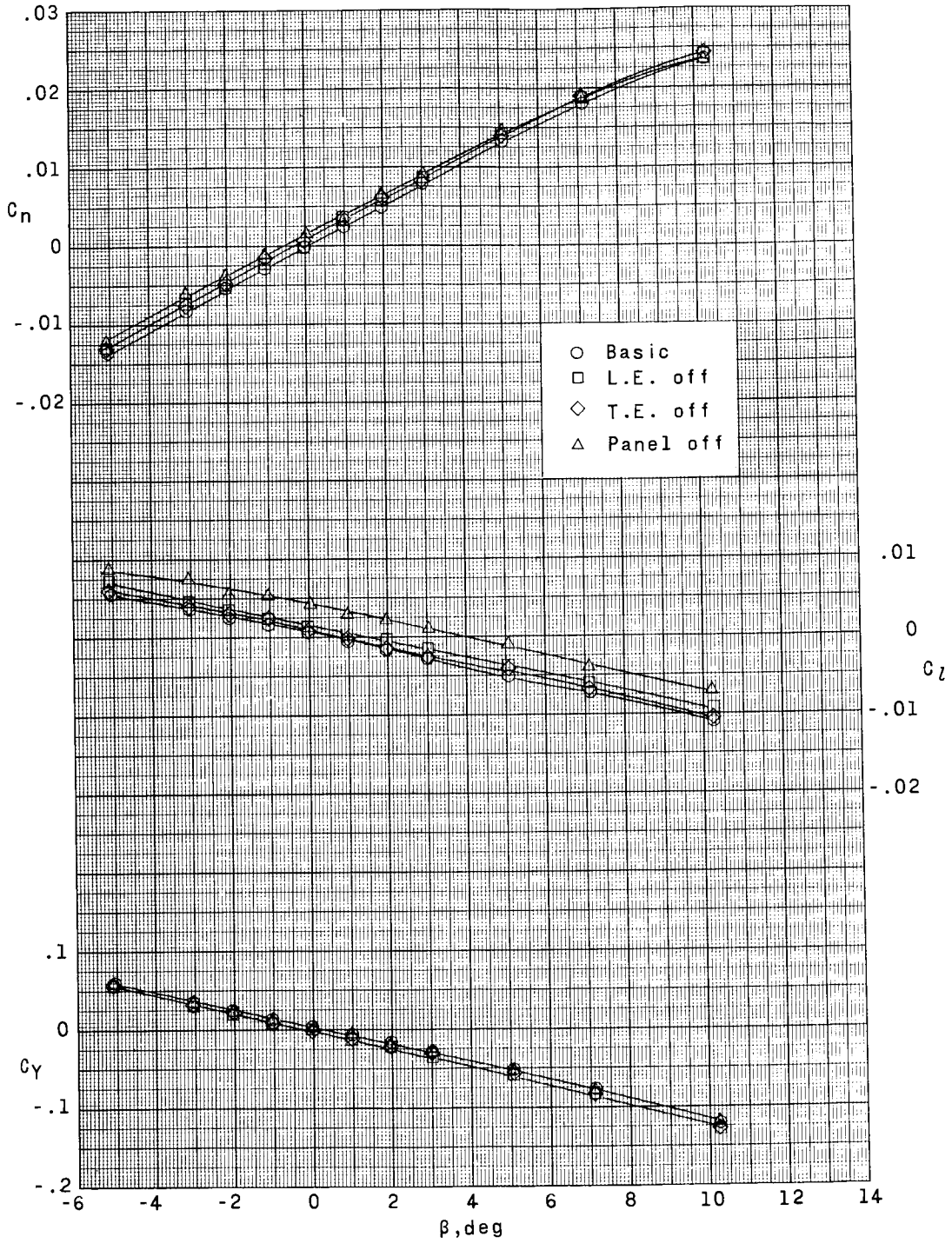

(a) $\alpha = 0^0$.

Figure 11.- Effect of wing asymmetry on the lateral-directional aerodynamic characteristics with sideslip. M = 2.36.

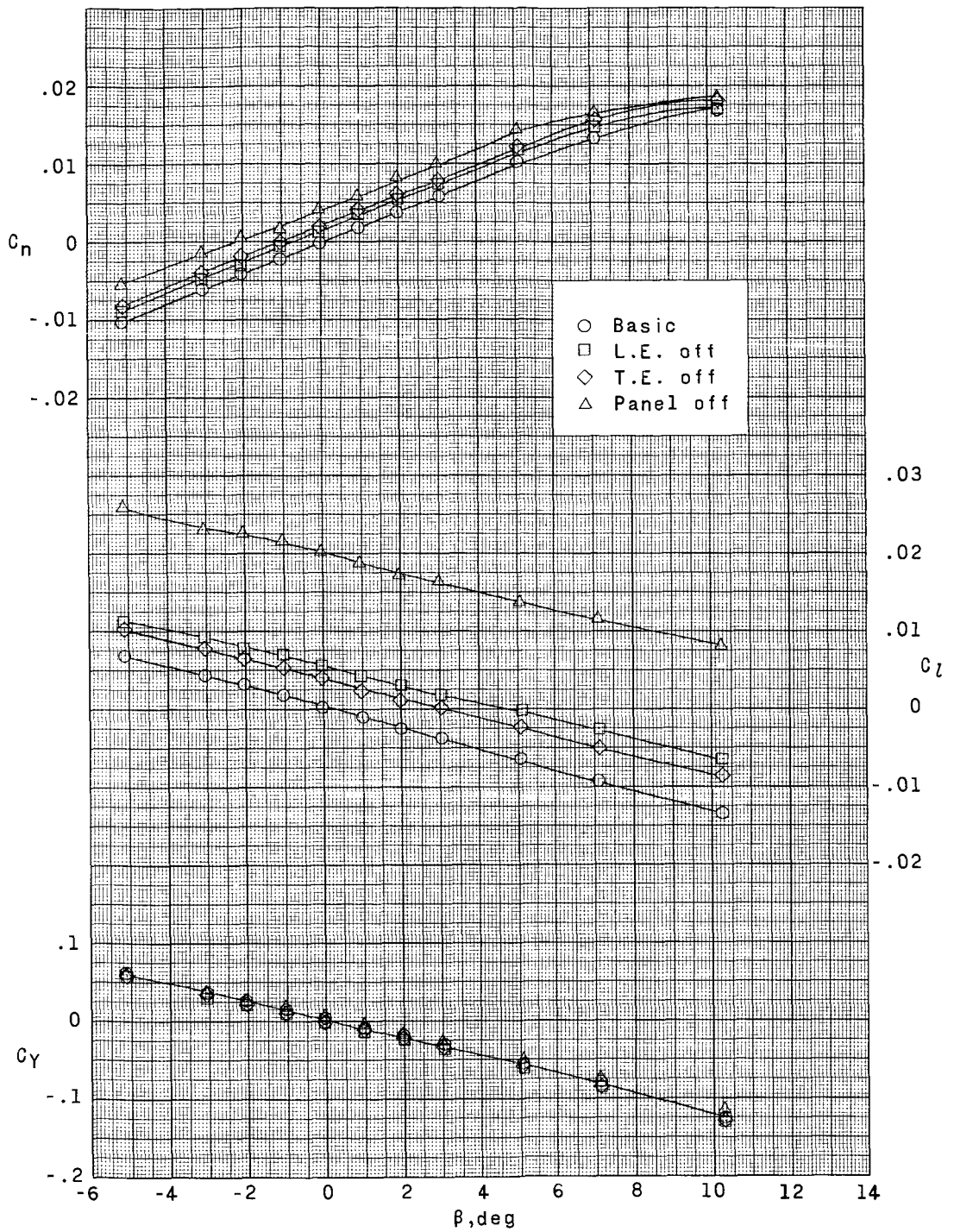

(b) $\alpha = 5^0$.

Figure 11.- Continued.

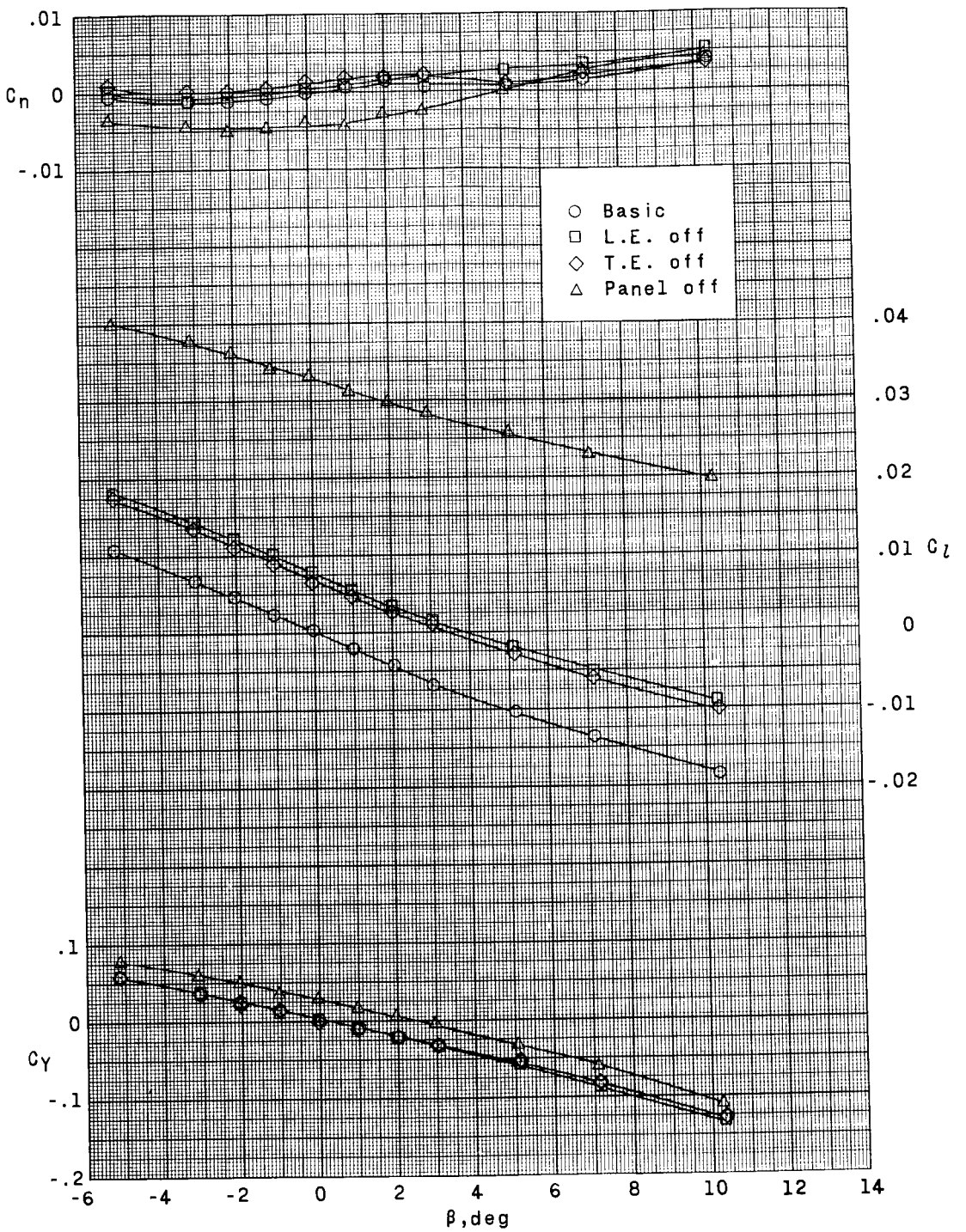

(c) $\alpha = 10^0$.

Figure 11.- Continued.

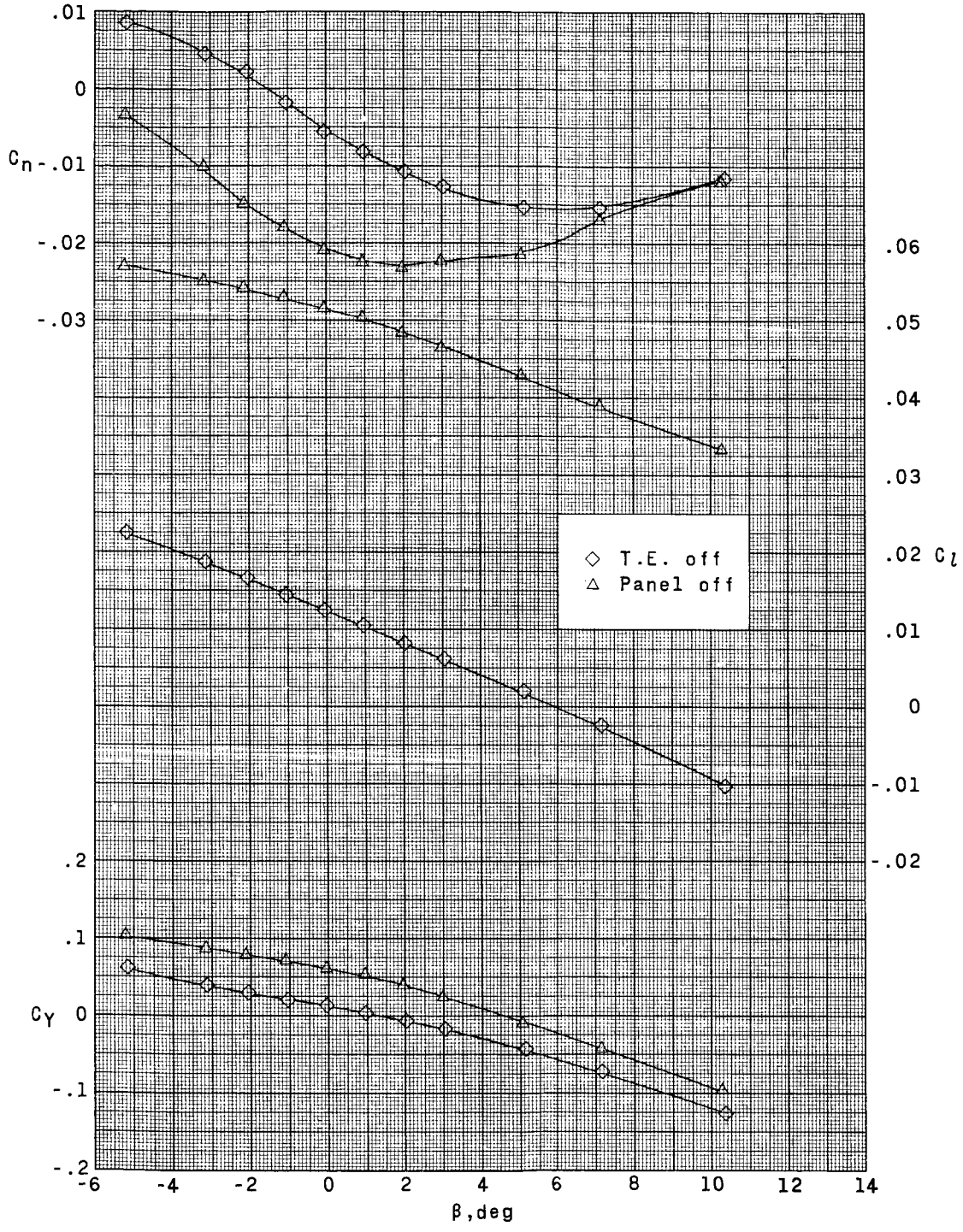

(d) $\alpha = 18^0$.

Figure 11.- Concluded.

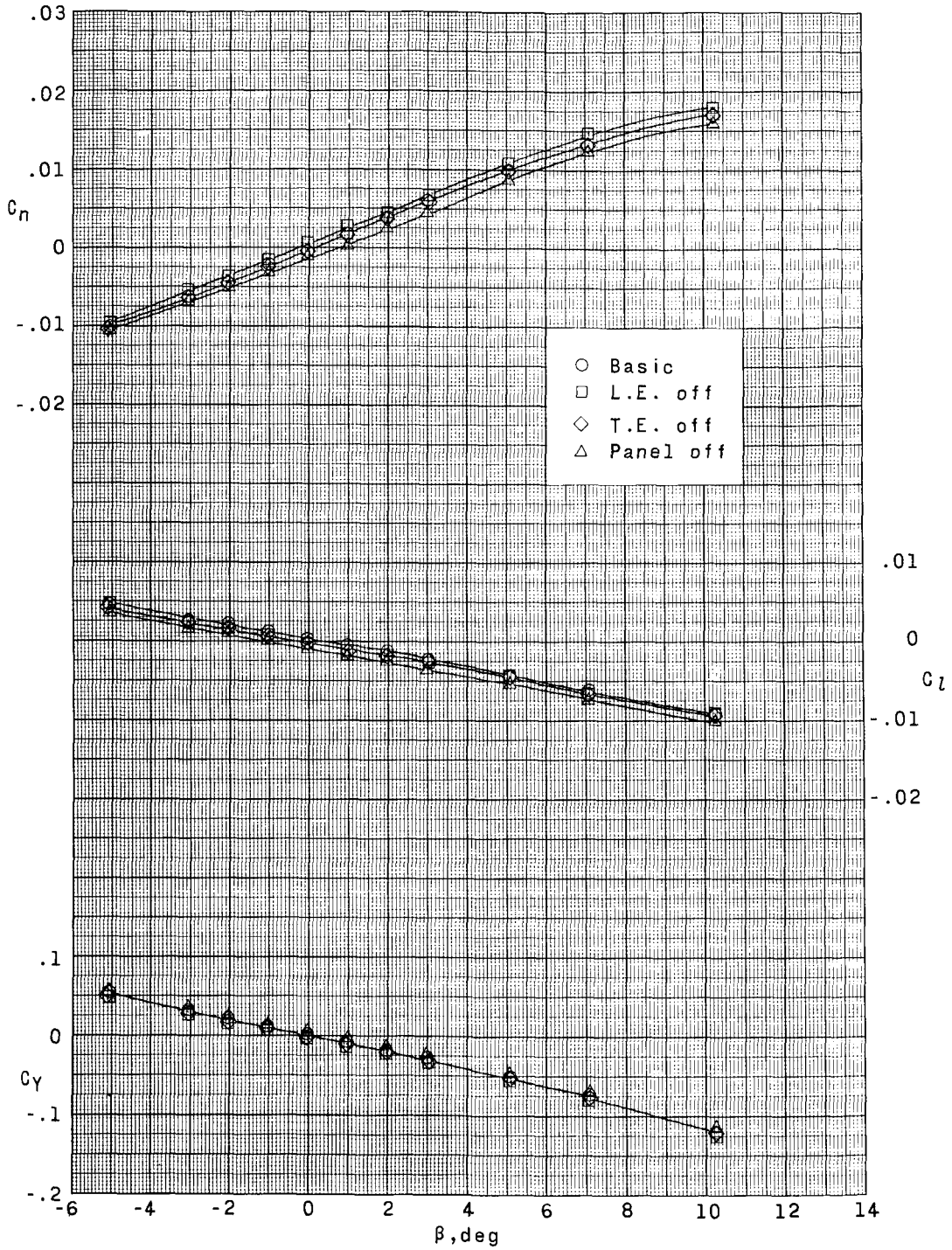

(a) $\alpha = 0^0$.

Figure 12.- Effect of wing asymmetry on the lateral-directional aerodynamic characteristics with sideslip. M = 2.86.

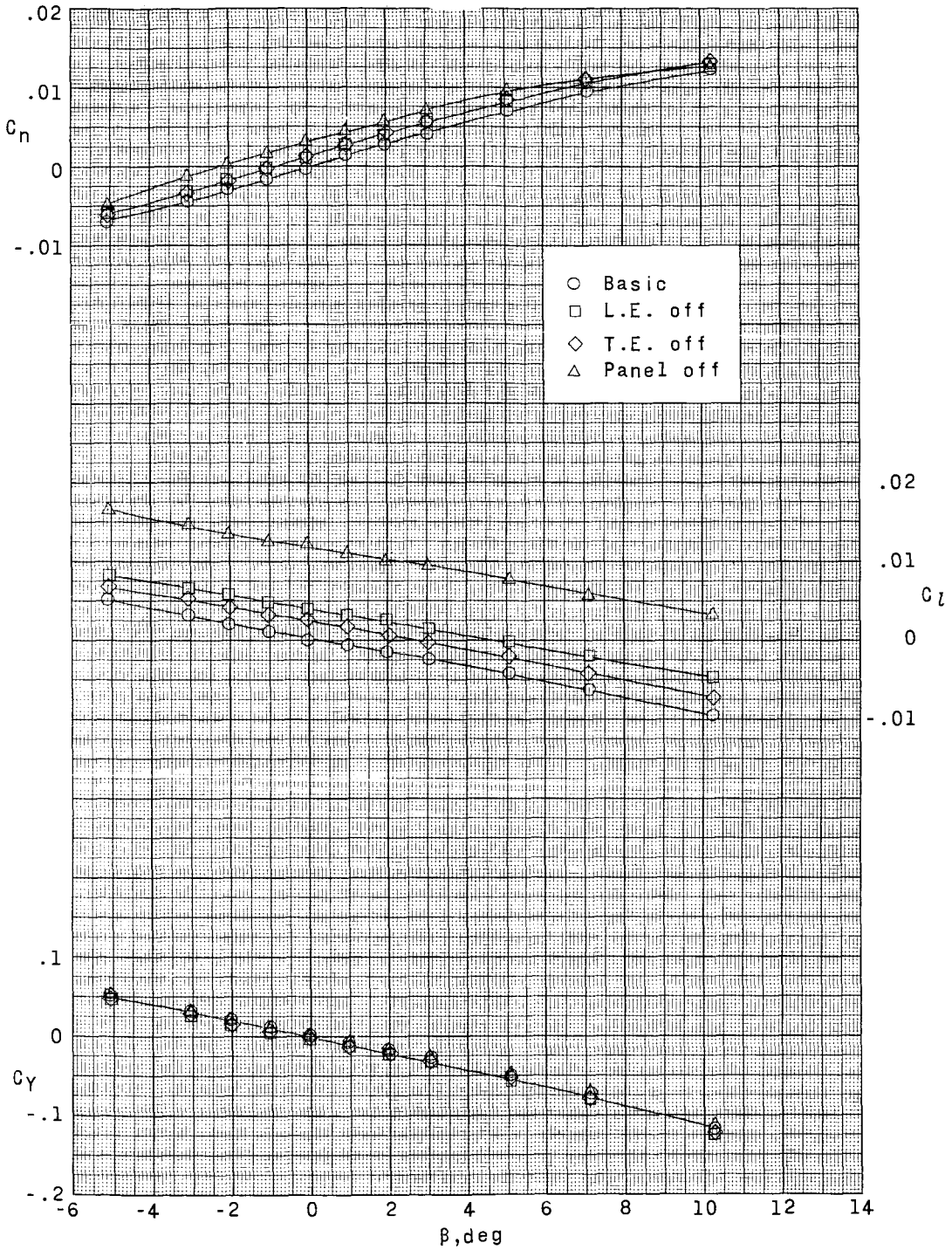

(b) $\alpha = 5^0$.

Figure 12.- Continued.

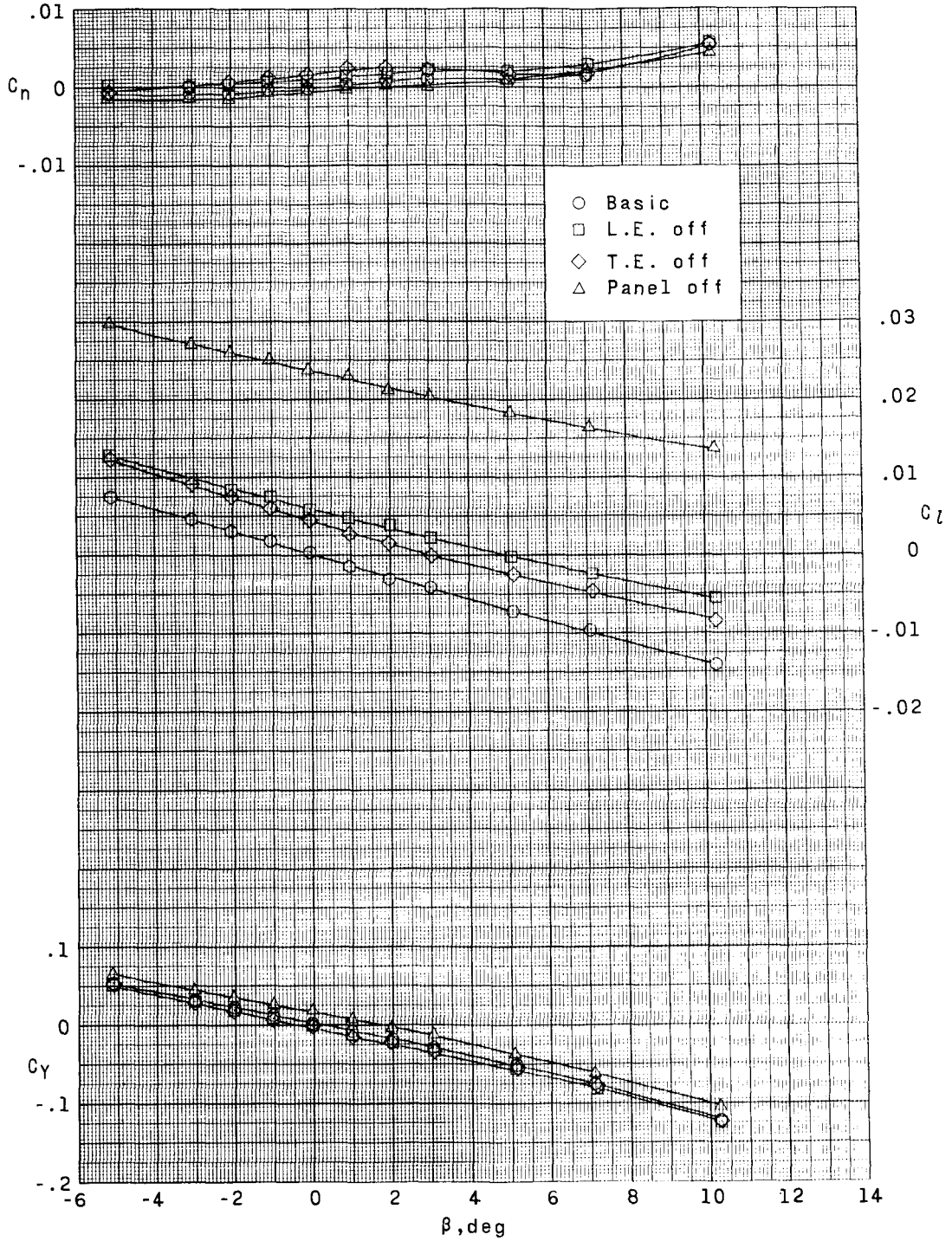

(c) $\alpha = 10^0$.

Figure 12.- Continued.

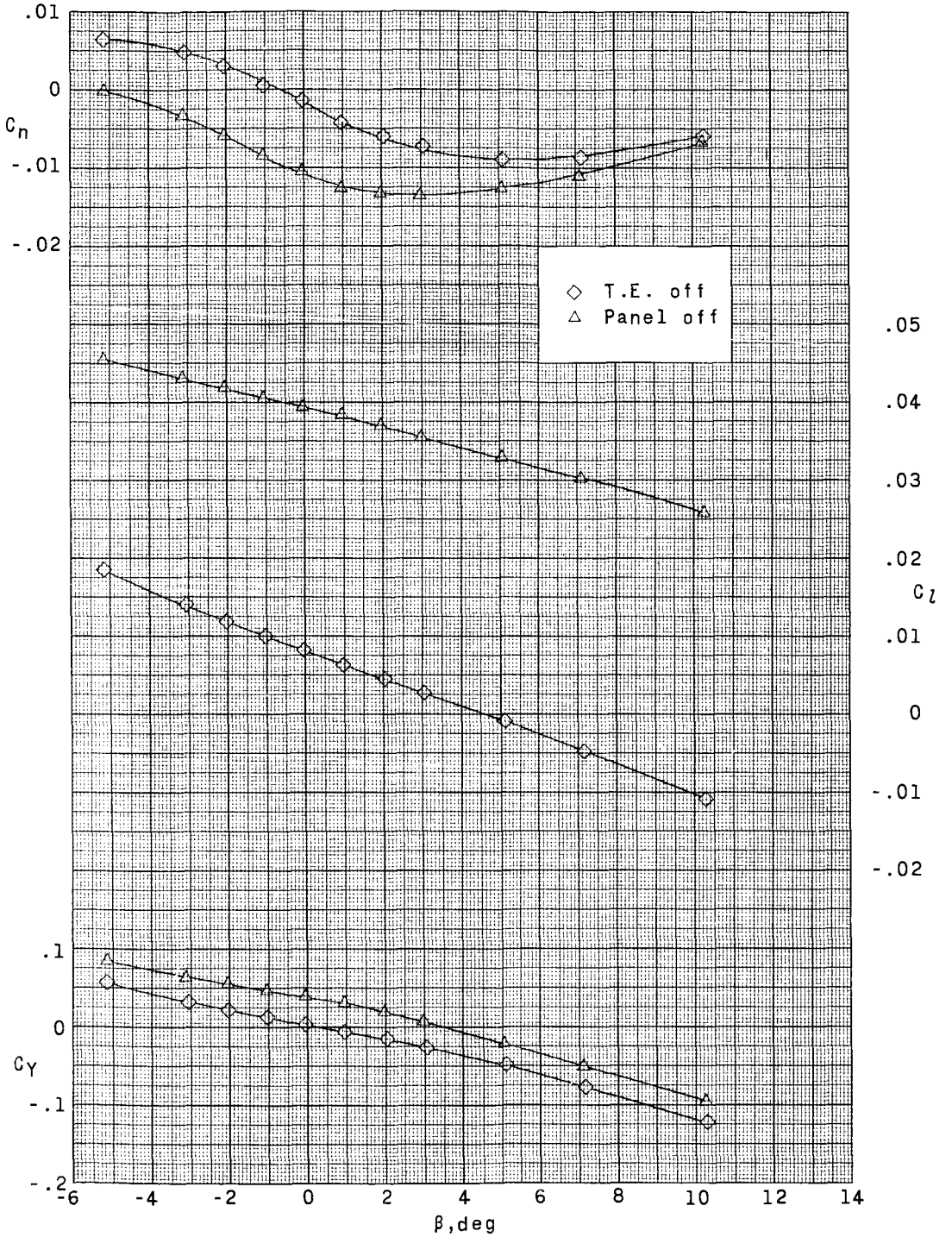

(d) $\alpha = 17^0$.

Figure 12.- Concluded.